Study on the controlling seawater intrusion for irrigation water quality conservation

Name HAISHENG LIU

Doctoral Program in Environmental Science and Technology

Graduate School of Science and Technology

Niigata University

Abstract

The seawater intrusion renders the quality of river water unsuitable for agricultural use. It is likely to occur near the estuaries of rivers draining into the sea. The agricultural area irrigated using the water from Shinkawa River has been suffering from the presence of saltwater. To avoid saltwater mixture to the irrigation water, closing the sluice gates at the river mouth and stopping intake pumping stations have been implemented when the salinity of water is expected to the standard of irrigation water. However, operating drainage pumps incurs a cost and stopping pumps causes shortage of irrigation water. In fact, the first class rice harvested in the year 2010 remained only 10 % of the total rice production of this area (Average rate 75 % for the whole prefecture). This study, therefore, aims at finding inexpensive but effective countermeasures to control the seawater intrusion for the irrigation water quality conservation.

To start with the study, the characteristics of seawater intrusion in Shinkawa River were investigated by visualizing the behavior of seawater intrusion through field surveys and numerical calculation. In the field survey, an acoustic reflection profiling system (SC-3) and electronic conductivity (EC) meters were employed to obtain the longitudinal and vertical profiles of the seawater intrusion. Then, the behaviors of the seawater intrusion, in response to the tidal force and the discharge change from upstream during the whole irrigation season without operation of sluice gates, were reproduced by a numerical calculation with a one-dimensional and two-layer unsteady flow model. As a result, it was clarified that when the interface between the saltwater and freshwater rises as high as 1.2 m below the inlet of intake pump, electrical conductivity of irrigation water exceeds the standard of irrigation water, 1500 μs/cm, which was evaluated as about 23 % of the irrigation period if the countermeasures were not practiced.

Based on this analysis, three countermeasures, discharge increase, the operation of sluice gates and selective intake, were conducted to control the seawater intrusion in Shinkawa River. The discharge increase was achieved by the operation of all drainage and irrigation pumping stations. The method of the operation of the sluice gates is to

create a submerged orifice by controlling the aperture of sluice gates to keep the constant water level difference of 25 cm between inside and outside the gates, pushing-out the saltwater layer outside the river. The basic idea of selective intake is constructing one kind of structure which can only let freshwater freely enter the gate of pumping station, and block saltwater outside of the gate. As a result of these three countermeasures, the operation of the sluice gates was determined as the most effective method. The elevation of the density interface between saltwater and freshwater decreased by 1.04 m, and the extent of seawater intrusion decreased by 1.85 km within 3 hours.

Therefore, the most inexpensive and effective countermeasure for controlling seawater intrusion is the operation of sluice gates, and this method can be applied to other estuaries suffering from the presence of seawater intrusion.

Acknowledgements

My deepest gratitude goes first and foremost to Professor Natsuki Yoshikawa, my supervisor, for his constant guidance in the writing of this dissertation, as well as during my whole doctoral period. His perfect-pursuing character, which makes the high quality of all the work be ensured, has been a goal for me to pursue. His deliberate mind, diligence and dedication to his work, and rigorous attitude of research motivate me to move forward all the times.

I would also like to extend my sincere acknowledgement to all the other supervisors, Professor Shin-ichi Misawa, Professor Toshihiro Morii and Professor Kazuhiro Nakano, for their all aspects of instructive advices and useful suggestions on my dissertation, and kind help to my daily research and study.

Furthermore, I am greatly indebted to every member in my laboratory, who has offered me invaluable help in the field surveys and daily life. Under the situation of my poor Japanese, they always communicated with me and help me patiently, and without them my life in Japan would have become much harder and duller.

Also, I am grateful for the experiment support from the Ministry of Agriculture, Forestry and Fisheries, Ministry of Land, Infrastructure, Transport and Tourism, Niigata Prefectural Government, and Nishikanbara Water Management Office of Niigata city, Japan. I would like to thank the Niigata University and the China Scholarship Council as well, for providing me the study opportunity and full financial support.

Last but not least, my thanks goes to my beloved family for their thoughtful concern and great confidence in me through all these years. I also owe my sincere appreciation to my friends who spent plenty of time on my dissertation's language modification and problem solution during the difficult course.

Contents

Figures

Tables

Symbols

B	river width
E	saltwater entrainment coefficient
F_P	net landward force of unit mass of water
F	internal Froude number
f_i	interfacial friction coefficient
f_b	riverbed friction coefficient
D_x	vertical diffusion coefficient
g	gravitational acceleration
h	water depth
i_f	friction slope
i_0	riverbed slope
m	grid-point number counted from downstream
n	time step
ρ_1	cross-sectionally averaged density of freshwater
ρ_2	cross-sectionally averaged density of saltwater
ρ	density of given mass of water
$\Delta\rho$	density difference between river water and sea water
$\bar{\rho}$	average density of water column with length
P	hydrostatic pressure
P_t	tidal prism

Q_1	discharge of freshwater
Q_2	discharge of saltwater
Q_r	volume of river flow during one tidal period
Ri_E	Estuarine Richardson number
δS	salinity difference from top to bottom
S	tide level
S_0	mean area of the cross-section of saltwater lay
U	typical tidal current
U_s	surface current
U_f	mean current of freshwater over the cross-section
u_1	flow velocity of freshwater
u_2	flow velocity of saltwater
u_{*2}	shear velocity
V_r	freshwater discharge
W	width of the estuary
η	ratio of the tidal prism and the volume of river flow
ε	relative density difference
x	horizontal distance
z	vertical coordinate

1. Introduction

1.1 Background

1.1.1 Seawater intrusion into rivers

Seawater intrusion is that saltwater from the sea tends to propagate into the river mouth from where river carrying freshwater flows into the sea, making some good and bad effects to the estuarine area (Tuin 1991). The saltwater, with a density of 2 % to 3.5 % higher than freshwater, slopes to the riverbed and spreads in the landward direction against the river flow, whether mixes well or not with the river water. The mixture degree between freshwater and saltwater entirely depends on the specific condition of the river mouth. This seawater intrusion is subject to both marine influences, such as tides and the influx of saline water, and riverine influences, such as flows of fresh water and sediment (McLusky and Elliott 2004). The seawater intrusion can propagate to a great distance from the coastline, especially as the river discharge is small. Extent of some tens of kilometers frequently occurs, and it is possible for the distance of more than two hundred kilometers to take place under extreme conditions.

The effect of seawater intrusion on estuarine region is mainly represented in three aspects, topography evolution, estuarine water environment and human development activities. The mixture of freshwater and saltwater in estuaries has functions on riverbed topography by changing the velocity and characteristics of sediment movement and hydrodynamics, such as the flocculation of sediment can be strengthened by saltwater, causing the formation of sandbar in the tidal estuaries (Huang 2006; Li 1990). Besides, the environment of high salinity in estuaries, caused by seawater intrusion, not only provides good living environment for many marine organisms, but also functions in the chemical processes (Li 1990; Xu et al. 2004; Zhu 2006). For instance, some heavy metal ions can be precipitated by the chemical reaction due to the mixture between saltwater and freshwater. However, the seawater intrusion may contaminate the freshwater in the lower river reach, making salinity of river water too high to be used in domestic, agricultural, industrial and other aspects, threatening the interests of the people who live in this area, especially when the freshwater requirements are relatively higher.

1.1.2 Influence of seawater intrusion

Since ancient times, estuarine region, where seawater intrusion often occurs, have generally focused the human production, living, market trade and tour because of its convenient traffic and plenty of coast resources. Most of people in the world live near coast and river mouth areas, and many cities originated here are the centers of polity, economy, culture, education and transportation hubs. Seawater intrusion can have an enormous impact on the features of physics, chemistry and biology of river mouth areas, influencing human health, agricultural production, industry and economic development.

(1) Human health

The chloride content is stipulated less than 250 mg/L in international drinking water standard. In estuaries, it can be increased when seawater intrudes into the lower reach of river, contaminating the drinking water resource. If the salinity of water is higher than 250 mg/L, it is not safe for the people who suffer from high blood pressure, heart disease or diabetes.

According to the monitoring data provided by the Shanghai Yuanshui Limited Corporation (named Chengtou Holding), the largest concentration of chloride appeared from December, 1998 to April, 1999 in the Wusong water utility company along the Yangtze River estuary in China, was over 1360 mg/L. In 2001, this concentration in Baogang Chengxing reservoir located along Yangtze River was more than 400 mg/L (Song and Mao 2002). In addition, the other minerals in seawater that exceeds the standard of drinking water will also cause some diseases, harming human health.

(2) Industry

Normally, the surface of metal container in the estuary industry zone is easily oxidized when it contacts with high salinity water, leading to age equipment, short useful life and low production efficiency, even losing safety guarantee (Yang 2007). In the case of some coastal engineering, the high salinity water can also make the risk of equipment erosion higher, since some metal can be damaged owing to the interaction with different kinds of substances of seawater, lowering the thickness and intensity of material, even perforating or fracturing.

(3) Agriculture

High saline water can influence the agriculture production in two main ways. Firstly, the irrigation water mixed with seawater is directly pumped to the irrigation channel, then watered crops. If the salinity in the irrigation water were higher than the limits, the plant would lose water, even wither, because the concentration of fluid inside the plant cells is lower than outside. Secondly, high saline seawater can infiltrate the soils through streams and canals, causing the variation of the pH and having harm to the growth of crops and other plants, even making soils compaction.

In irrigation water, the chloride content is strictly limited for different crops. Usually, the standard of irrigation water for paddy field is limited less than 1200 mg/L, but is proposed less than 600 mg/L during the period of raising rice seedlings. When seawater intrudes into the low river reaches, the high saline water would cause the concentration of the chloride high. During the dry water period from Dec 1978 to Mar 1979, the seawater intruded heavily along the estuary of Yangtze River in China. The water chlorinity was over 4000 mg/L at about 30 km from the East China Sea, and the Chongming Island where is located in the estuary of Yangtze River was surrounded by the saline water, causing the lost area of paddy field grown by about 1000 hm^2 (Mao et al. 1993; Shen et al. 1980). In the case of Nile River in Egypt, the seawater intrusion made the salinity of soil increase not only in the delta, but also in the upper reaches of Nile River, adversely effected the crop plants' growth and yield in recent years (Van 1993).

(4) Economy

Seawater intrusion can threaten the safety of drinking water, hinder the industry production and lower the quality of irrigation water, while all of these results in significant economic losses. In coastal cities, where the economy is more developed, the more economic losses might be caused once the seawater intrusion happens. The most serious consequence would be the relocations of factory and town, and nothing could grow in the region intruded by seawater. During the period from Dec, 1978 to Mar, 1979, the seawater intrusion was so serious that the whole Chongming Island was surrounded by saline water, caused a direct economy loss of more than 14 million Yuan and an indirect economy loss of more than 0.2 billion Yuan in Shanghai city, China

(Mao et al. 1993; Shen et al. 1980). In the case of Nile River in Egypt, billions of dollars were spent to cure the high salinity soil caused by the seawater intrusion in upper reaches after the Aswan Dam built in this river (Van 1993).

1.2 Seawater intrusion

1.2.1 Mechanism of Seawater intrusion (Tuin 1991)

Salinity of seawater is higher than that of freshwater. This makes the density of seawater higher than the density of freshwater, that is to say, the mass of seawater per unit volume is greater than that of freshwater. In estuaries, this density difference between seawater and river water has a large effect on the flow scheme since the density difference tends to cause stratification and has effect on pressure.

The horizontal landward pressure of a given mass of water is larger than seaward because of the density difference of the water bodies on both sides. This will generate a net landward force, causing acceleration in the same direction. This net landward force can be given by the following formula

$$F_P = -\frac{1}{\rho}\frac{\delta P}{\delta x} \tag{1-1}$$

where F_P is net landward force of unit mass of water. ρ is the density of given mass of water. x is horizontal distance, with the positive direction of seaward. P is hydrostatic pressure, and can be calculated by given formula as follows

$$P = \bar{\rho} g (h + h_b + z) \tag{1-2}$$

where g is gravitational acceleration. $(h + h_b + z)$ is length of considered water column "(see Fig. 1-1)". z is vertical coordinate (see Fig. 1-1). h is water depth. $\bar{\rho}$ is average density of water column with length $(h + h_b + z)$. h_b is vertical coordinate of bottom.

Difference between the pressures on both sides of the given mass of water may be caused by two factors: density difference and water surface slope. The pressure difference caused by the former factor increases with the river depth from the water surface, but is same anywhere over the entire depth of water for the latter one.

If ρ does not vary over the depth, $\rho = \bar{\rho} = f(x,t)$, and $h = f(x,t)$. The F_P of a unit mass of fluid can be given at any time by

$$F_P = -g\frac{\delta(h+h_b)}{\delta x} - \frac{1}{\bar{\rho}}(h-z)g\frac{\delta\bar{\rho}}{\delta x}$$

$$= -g\frac{\delta(h+h_b)}{\delta x} - \frac{1}{\bar{\rho}}\frac{1}{2}hg\frac{\delta\bar{\rho}}{\delta x} - \frac{1}{\bar{\rho}}(h/2-z)g\frac{\delta\bar{\rho}}{\delta x}$$

$$(a) \qquad (b) \qquad (c) \tag{1-3}$$

Term (a) descripts the effect of the water surface slope caused by tide on F_P, without varying over the depth. Term (b) is the effect of the density differences on the tidal flow over the depth. Term (c) is zero as it is averaged over the depth, implying that it does not function on the tidal flow over the depth. But it varies linearly over the depth, causing the velocity of flow to change with the direction in depth.

In estuaries, $\delta\bar{\rho}/\delta x$ keeps negative quantity due to the water density decreases with increasing distance from the sea, causing the variation of the direction of F_P over the depth. When 0 < z <1/2 h, F_P is positive and the water suffers a landward force. When 1/2 h < z < h, F_P is negative and the water suffers a seaward force. This illustrates the gravitation circulation is the driving mechanism of seawater intrusion into estuaries.

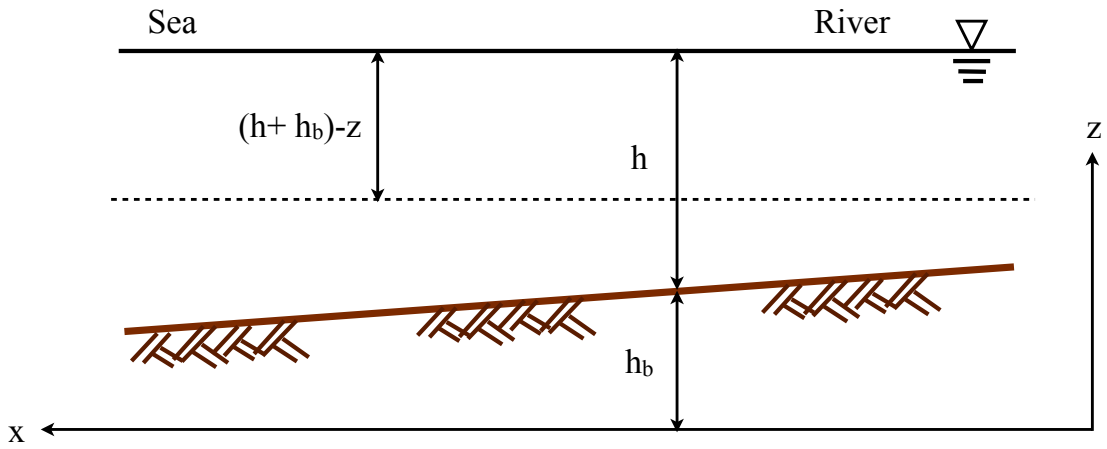

Fig. 1-1 Definition sketch for notation

The extent of seawater intrusion is limited by the vertical turbulent mixing and the vertical flow. The tip of seawater intrusion is directed upward, and the saltwater in bottom layer can be also brought to upper layer, and then flows to seaward with the freshwater in upper layer.

1.2.2 Factors of Seawater intrusion

Changes of seawater intrusion can be affected by natural factors and human development activities. The terms of the impacts on seawater intrusion are listed as follows:

(1) Freshwater discharge

The river runoff, one of the most important factors that influence seawater intrusion in the river mouth area, not only influences the mixture type between freshwater and seawater, but also works on the extent of seawater intrusion.

In general, the larger the river runoff becomes, the shorter the seawater intrusion extends, and vice versa. The river runoff varies with the seasons. The rainfall, influencing the runoff, is different because of climate and location. For example, Yangtze River's flood generally appears from May to October, during when the discharge takes 71.4 % of whole year. During the other months, the mouth area of this river is usually occupied by saline water (Song and Mao 2002; Yang 2007). The runoff not only varies with time, but also changes with spatial, thus causes the spatial distribution of seawater intrusion in the same river. This is reflected in the rivers that have many branches and estuaries. In the case of Yangtze River, its discharge is divided into four parts by four inlands, forming four outlets to drain the freshwater, causing different features of seawater intrusion. This is because that the different discharges, in four estuaries of this river, are determined by the different diversion ratio of upstream river section (Mao and Shen 1995).

(2) Tide and tidal current

Tide is another important factor that influences the seawater intrusion in estuaries. It is the rise and fall of sea level caused by the gravities between different celestial bodies and earth, especially by combined effects of the gravitational force exerted by the Moon

and the Sun and the rotation of the Earth (Huang 2006). Because of the earth's rotation, the positions of the Moon and the Sun relative to Earth changes, thus the tide varies on timescales ranging from hours to months and years, leading to the different periodicity of flood tide and ebb tide and tidal range (semidiurnal tide, diurnal tide and mixed tide) (Huang 2006; Zeng 2007), which play a role in seawater intrusion. In most oceans, the tidal change mainly refers to daily and semimonthly spring tide and neap tide, because of which the extent of seawater intrusion has the same time variation rules as well.

The tidal current is the periodic horizontal motion of seawater accompanying the rise and fall of the sea level. The tidal current provides the sustainable resource of seawater for the saltwater intrusion in estuaries. Tidal current has function on the driving force of seawater intrusion with the vertical variation of tide amplitude, remaining the density difference. What's more, it determines the movement direction of seawater. When the flood tide occurs, the tidal current moves inland, and vice versa.

(3) Ocean wave and wind

Ocean wave is one of the common phenomena in nature, while the ocean wind is the one of the reasons causing ocean wave. In general, ocean wave can be classified into wind wave that directly caused by wind and swell that generates from the wind wave subsequently. When the ocean wave propagates to the shallow water region near coast or in estuaries, it also plays a promoting role in the hydrostatic pressure of water.

Wind wave is directly influenced by the sea surface wind, so its direction is the same with the sea surface wind, whose features such as speed, fetch and duration, can determine the height and period of wind wave. If the directions of wind and tidal current are the same, the tidal current can be propagated landward faster (Huang et al. 2006). He (2010) found that in winter, the influence of wind on seawater intrusion is more obvious in the estuary of Modaomen, in China. Compared with the situation under no-wind, the ebb of surface layer and flood of underlying layer in this region were enhanced by the real wind in same direction, which exacerbated the development of vertical circulation, made the underlying salinity increase, lengthened the intrusion distance in bottom layer and made the trend of stratification between freshwater and saltwater more clear. In addition, the types of wind also had different impacts on the seawater intrusion under the average discharge. For instance, north wind can cause the

worst seawater intrusion in Yangtze River, in China, leading to the highest salinity in all layers, the longest intrusion distance at the bottom, the largest salinity flux transporting landward, and the most obvious stratification. The results caused by south wind are opposite, since it blocks the seawater intrusion to some extent in Yangtze River, leading to the lowest salinity in all layers, the shortest intrusion distance at the bottom, the smallest salinity flux transporting landward and the largest mixture (Xiao and Shen 1998).

(4) Topography

The topography of estuaries, an important carrier of fluid transport, plays a role in the interaction between seawater and freshwater. The depth and shape of estuary can determine the boundary condition and flow field of fluid, which determine the flow regime to a large extent (Liu 2010). The complexity of topography directly causes distinct mixture features between freshwater and seawater. Take Yangtze River estuary in china as an example, the intrusion means of seawater mainly includes (Mao and Shen 1995; Nguyen and Savenije 2006): (1) directly intrusion from open sea, (2) seawater propagated from north branch flows back through the south branch owing to the different flow diversion ratios, and the sedimentation appears in north branch, causing the saline water intruded from the south passage to flow back toward the north passage, (3) the water exchange between south branch and north branch through the passages of shoals, and (4) unsynchronized seawater intrusion in each branches. The complex seawater intrusion means, caused by topography, also appear in other branched alluvial estuaries in the world, such as the Loire estuary in France, the Tanintharyi estuary in Myanmar, the Hau and CoChien branches of the Mekong Delta in Vietnam, the Dhamra estuary in India and the Mekong Delta in Vietnam (Nguyen and Savenije 2006).

(5) Human activities

Basically, the estuarine regions are characterized by human highly development activities, which can cause the changes in estuarine configuration, modification of freshwater inputs and net salinity flux transported from open sea, influencing the behavior of seawater intrusion near river mouth areas.

As for the use of the natural resource of a river mouth ecosystem, some economic

development activities, such as aquaculture, agricultural irrigation and transportation, may cause important effects on the seawater intrusion and are aimed at restraining seawater intrusion. Moreover, the dam built upstream river makes the water supply of downriver decrease, causing the larger range and longer period of seawater intrusion. For example, the Three Gorges Dam on the Yangtze River and the South-North Water Diversion Project in China decreased the discharge downstream, especially in very low flow years, thereby having more obvious influence on seawater intrusion (Wang et al. 1997). Besides, the salinity increase of the soil in upper and middle reaches of the Nile River in Egypt is because the Aswan Dam on the Nile River decreased the discharge drained downstream during dry season, seriously aggravating the seawater intrusion (Van 1993). In addition, other coastal estuarine engineering also has impacts on the range of seawater intrusion. For example, sluice gates or dikes are constructed in the river mouth to control seawater intrusion, and deepening usually adopted to maintain navigation channels, as well as sediment collection, reservoir construction and harbor building also change the natural river at different level, effecting on the seawater intrusion to some extent (Tuin 1991).

1.2.3 Classification of Seawater intrusion

The independent variables mentioned last section, govern the seawater intrusion. Different relationships between variables can result in different intrusion types. Commonly, there are three intrusion appearance types: stratification type, partially mixed type and well-mixed type (Tuin 1991).

Stratified type: This type of seawater intrusion is featured by clear stratified flow, while overlying freshwater moves downstream, and underlying seawater flows upstream along the riverbed from the river mouth, generating an arrested saltwater wedge. It forms as the freshwater discharge is large and tidal amplitude is small, with weak turbulence in the river (Fig. 1-2 (a)), and generally occurs in rivers draining into the Sea of Japan due to its relatively small tidal range.

Partially mixed type: The interface between freshwater and seawater is not so clear as in the stratified type, yet there are both horizontal and vertical variations in the salinity field. It is shown in Fig. 1-2 (b). Geographically, this type is also distributed in the river mouths along the Pacific Ocean in Japan where the water depth is not too deep and the

tidal range is relatively large.

Well-mixed type: When the tidal range is large, and freshwater and seawater mix strongly because of the tidal current, the salinity in a vertical direction becomes uniform and only varies toward to upstream as shown in Fig. 1-2 (c). This type generally appears in the estuaries along the Pacific Ocean in Japan because of the relatively large tidal range.

The stratified and the well-mixed types are extremes of the mixing types. When the vertical density gradient of partially mixed type reaches the maximum, the former type appears; conversely, when the vertical gradient of density decreased to the minimum, the latter type appears. However, these three types are not always distinguished definitely, but quite ambiguously, and are frequently changing with the time and the space. Different types of flows are even generated in the same river mouth. This is usually caused by the change of river discharge, tidal level, tidal range, estuary topography and so on.

1.2.4 The determinants of mixture types

Based on these influence factors and driving mechanism of seawater intrusion, there are three ways to identify the classification of seawater intrusion.

(1) Estuarine Richardson number (Wang 2001)

The most basic definition is the gradient Richardson number, namely a ratio of stabilizing effect of stratification to the destabilizing effect of shear. In estuarine research field, it has another universal formulation, given by

$$Ri_E = g\frac{\Delta\rho}{\rho}\frac{V_r}{WU^3} \tag{1-4}$$

where g presents gravitational acceleration, V_r denotes the freshwater discharge, W denotes the width of the estuary, U denotes the typical tidal current, and $\Delta\rho$ denotes the density difference between river water and sea water. An experimental mixing classification scheme based on estuarine Richardson number suggests that when $Ri_E < 0.08$, the mixture is well-mixed type, $0.08 < Ri_E < 0.3$ indicates partially mixed type, and when $Ri_E > 0.8$, it turns to highly stratified type.

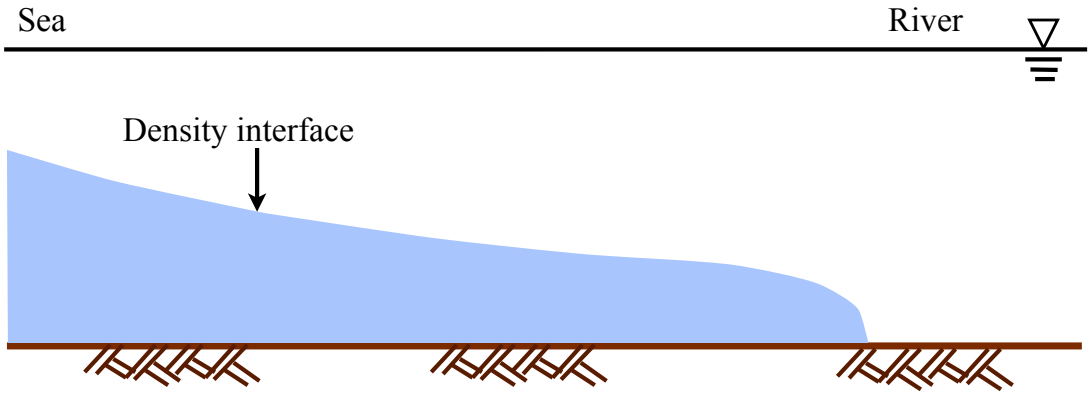

(a) Stratified type

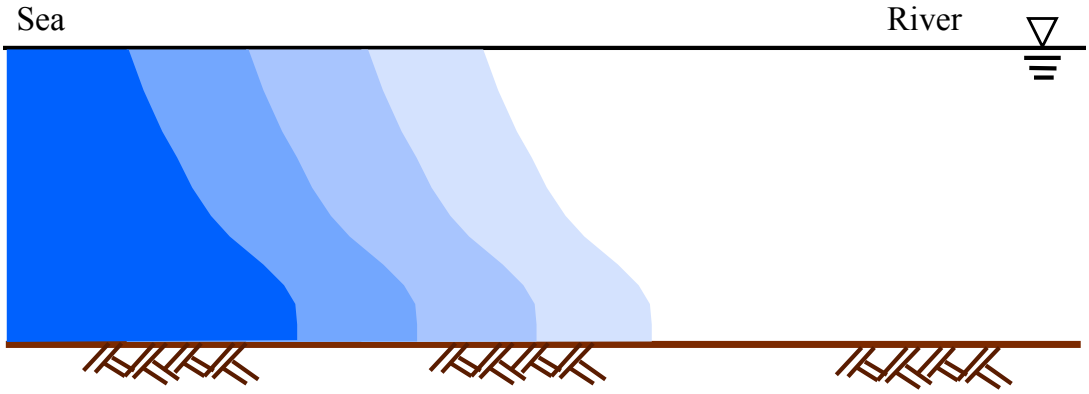

(b) Partially mixed type

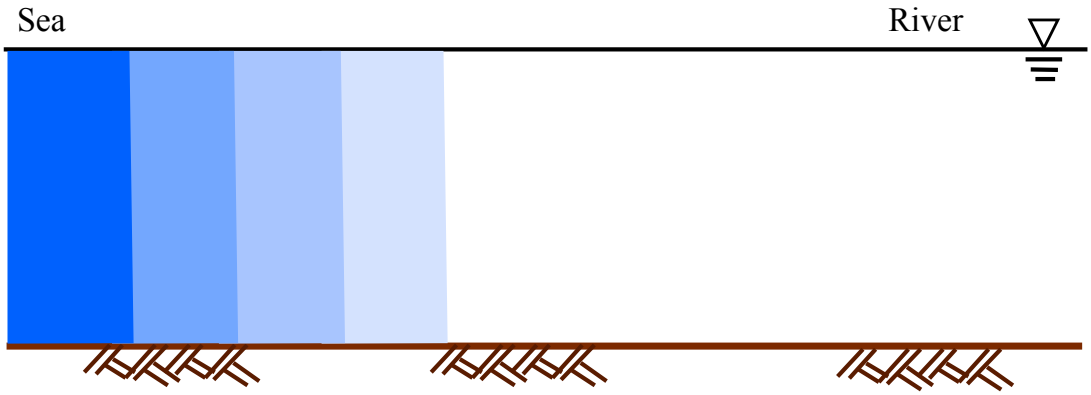

(c) Well-mixed type

Fig. 1-2 Seawater intrusion types

(2) Hanson-Rattray classification (Wang 2001)

Hanson and Rattray defined a classification scheme based on two dimensionless ratios: the top to bottom salinity difference δS divided by the mean over the cross-section S_0 ($\delta S/S_0$) and the surface current U_s to the mean current over the cross-section U_f, which is the fresh water flux (U_s/U_f). The Hanson-Rattray scheme aims to plot $\delta S/S_0$ versus U_s/U_f, and then to read off the type of estuary from the plot. The identifiable types are

Type 1 – Well-mixed

Type 2 – Partially stratified

Type 3 – The saltwater wedge

(3) Simmons and Brown (Simmons and Brown 1969)

The ratio of the tidal prism P_t and the volume of river flow during one tidal period Q_r are calculated to classify the density current η, as

$$\eta = \frac{Q_r}{P_t} \tag{1-5}$$

while

$\eta \geq 0.7$ Stratified type

$\eta = 0.2 \sim 0.5$ Partially mixed type

$\eta < 0.1$ Well-mixed type.

In this mean, the tidal prism is defined as the volume of seawater that flow into the river mouth during one tidal period.

1.3 Reviews on seawater intrusion

1.3.1 Research methods

Research by prototype observation

The key of this method is the field observation. A large amount of observation of the

salinity of the river water, for long term, should be recorded by reasonable experimental designs and equipment, then the intrusion rules of seawater can be summarized base on the relative theories and methods. What's more, some universal relationships between the observed parameters can be obtained to evaluate the seawater intrusion occurred in other estuaries. Suga (1979) investigated the concentrations of chlorine-ion at the surfaces and the bottoms in 90 rivers in Japan, calculated their ratios and summarized the flow regimes of seawater intrusion using the tidal ranges and the length of tidal areas. Hansen and Rauray (1966) classified the estuaries into three types according to the circulation coefficient and Simmon (1969) similarly classified the conditions of appearance of these three types, based on the ratio of river discharge and tidal prism in one tidal cycle. These classification methods are still used to recognize the seawater intrusion types in other estuaries by modern researchers. Wang et al. (2011) conducted three surveys along six sections around the Yellow River mouth to investigate how salinity changes with abrupt increases and decreases in river discharge. Besides, these recorded data in field observation can also be adopted in the numerical simulation to verify the model.

Although the prototype observation can obtain important information, the accuracy degree of its results mainly depends on the amount of observation data, which needs more monitoring stations and longer period of investigation to get a more precise result. Sometimes, the observed data is easily influenced by the external factors, such as weather and monitor equipment, causing a lower accuracy. It's also worth noting the disadvantages of expensive cost, high region restriction and the one-sidedness of recorded data.

Research by physical model

The flow conditions of water in real engineering are very complex. It's quite difficult to solve the hydraulic problems only by theoretical analysis, directly measurement or simplified experiment, but the model test is an efficient method applied to this research area. The model test is defined as that water flow condition similar with that in prototype can be reproduced in the model in order to analyze or observe the water movement law. In the model test, the geometrical shape, movement and dynamic characteristics of water current that are shrunk or enlarged based on the similarity

principle are similar with that in prototype, and these terms in prototype can be calculated or derived according to the similar ratio. The model test can be classified by the following methods (Zuo 1984; China Institute of Water Resources and Hydropower Research and Nanjing Hydraulic research institute 1985): (1) cross-section model and overall model by the space scale of experiment, (2) normal scale model and state-variable model by the geometrical shape, (3) fixed bed river model and mobile-bed river model by the boundary conditions, (4) clear water model and muddy water model by water current of single phase or multiphase fluid and (5) pipe, channel, building and machine model by the research subjects.

Farmer (1951) made an experimental study of saltwater wedge. He observed the phenomenon of the saltwater wedge in the experimental apparatus over a wide range of flow conditions, provided important reference to investigate the saltwater wedge in experimental apparatus to the future work and developed an experimental equation that can describe the saltwater wedge formed in the laboratory. This experimental equation can generally describe the mean horizontal distribution of salinity in estuaries where the freshwater and saltwater are well mixed. Kaneko (1965) observed the behavior of saltwater wedge in a channel of non-uniform depth, successfully measured the wedge shape and size, the surface slope, the interface slope between saltwater and freshwater, the velocity and density distribution, and also developed the profiles of stress and interfacial stress coefficient from this observation and the equation of motion. Grigg (1995) investigated the dynamics and mixing of a seawater intrusion in a long and level flume containing a contracting and diverging section. Physical model test can not only reproduce the process of seawater intrusion, but also quantify the variables governing seawater intrusion, specifically revealing the mechanism of seawater intrusion.

Research by numerical simulation

The numerical simulation is the most popular method not only in seawater intrusion, but also in other research fields, such as spaceflight and automobile industry, due to the advantage of saving considerable time and labor, avoiding external interference, and realizing the calculation under single and multiple conditions. The numerical simulation is also named as computer simulation, and is an attempt to model a real-life or hypothetical situation on a computer. It is generally applied to reveal how the archetype

system works under different conditions. By changing variables in the model, predictions about the behavior of the system can be made, therefore it's also used to explore and gain new insights into new technology and to estimate the performance of systems (Banks et al. 2001; Starogatz and Steven 2007). Numerical simulation generally consists of the following aspects: building the mathematical model which describes the substance of the problem, determining the solving methods, inputting the initial and boundary conditions and verifying the output. Currently, the simulation method adopted in the seawater intrusion field has been paid more and more attention with the fast development of computers and the improvement of the calculating methods.

(1) One-dimensional model

One-dimensional model of seawater intrusion mainly focuses on the distribution of salinity along the longitudinal direction changing with time. Suga (1977; 1979; 1981) developed the one-dimensional, two-layer, unsteady flow numerical model, in which the front position of saltwater wedge, the depth of density interface and the average velocities and concentration distributions in upper and bottom layer can be solved at the same time. Zhu (1980) calculated the longitudinal distribution of salinity and intrusion extent in Yangtze River estuary by the advection-diffusion equation and the mass conservation equation. Yi (1987) researched the variation of cross-section mean salinities and velocities in different positions by the one-dimensional flow model in the anabranched estuary.

(2) Two-dimensional model

Two-dimensional model of seawater intrusion mainly focuses on simulating the distribution of salinity in two directions changing with time. Arita and Gerhard (1987; 1987) developed the entrainment model of saltwater wedge. This model was applied in the prediction of overall wedge properties, i.e., length, shape, and internal circulation, in estuary. Good agreement was found between the available data spanning the full Reynolds number range from laboratory and the field conditions with relative intrusion lengths. Chen (2004) adopted an efficient laterally averaged model that is unconditionally stable with respect to gravity waves, bottom and wall frictions, and adopted the vertical eddy viscosity term to study the hydrodynamics and salt transport

processes in the Alafia River, in southwest Florida. Model simulations show that runoff from the un-gauged portion of the Alafia River watershed is an important factor controlling the salinity distribution in the Alafia River, even though the majority of the Alafia River watershed is gauged. Liu et al. (2004) investigated the change in seawater intrusion using a vertical two-dimensional numerical model in the Tanshui River estuarine system, Taiwan, when reservoir was built and bathymetric changed. This model simulation reveals that significant salinity increases have resulted from these combined changes.

(3) Three-dimensional model

Three-dimensional model of seawater intrusion is most complex, which focuses on analyzing the distribution of salinity in three directions changing with time. It has been widely used to reproduce the spatial and temporal mixing processes of saltwater and freshwater under partially or strongly mixed conditions. Meselhe and Nohsi (2001) researched the seawater intrusion under the climate change and intake water conditions by the three-dimensional numerical simulation model named SEAWAT. Jeong (2010) used a three-dimensional numerical model, called Environmental Fluid Dynamics Code (EFCD) to analyze the seawater intrusion characteristics and the influence range in the downstream of Geum River, Korea, when the gates near this river mouth were fully opened, indicating that the EFDC model used for numerical simulation has high accuracy. Gong and Shen (2011) investigated the salinity transport mechanisms and the response of seawater intrusion to the changes in river discharge and tidal mixing in the Modaomen Estuary, one of the estuaries of the Pearl River Delta in China, by adopting the Environmental Fluid Dynamics Code using nested grids.

1.3.2 Research status

The research of seawater intrusion in estuaries started from 1930's in the world, while the Waterways Experiment Station (WES) of the United States and the hydraulic experimental laboratory of the Delft in Netherlands have done huge scale amount of work involved the in-site observation and pilot research in this research field (Liu and Tong 2004). The research results generally include: (1) revealing the characteristics of seawater intrusion based on field survey, (2) analyzing the reasons causing the seawater intrusion according to corresponding theory, (3) determining the factors influencing the

seawater intrusion, (4) discovering the harm on surround environment and (5) attempting to control or prevent the seawater intrusion by various countermeasures.

Survey

In early research concerns, many researchers paid more attention to the extent of the seawater intrusion. Schonfeld (1953) derived the analytic solution of the intrusion length of saltwater wedge based on the theory of saltwater wedge. Pritchard (1952,1954), Bowden (1959,1963,1966) and Hansen (1965) respectively discussed the seawater intrusion range, the mixing process between freshwater and saltwater, the distribution of salinity and the influence on movement of water flow and sediment. After these, the intrusion classification of seawater in estuaries was discussed from distinct aspects. Hanson and Rattray (2001) defined a classification scheme based on two dimensionless ratios which are the top to bottom salinity difference divided by the mean over the cross-section and the surface current velocity to the mean current over the cross-section. Simmons (1969) defined a mixed coefficient that is the ratio of the tidal prism and the volume of river flow during one tidal period, to classify the density current. Bowden (1967) and Pritchard (1967) classified the mixture types between saltwater and freshwater in the saltwater wedge (well stratified type), two-layer flow (moderate stratified type) and vertical homogeneous type.

In subsequent researches, the mechanism of seawater intrusion and driving force factors are the emphases. Hanawa and Sugimoto (1980) explained that the combined effect of vertical circulation and vertical eddy diffusion was responsible to the predominant longitudinal dispersion process and the water renewal process in the saltwater wedge according to a series of measurements of salinity and temperature carried out at a fixed station along the Nanakita River estuary, Japan. Uncles and Stephens (1996, 1997) studied the variation of driving force of seawater intrusion in Tweed estuary and its impact on the seawater intrusion based on analyzing the salinity under different tidal and river discharge. Austin (2004) used seventeen years' hydrographic data taken along the main stem of the Chesapeake Bay in US to analyze the mean salinity structure, the stratification structure, and the infer trends in the effective longitudinal dispersion of properties. Lerczak and Geyer (2006) used an array of cross-channel moorings and shipboard surveys to study the salt balance in the

Hudson River estuary in New York, illustrating that steady vertical shear dispersion, resulted from the estuarine exchange flow, is the dominant mechanism which drives the down gradient salt flux at that location, while the salt flux, resulted from tidal correlations between currents and salinity (tidal oscillatory salt flux), is an order of magnitude smaller than that resulted from steady shear dispersion.

Numerical simulation

For prototype survey, the corresponding conclusions are usually summarized based on the original obtained data. Nevertheless, this research mean is very easily interfered by external factors, such as weather and apparatus. In order to overcome these lacks, the numerical simulation method is gradually becoming another main mean for the study of seawater intrusion. Numerical simulation is generally applied to reproduce the temporal and spatial distribution of salinity under real conditions, to analyze the intrusion rules under single condition or combined conditions and to explore the mechanism of the seawater intrusion. Ippen and Harlemen (1961) built the one-dimensional model of seawater intrusion to analyze the basic factors that determine the instantaneous longitudinal distribution of salinity in a partially mixed estuary. They revealed that in the steady-state portion, the apparent longitudinal diffusion coefficient was a function of the turbulence induced by the tide and of the internal circulations induced by the density difference. And then they developed a function for the intrusion length as a expression of the estuary length, mean depth, tidal amplitude and period, freshwater discharge, ocean salinity, and estuary roughness. Leenderlse et al. (1973, 1975) proposed the earliest three-dimensional numerical calculation method, and Backhaus (1983) developed a semi-implicit scheme for the numerical solution of the shallow water equations that is suitable for the simulation of shelf sea dynamics.

After 1990's, the research on seawater intrusion was more and more carried out by numerical simulation. In 1990s, Simpson et al. (1990) built a numerical model to analyze the influence of tidal straining and density current on the stratification in Liverpool bay, England. In 1998, Gillibrand and Balls (1998) used a one-dimensional seawater intrusion model to investigate the hydrography of the Ythan estuary in the north-east of Scotland, and successfully simulated the salinity distributions for periods of high and low river flow. In 2000, Hagy, et, al. (2000) developed a box model based

on salinity distribution and freshwater inflow measurements, and estimated net non-tidal physical circulation and hydraulic residence times for Patuxent River estuary, Maryland. Acerts et al. (2000) developed a river basin management instrument based on GIS tools and rapid assessment techniques, aiming at assessing the effects of seawater intrusion on freshwater availability, fish stocks and agricultural production in Gorai region in Bangladesh. In 2004, Hetland and Rockwell (2004) configured a model using an idealized estuary/shelf domain with rectangular cross section, constant vertical mixing, and steady riverine discharge, and then they estimated the estuarine adjustment time scales of the model. They also examined the response to a step change in riverine discharge and estuarine response to changes in vertical mixing. In 2006, Sylaios et al. (2006) developed and applied a stratification-mixing model that intended to assess the influence of water retention by a man-controlled artificial reservoir on the stratification extent at the mouth of Strymon River in Bulgaria and Greece. In 2008, Zahed et al. (2008) applied the model (CE-QUAL-W2) to assess the impacts of river discharge reduction on seawater intrusion in Arvand River estuary in Iran and Iraq, and obtained a simple equation for estimation of the intrusion length using upstream freshwater discharge. In 2009, Xue et al. (2009) applied the high-resolution unstructured-grid Finite-Volume Coastal Ocean Model to study the physical mechanism leaded to the seawater intrusion in the Yangtze River in China, and found that the intrusion was caused by a complex nonlinear interaction process in relation to the freshwater flux upstream, tidal currents, mixing, wind, and the salt distribution in the inner shelf of the East China Sea. Twigt et al. (2009) applied a modeling system coupled a one-dimensional (1D) river network model with a three-dimensional (3D) coastal model to the Pearl River Delta (PRD) in China, and successfully provided an accurate representation of the discharge volume and distribution as well as water levels in the PRD under a wide range of hydrological conditions, which varies from very low to very high river discharges. In 2010, Ralston et al. (2010) used an unstructured grid hydrodynamic model to simulate the conditions in the Merrimack River estuary in US, achieving a high skill against time series of water level, salinity and velocity, and captured the spatial structures of salinity, velocity and salt flux observed in along and across-estuary transects. In 2012, Zhang et al. (2012) established a one-dimensional flow and salinity model of the Pearl River networks in China to reproduce the seawater intrusion process.

Control method

After having mastered the characteristics and mechanism of seawater intrusion, many researches paid attention to methods of controlling or preventing the seawater intrusion to decline its impact on estuary surrounding environment. Several control methods of seawater intrusion that have been implemented, either laboratory experiments or engineering practices, are all based on the way of disturbing the turbulence structure of the tidal current to weaken or block the driving force of seawater intrusion. These methods generally include that (Abraham et al. 1973; Army U.S. Army Corps of Engineers 1993; Zhu 1996) (1) flushing the waterway with freshwater upstream, (2) setting pneumatic barriers to create air bubbles curtain in the path of seawater intrusion, (3) setting water barriers induced by pumping water to create a vertical water curtain in the path of seawater intrusion, (4) selectively withdrawing freshwater, (5) building a sluice gate nearby the river mouth, (6) constructing the structure or sill at the bottom of river to block the seawater intrusion, (7) digging a slot at the riverbed in the path of seawater intrusion and (8) reducing the local width or depth of the estuary to increase the velocities downstream and decrease the external pressure gradient causing by density difference.

Currently, many researches of control techniques of seawater intrusion mainly aimed at the type of saltwater wedge (well stratified estuary). In the engineer technical letter by the Department of the Army U.S. Army Corps of Engineers (1993), there are three basic types of control methods mentioned, which are Venture control, static control and dynamic control, respectively. The type of static control was successfully used in Mississippi River in 1988 during a low river discharge period to block seawater intrusion from Gulf and protect freshwater intakes for the city of New Orleans (Fagerburg and Alexander 1994). Jirka and Arita (1987) introduced the concept of dynamic control, which is an obstruction into the path of the saltwater wedge that synchronously blocks the wedge and provides a sudden constriction of the approach flow, altering the near bottom boundary layer and eliminating the zone of low flow speed. Jirka and Sutherland also showed the average ratio of dynamic-to-static control device height based on experiment. The air curtain mechanism has been tested not only in laboratory experiments but also in several navigation locks adjoining the sea in the Netherlands. Nakai and Arita (2002) experimentally investigated the behavior of steady

saltwater wedges in the presence of an air curtain, and found that the buoyancy due to an air curtain, the intrusion force of a saltwater wedge and the inertial force of a freshwater flow govern variously behave of the saltwater wedges around an air curtain. Haralambidou et al. (2003) tried to apply the combination of the air curtain method and the results of a mathematical model to the estuary of Strymonas River in Greece. Luyun et al. (2009) investigated the effect of the application of surface recharge, injection recharge and the installation of a cutoff wall in repulsing seawater intrusion by laboratory experiments and determined the optimum location for injection recharge application by numerical simulation.

1.4 Purpose and objectives

Although there are many existing studies and models that attempt to predict or prevent the seawater intrusion in the estuaries of the world, only some of them, not many, can really control the seawater intrusion to some extent. However, It is difficult and expensive to build these methods mentioned in last part to some estuaries, even the adverse effect will occur when these methods are applied. What's more, almost all control methods applied either in lab or practical engineering can't be directly transplanted to other estuaries due to the complexity of conditions in different estuaries.

In this study, the major objective is to determinate one effective and inexpensive countermeasure to limit or prevent seawater intrusion by verifying the practical effect in field experiments. The important two aspects of seawater intrusion, longitudinal profile and vertical distribution of salinity, will be recognized by the field surveys and numerical simulation. The specific objectives are shown as the following:

(1) Visualization of the seawater intrusion in Shinkawa River

The behavior of seawater intrusion in Shinkawa River will be visualized by two aspects: longitudinal and vertical direction. The longitudinal and vertical distribution of salinity will be observed by an acoustic reflection profiling system (SC-3) and the electronic conductivity (EC) meter. This process will be conducted under different discharge and tide stage. Besides, the velocities and flow directions of saltwater and freshwater will be recorded by current meters as well (chapter 3).

(2) Reproduction of the seawater intrusion by numerical simulation

The behavior of seawater intrusion in the Shinkawa River will be reproduced by a one-dimensional, two-layer, unsteady numerical flow model. This model will be implemented during the whole irrigation season to obtain a long series data of seawater intrusion without external influence (chapter 4).

(3) Evaluation of the impact of seawater intrusion on irrigation water

The simulated salinity distribution will be compared to the observed salinity of irrigation water during the whole irrigation season. The period of high saline irrigation water contaminated by seawater intrusion will be evaluated (chapter 4).

(4) Verification of the propositional methods of controlling seawater intrusion

Three countermeasures, as discharge increase, freshwater selective intake and operation of sluice gates near the river mouth, will be verified to control or limit the seawater intrusion by in-site experiments. The effect of each method will be discussed and analyzed from two aspects after it is conducted: longitudinal distribution and vertical distribution of salinity (chapter 5).

2. Study field

2.1 Overview

2.2.1 General description of study field

The study river is a man-made river named Shinkawa River, which flows through the Nishikanbara district in Niigata City, Japan (Fig. 2-1) and services this area. The topography of this district is characterized by a low-lying plain with approximately one-third of the land dipping below sea level and surrounded by the mounts and hills, leading to a large amount of rainy water retention. The Nishikanbara district is a part of the alluvial plain created by the Shinano River and Agano River, and has fertile soil. This district covers an area of 350 km^2 in the Niigata City, and paddy production is the dominant land use, occupying about 198 km^2, 57% of the total area.

The entire length of the Shinkawa River is approximately 13.5 km (Fig. 2-2). The Shinkawa River started to be canalized in 1818 for draining not only the rainwater and surface drainage from paddy fields, but also the house sewage along this river. However, the river water is also recycled as irrigation water in the downstream area where there is a shortage of irrigation water, especially during irrigation season. The most important facility along the river is the river mouth drainage pumping station and sluice gates (Fig. 2-3). Its main purpose is to control floodwater, but it also functions to limit seawater intrusion when salinity of river water is expected to exceed the level at which it would affect irrigation water. In order to supply irrigation water for paddy fields efficiently in this district, nine irrigation pumping stations have been equipped along the river (Fig. 2-3), having a beneficiary area of 33.3 km^2, which accounts for 17% of the total paddy field areas in the district. Ten drainage pumping stations are also equipped along this river to ensure the demand of drainage as shown in Fig. 2-3.

2.1.2 Seawater intrusion and present strategies

Paddy fields irrigated with water from the Shinkawa River have experienced significant yield loss and deterioration in rice quality. In order to obtain the timely salinity data of this river water, two salinity monitoring stations with electronic conductivity (EC) meters have been set at 3.21 km and 3.59 km from the sluice gates,

near the intake inlet of the Nakasai and Nishikawa-karyu irrigation pumping station, respectively, by the Water Management Office of Nishikanbara district (Fig. 2-3).

Attempts to avoid saltwater mixture into irrigation water have been made by the Water Management Office of this area based on the data recorded by the EC meter at the Nakasai irrigation pumping station. One such measure is the closure of the river mouth sluice gates near the river mouth when salinity, indirectly measured by EC meters at the Nakasai irrigation pumping station, reaches an unallowable level. At this point, the drainage pumps, at the Shinkawa River mouth drainage pumping station, drain saltwater along with freshwater out of the river. During periods of high salinity, intake pumps that supply irrigation water along this river cease to operate so that high saline water is not pumped into irrigation channels. The detailed operation standard of each pump is listed in the Table 2-1 and 2-2, and the pumping stations which needed operation mainly include Shinkawa River Mouth drainage pumping station and Nishikawa Suirokyou, Shindorimakio, Nakasai, Chyokusenbo and Nishikawa-karyu intake pumping stations. The distance of each irrigation pumping station from the sluice gates is 2.20 km, 2.22 km, 3.06 km, 3.23 km and 3.59 km, respectively.

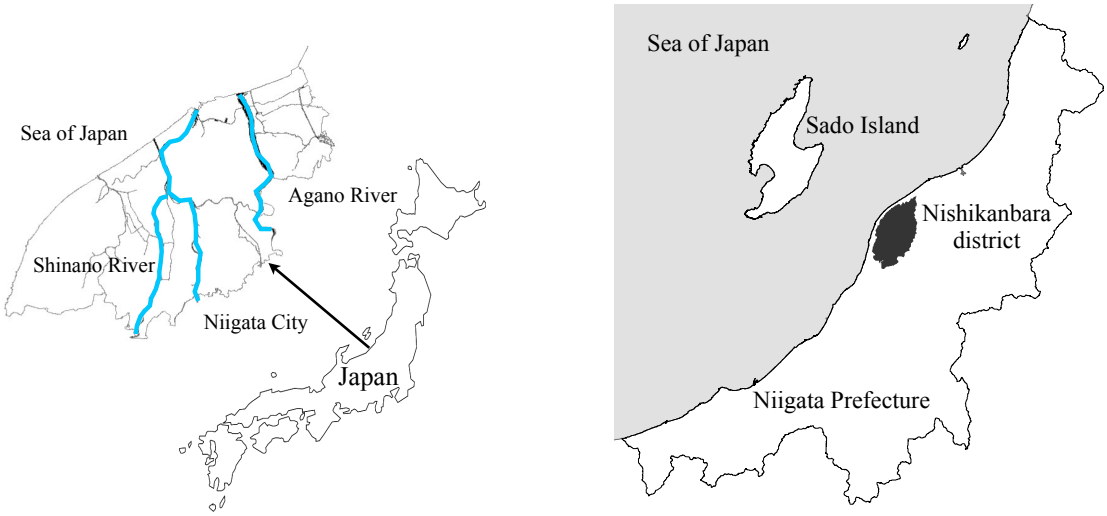

Fig. 2-1 Location of study field

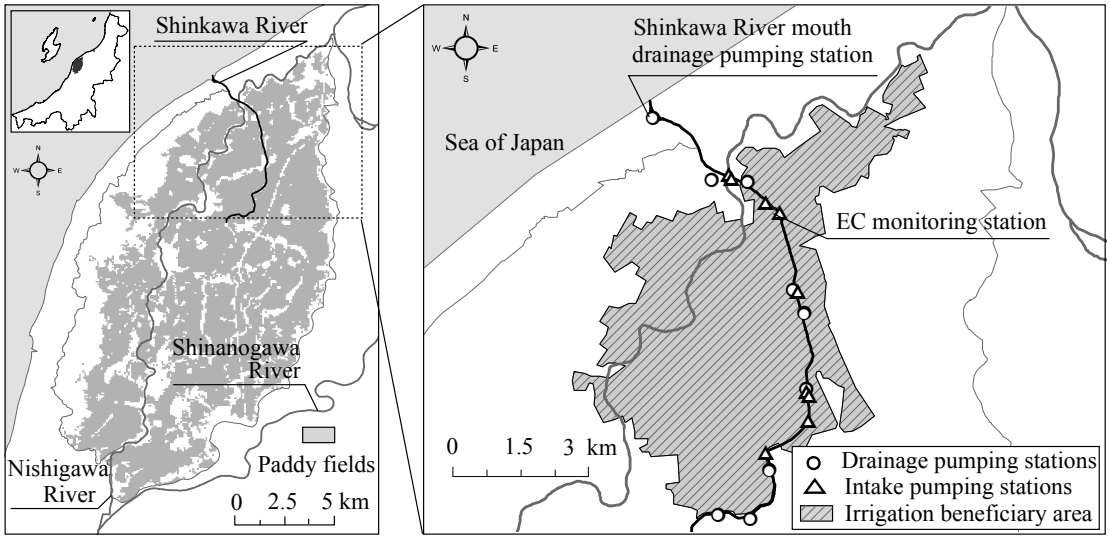

Fig. 2-2 Location of study river

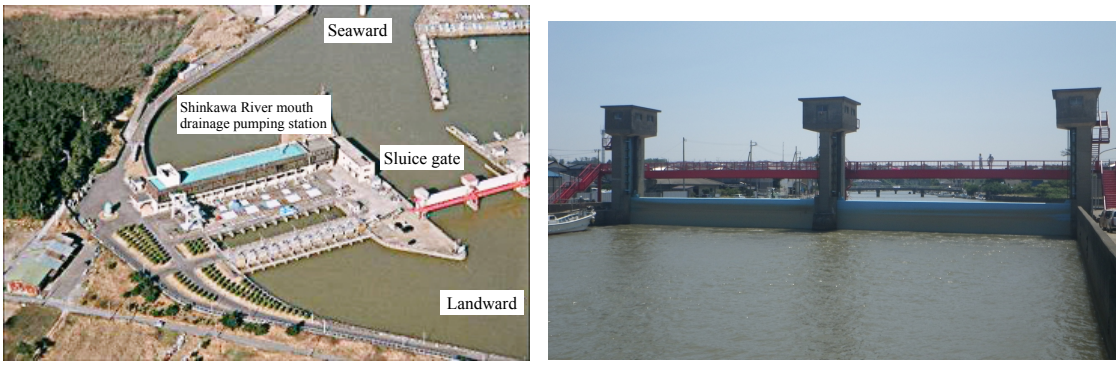

Fig. 2-3 Shinkawa River mouth drainage pumping station and sluice gates

Table 2-1 Operation standard of pumping stations

EC Value (μs/cm)	Name of pumping station	Operation status
700	Shinkawa River Mouth drainage pumping station	Attention and prepare
1000		Closure of the sluice gates
1300	Nishikawa Suirokyou irrigation pumping station	Stop
	Irrigation pumping station	Stop
1500	Nagasai irrigation pumping station	Stop
2000	Cyokusenbo irrigation pumping station	Stop
	Nishikawa downstream irrigation pumping station	

Table 2-2 Rerun standard of pumping stations

EC Value (μs/cm)	Name of pumping station	Operation status
1300	Nishikawa Suirokyou irrigation pumping station	Run
	Irrigation pumping station	
	Nagasai irrigation pumping station	
	Cyokusenbo irrigation pumping station	
	Nishikawa downstream irrigation pumping station	
700	Shinkawa River Mouth drainage pumping station	Open

However, this measure has some drawbacks. The operation of the drainage pumps of the Shinkawa River mouth drainage pumping station is costly, and part of that cost is reimbursed by farmers. The total electricity cost of Shinkawa River Mouth drainage pumping station was 38,775,473 Yen during the irrigation seasons (April to September in 2010, 2011 and 2012), and the specific cost in each year is shown in Table 2-3. Regarding water balance, irrigation water becomes scarce and may be insufficient to meet the demands of the paddy fields when high salinity is detected and intake pumps cease to run. Despite the countermeasure efforts, the first class of rice harvested in the year 2010, made up only 10 % of the total rice production of this area, the average rate of whole prefecture was 75 %. This degeneration was presumably caused by insufficient irrigation water supply during the high water demand period due to halted operation of irrigation pumps under high-saline conditions. Therefore, the specific characteristics of this estuary should be researched so that the more suitable and inexpensive countermeasures can be proposed to control or prevent the seawater intrusion.

Table 2-3 Electricity cost of Shinkawa River Mouth drainage pumping station

Year	Total cost (En)	Control seawater intrusion (%)	Control flood (%)
2010	14, 664, 533	33 %	67 %
2011	12, 288, 753	16 %	84 %
2012	11, 822, 187	31 %	69 %

2.2 River discharge

River discharge is one of the important factors influencing the penetration of the seawater intrusion. A large number of researches indicated that the salinity or distance rapidly decreases in upstream direction with a larger river discharge. On the contrary, the decreasing of the river discharge can promote the intrusion of seawater (Ranganna 1975; Garvine et al. 1992; Hu et al. 2003; Tang and Mao 2004).

The river discharge was calculated by the recorded discharge data of every pumping station along the Shinkawa River. The variation trends of average daily discharge in 2011, 2012 and 2013 are shown in Fig. 2-4. Average discharges during irrigation season in 2011, 2012 and 2013 are 38 m^3/s, 32 m^3/s and 43 m^3/s, respectively. The irrigation season in this district starts from late April, and ends in early September. It can be found that the river discharge increases from about the end of April every year, and decreased from about the beginning of September in Fig.2-4. The river discharge varies with the demand of irrigation water and rainfall.

2.3 Tidal characteristics

The characteristics of tide near this estuary were analyzed using the tide data of Niigata West Port (the homepage of Japan Meteorological Agency) which is the closest monitoring position to the study estuary. The tide variation in Shinkawa River estuary during one tidal day, half lunar month and annual cycle is shown in Fig. 2-5. As shown in Fig. 2-5 (a), it is obviously that there are two tidal periods in one tidal day, occurring two uneven flood and ebb tides with different tidal amplitudes. The tide level also raises and falls with the relative position between the Moon, the Sun and the Earth. In Fig. 2-5 (b), it can be found that the tide level changed from high to low, then returned to high, within approximately half lunar month (from New Moon to Full Moon), or changed from low tide level to high tide level, then returned to low tide level (from the First Quarter to the Full Moon, thus to the Last Quarter). This conversion process from neap tide to spring tide illustrates that tide has a variation periodicity of half lunar month. Besides, the tide level has annual variation rules as well. It is lowest in April, reaches crest in August, and then returns to the lowest value next April as shown in Fig. 2-5 (c).

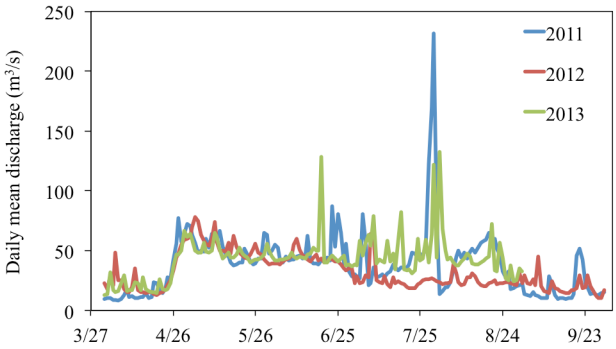

Fig. 2-4 The variation trends of daily average discharge during irrigation season

According to the characteristics of tide near this estuary analyzed above, the tide belongs to the mixed type. Because the frequency of semi-diurnal tide is higher than diurnal tide within one semi-month cycle near Shinkawa River estuary, the tide type is classed as irregular semi-diurnal tide. The largest tide levels during the irrigation periods in 2011, 2012 and 2013 are 0.44 m, 0.45 m and 0.44 m, respectively.

2.4 Summary

Because of this small river discharge and tidal range near Shinkawa River mouth, the type of seawater intrusion in this river are likely to be highly stratified, forming a saltwater wedge with a overlying freshwater layer and underlying saltwater layer.

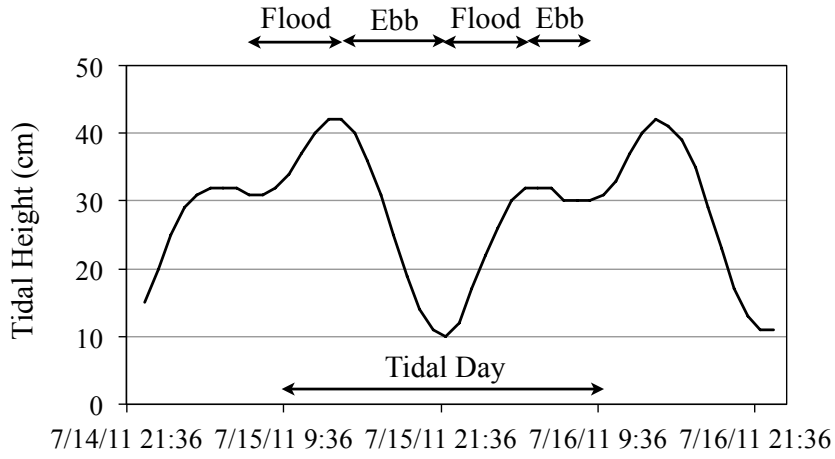

(a) Diurnal tidal stage fluctuation

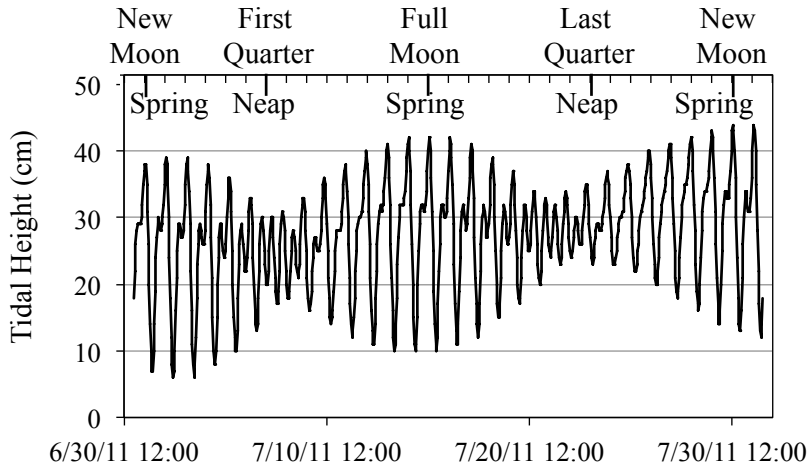

(b) Monthly tidal stage fluctuation

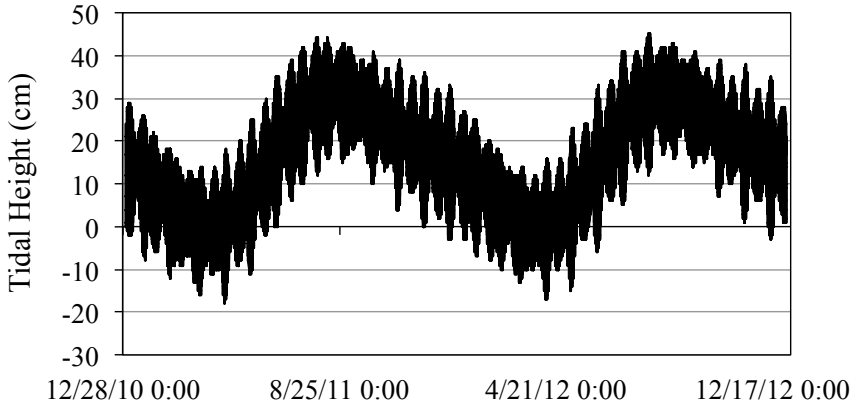

(c) Annual tidal stage fluctuation

Fig. 2-5 Tide characteristics in Shinkawa River estuary

3. Characteristics of seawater intrusion in Shinakwa River

One of the most important methods to reveal the rule of seawater intrusion is the prototype observation. A large amount of data obtained from in-situ experiments can illustrate the specific physical process. In this chapter, the long-term measurements of salinity in Shinkawa river estuary were implemented to survey the longitudinal profile, the vertical distribution of the seawater intrusion and the velocities of freshwater and saltwater.

3.1 Methods and materials

3.1.1 Survey design

Seawater intrusion is embodied by the vertical and horizontal variations of salinity in estuaries. Vertical measurement is focused on recognizing the salinity difference from water surface to the bottom of river, and longitudinal observation aims at ensuring the range of seawater intrusion. In this survey design, the measurement of longitudinal profiles and vertical distributions of the seawater intrusion in Shinkawa River were conducted under different conditions, such as flood tide and ebb tide, spring tide and neap tide, and different discharge since the tide and river discharge are two main factors that influence the movement of seawater into river.

The field surveys of seawater intrusion in Shinkawa River were conducted from May 2011 to September 2013 under different tide stages and different river discharges. The more specific survey dates and investigation contents are listed in Table 3-1. In addition, it is worth noting that the seawater intrusion will also be influenced by the operation of sluice gates near the river mouth. Seawater intrusion in Shinkawa River were observed under two special status as well, one of which was the process of draining seawater out the river by pumps at river mouth after the sluice gates were fully closed, and the other was that seawater started to intrude upstream after the sluice gates were fully opened.

During the survey period, an acoustic reflection profiling system (SC-3), electronic conductivity (EC) meters and current meters were applied to measure the items of characteristics of seawater intrusion. Among them, the SC-3 was only used within short period due to the various constraints. But EC meter was adopted as a long-term

observation instrument, complementing the disadvantage of SC-3.

Table 3-1 The specifications of the survey design of seawater intrusion

Condition	Survey period	Survey date	Survey equipment	Measure time
Tide	Flood, Ebb tide	May 26-28, 2013	EC meters	High and low water
	Flood, Ebb tide	June 24-25, 2013		24 hours
	Spring tide	July 15, 2011	SC-3	Around high water
	Neap tide	Aug 23, 2011		Around low water
Discharge	Irrigation	Jul 2, 2011	EC meters	Around high water
	Non-irrigation	Sep 29, 2011		Around high water

3.1.2 Experimental apparatus

An acoustic reflection profiling system was used to survey the longitudinal profiles of seawater intrusion. The acoustic reflection profiling system was specially developed by Tokuoka et al. (2005) and Tateshi et al. (2006; 2007) to recognize the halocline in tidal rivers and coastal lagoons, while it was improved with a 200 kHz precision echo-sounder made by the Senbon Denki company (Co. Ltd., Shizuoka, Japan). It mainly consists of a recording unit, a digital recorder, a transducer, and a global positioning system (Fig. 3-1). This system determined the longitudinal and cross-sectional position of the halocline by directing and receiving ultrasonic waves to the river floor from the transmitter fixed on a boat. The ultrasonic waves were reflected because of the density difference at the interface between freshwater and saltwater, and at the surface of the riverbed between saltwater and mud. The reflected ultrasonic was converted to digital signals and recorded by a digital data logger and thermal paper. The net depths of the halocline and riverbed were determined based on the sonic velocity and the time differences between the transmitted and reflected signals. Its operation principle can be illustrated in Fig. 3-2, and basic specifications of this measurement system are shown in Table 3-2.

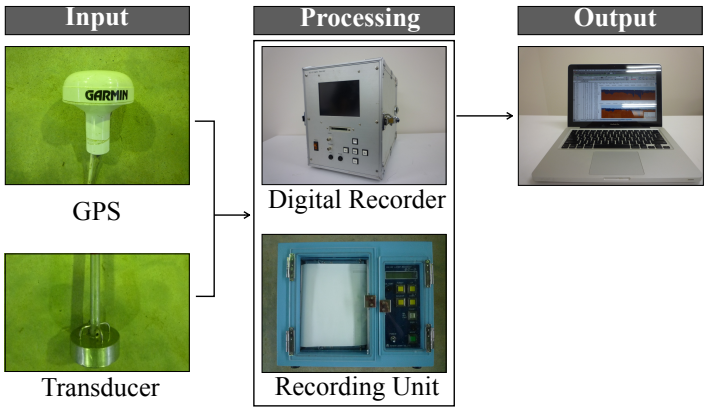

Fig. 3-1 Acoustic reflection profiling system

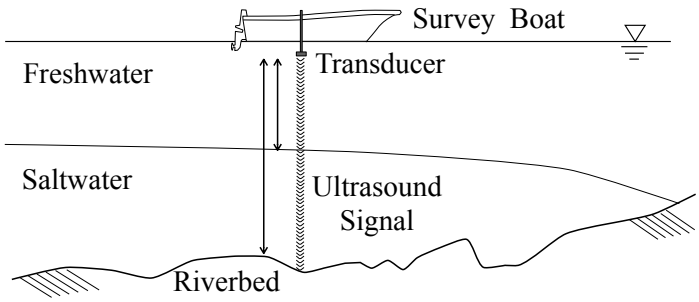

Fig. 3-2 The operation principle of SC-3

Table 3-2 Basic specification of SC-3

Transducer	Frequency	200 KHz
	Beam angle	6 degree
Power supply	Internal	NI-Cd battery
	External	DC 12 V, 0.6 A

Along with profiling halocline by using SC-3, vertical profiling of salinity was also carried out by EC meters. Although, the EC meter was also used to observe the extent of seawater intrusion when the SC-3 could not be applied. In this measurement, the EC meters of CM-21P type made by DKK-TOA Corporation, Tokyo, Japan, was adopted as shown in Fig. 3-3 (a). This instrument indirectly measures salinity of river water converted from the electrical conductivity of river water that can be measured by

determining the resistance of the river water between two cylindrical electrodes separated in a fixed distance. The vertical profiling of salinity in this river was conducted at 10 cm intervals from the water surface to the riverbed at bridges crossing the Shinkawa River. The length of sensor cable of the common laboratory conductivity meter could not meet the entire height from bridge deck to riverbed, so a 30 m sensor cable was used to satisfy the measurement distance. Another notable problem was that the sensor of EC meter could not straightly sink to the bottom of the river as a result of its insufficient weight, so one cylindrical metal case matching with the sensor was connected to the sensor cable to guarantee enough weight to let the sensor can straightly reach the riverbed. Besides, in order to read the depth of water more easily and quickly, the marks with interval of 50 cm were attached to the sensor cable, and the ameliorated EC meter is as shown in Fig. 3-3 (b). The detailed operation method of the EC meter is shown in Fig. 3-4, and the more specific information of observation positions, such as the distance of every bridge form the sluice gates, are shown in Fig. 3-5 and Table 3-3.

The velocities and flow directions of freshwater and saltwater were measured using electromagnetic current meters simultaneously. The current meter mainly includes two types. One is the INFINITY-EM type made by JFE Advantech Co. Ltd, Hyogo, Japan, as in Fig. 3-6 (a). It features fast transmission of data, great memory capacity, camera lithium battery (CR-V3) and user-friendly software interface, while its specific parameters are shown in Table 3-4. The other is the COMPACT-EM type made by ALEC Electronics Co. Ltd, Hyogo, Japan, as in Fig. 3-6 (b). It is featured by high resolution, small size, lightweight and great memory capacity, flash memory, calibration coefficient and friendly windows program, with detailed parameters shown in Table 3-5. Both of them can automatically record the velocity and flow direction after the time interval and measurement period are set. Their positions in freshwater and saltwater layers depend on the depths of river water and halocline at the survey time. The detailed method is that the depths of the density interface and river water should be measured first, and then the positions of two current meters are determined according to the measured results on that day and historic data, while the scheme of setting method is shown in Fig. 3-7. In this study, all acquisition intervals were fixed of 10 min, and the amount of samples was 30 for each data acquisition, while each sample was recorded every second. Two EC meters of INFINITY-EM type were set up under bridge 1 (in Fig.

3-5) to record the velocities of freshwater and saltwater, and one EC meter of COMPACT-EM type was located under bridge 6 (in Fig. 3-5) to measure the velocity of saltwater only.

(a) Common laboratory EC meter

(b) The improved EC meter improved

Fig. 3-3 Electronic conductivity meter

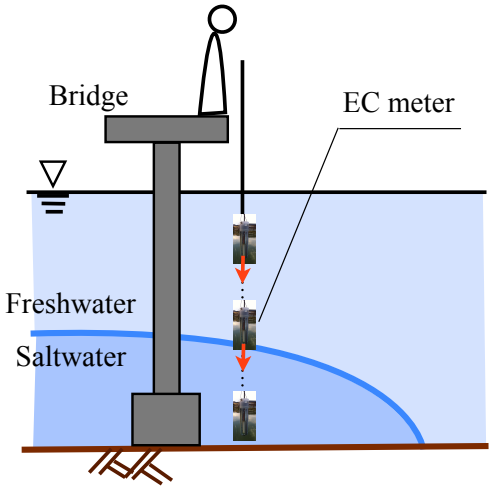

Fig. 3-4 Measurement method of EC meter

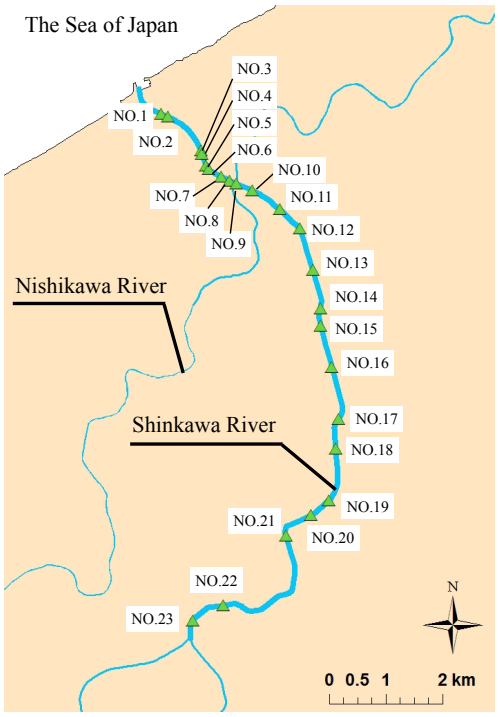

Fig. 3-5 The observation positions by EC meter

Table 3-3 The information of observation positions

Order	Bridge name	Distance from sluice gates (km)	Order	Bridge name	Distance from sluice gates (km)
1	Nagisa	0.26	13	Kasagi	4.33
2	Kourai	0.39	14	Tagatao	5.04
3	Gakkoyama	1.25	15	Tagata	5.36
4	Migatsuki	1.32	16	Doujigahara	6.12
5	Tsukimi	1.53	17	Shinkawa	7.07
6	Sakiyama	1.62	18	Hanami	7.62
7	Oohagi	1.87	19	Boubouoo	8.58
8	Nourinsyo	2.04	20	Boubou	8.99
9	Nishiikawasuiro	2.16	21	Hayadoori	9.64
10	Takayama	2.48	22	Yoroiko	12.0
11	Takanaka	3.07	23	Benten	12.6
12	Nakashin	3.56			

(a) INFINITY-EM type

(b) COMPACT-EM type

Fig. 3-6 Electromagnetic current meter

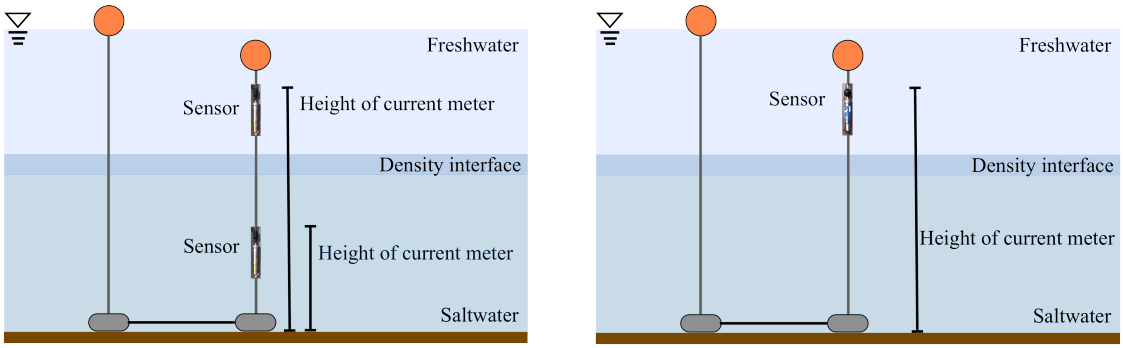

(a) INFINITY-EM type (b) COMPACT-EM type

Fig. 3-7 The setting method of current meter

Table 3-4 The specifications of the EC meter of INFINITY-EM type

Items	Velocity	Direction	Water Temperature
Measuring range	0 - ± 500 cm/s	0 – 360 °	−5～45 ℃
Accuracy	± 1 cm/sec (± 2 %)	± 2 °	± 0.02 ℃
Current consumption	90 mA		
Memory capacity	8, 500, 000 Data		
Power supply	Lithium (3.3 Ah)		
Burst interval	1 – 999 min		
Case material	Titanium		
Pressure-resistant	1000 m		
Weight	1kg (In air), 0.6 kg (In water)		

Table 3-5 The specifications of the EC meter of COMPACT-EM type

Items	Velocity	Direction	Water Temperature
Measuring range	0 - ± 500 cm/s	0 - 360°	−5～40 °C
Accuracy	±1cm/s (± 2 %)	± 2°	± 0.02 °C
Current consumption	110 mA		
Memory capacity	17, 9178 Data		
Measuring mode	Continuous Mode, Burst Mode		
Power supply	Lithium (7 Ah)		
Measuring interval	0.5, 1, 2 s		
Burst interval	1 – 999 min		
Samples	1, 10, 15, 20, 30, 60, 120, 180, 240, 300, 600, 1,200		
Case material	Titanium		
Pressure-resistant	1000 m		
Weight	870 g (In air), 0.6 Kg (In water)		

3.2 Survey results

3.2.1 The variation of seawater intrusion under different tide stage

3.2.1.1 The variation of seawater intrusion during flood tide and ebb tide

The daily variations of seawater intrusion were observed twice by discontinuous and continuous salinity measurements of river water using EC meters. For discontinuous observation, the salinity was only observed around 1 hour before and after low water and high water during 22:10 May 26, 2013 and 0:35 May 28, 2013. For continuous observation, the salinity measurement was conducted from 21:40 June 24, 2013 to 23:30 June 25, 2013. The specific tide conditions of survey days are listed in Table 3-6.

Discontinuous measurement

On the discontinuous survey day, the average river discharge during the survey period was 43 m^3/s, and the tide level difference between lower low water and higher high water was 37 cm.

(1) Vertical distribution

The vertical distributions of salinity at the position of 0.39 km from the sluice gates are shown in Fig. 3-8. It can be found that there were two layer water bodies from surface to riverbed, freshwater layer and saltwater layer, with a transition zone between them. This transition zone was defined as density interface between saltwater and freshwater, and was featured by the EC value of 20,000 μs/cm. The salinity changed abruptly when EC meter passed from freshwater layer to saltwater layers revealing an average halocline of 0.25 m, which suggests the existence of a fairly stable saltwater wedge in Shinkawa River. Moreover, the vertical distribution of salinity changed with the tide. The thickness of saltwater layer (under the transition zone) increased all the time from lower low water to higher high water, and then decreased from higher high water to next lower low water. After one tidal day, the thickness of saltwater layer was similar with that at first lower low water, and this variation trend of density interface with the change of tide level is shown in Fig. 3-8 (f). Taking the position of 0.39 km from the sluice gates for an example, the elevation of the density interface was -3.08 m at lower low water, but increased to -1.56 m at higher high water. From higher high water to next lower low water, the elevation decreased to -3.03 m, being similar to that at first lower low water. The whole variation processes of the density interface are shown in Fig. 3-8 during one tidal day. For other measurement positions, the variation tendencies of density interface were all similar within this river.

Table 3-6 Tide information on continuous and discontinuous survey days

	Higher low water	Lower high water	Higher low water	Higher high water	Lower low water	Lower high water
Date (2013)	05.26 14:12	05.26 22:20	05.27 05:25	05.27 09:07	05.27 15:03	05.27 23:13
Tide level	29 cm	-7 cm	21 cm	17 cm	30 cm	-7 cm
Date (2013)	06.24 14:02	06.24 22:12	06.25 05:11	06.25 08:52	06.25 14:58	06.25 23:04
Tide level	39 cm	1 cm	29 cm	24 cm	39 cm	2 cm

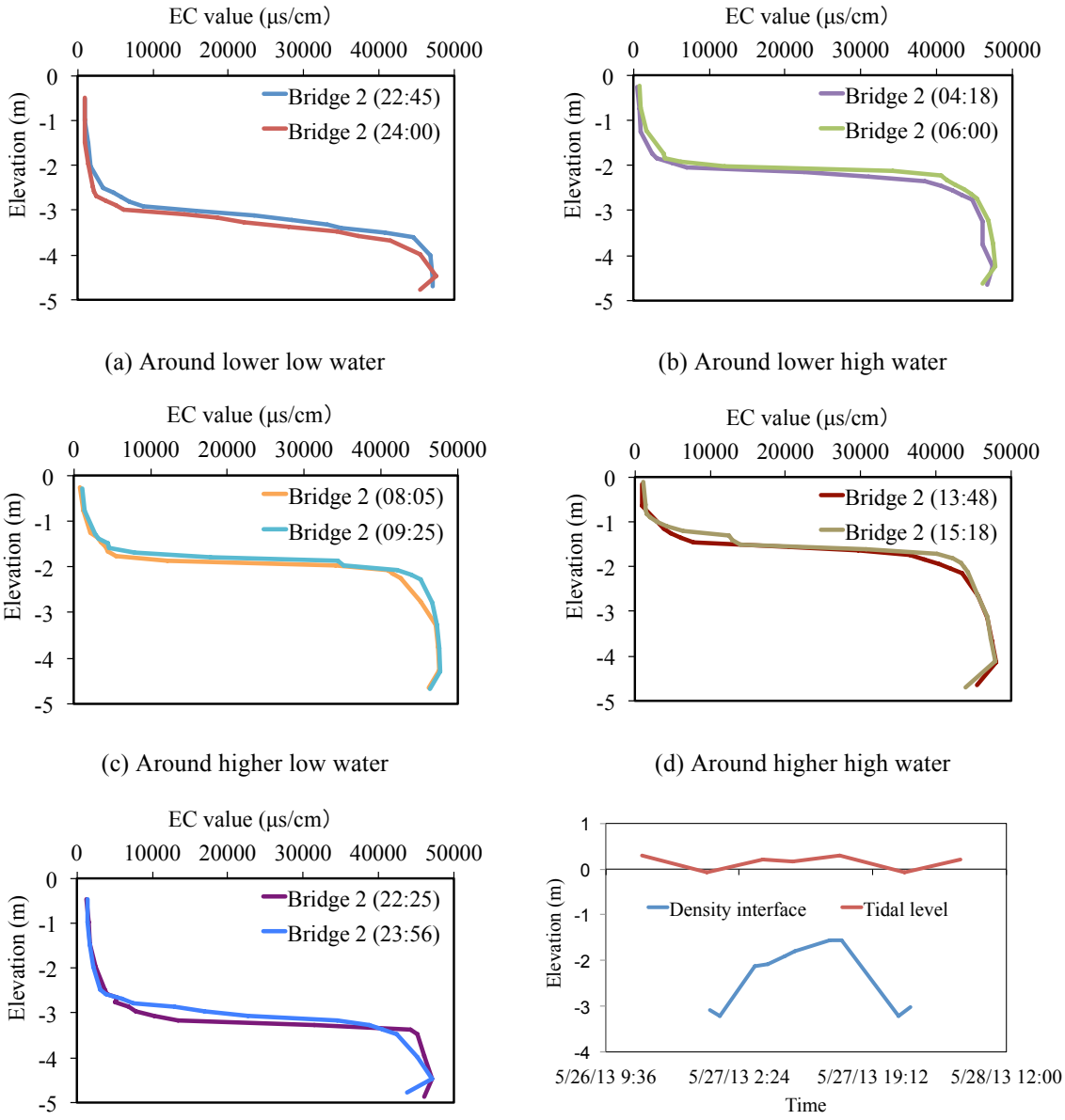

(a) Around lower low water

(b) Around lower high water

(c) Around higher low water

(d) Around higher high water

(e) Around next lower high water

(f) Density interface at bridge 2 and tide level

Fig. 3-8 The vertical distribution of salinity on the survey day of discontinuous measurement at the position of 0.39 km from the sluice gates

(2) Longitudinal distribution

Along with the vertical variation, the longitudinal changes were also observed, and its results are shown in Fig. 3-9. Around lower low water, the length of saltwater wedge was only 1.53 km as shown in Fig. 3-9 (b), and then it continuously moved upward, elongated to about 2.04 km around lower high water in Fig. 3-9 (c). The saltwater wedge didn't move downward during first ebb tide with a tide range of 4 cm, but

extended to 2.16 km around higher low water as shown in Fig. 3-9 (d), illustrating that seawater intrusion doesn't change its flow direction during the ebb tide with a smaller tide range in this river. With the following flood tide, seawater still intruded landward, and the front of saltwater wedge reached to 2.48 km around higher high water as in Fig. 3-9 (e). After this, tide transferred into ebb tide with larger tide range of 37 cm, and the range of saltwater wedge returned to that during the last lower low water as shown in Fig. 3-8 (f).

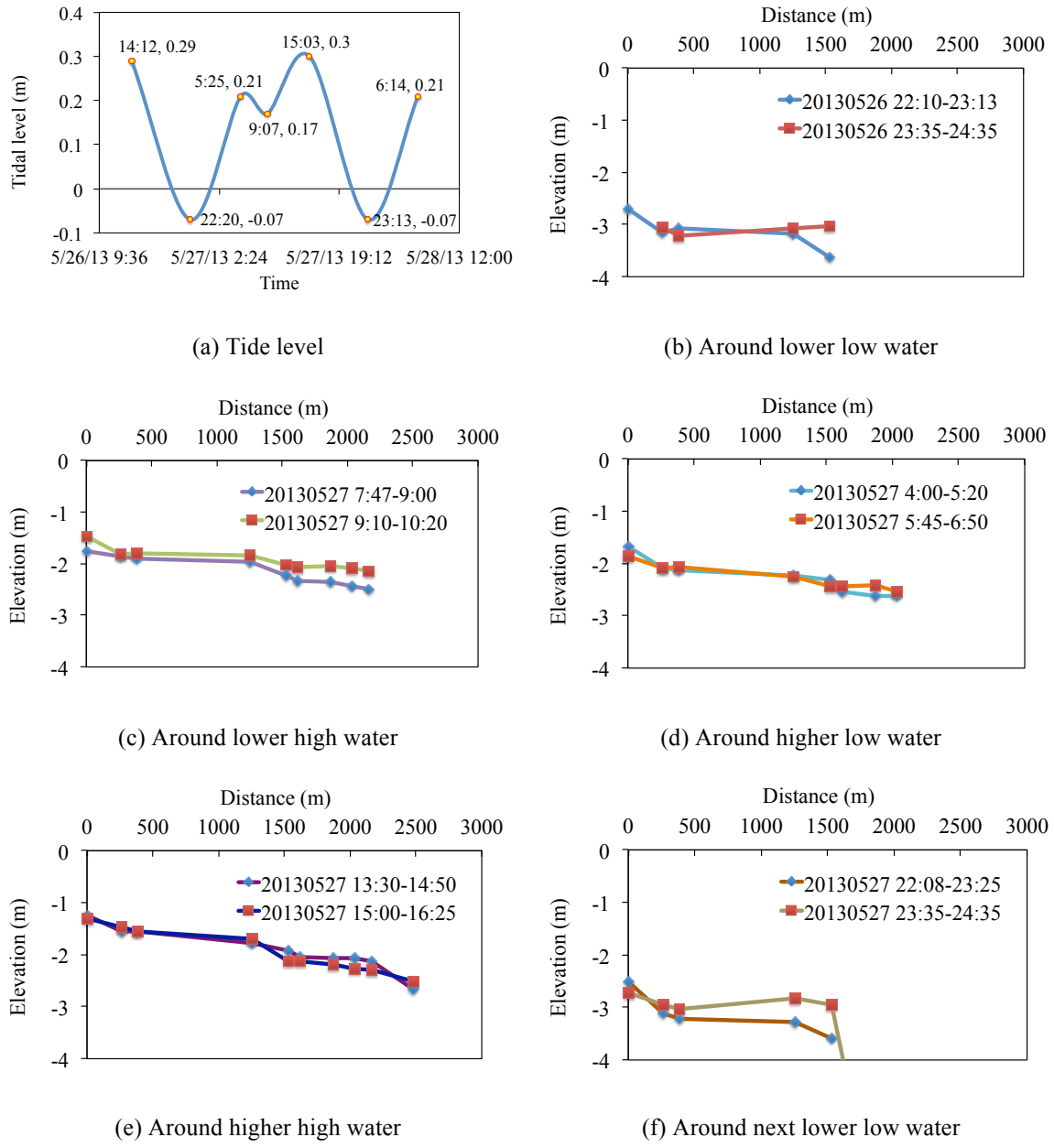

(a) Tide level

(b) Around lower low water

(c) Around lower high water

(d) Around higher low water

(e) Around higher high water

(f) Around next lower low water

Fig. 3-9 The longitudinal variation of seawater intrusion on the days of discontinuous measurement

According to the observation of salinity during one tidal day, the type of seawater intrusion in Shinkawa River estuary is classified to well stratified type with the shape of wedge and an obvious transition zone. The height variation of density interface at a certain position approximately declined from sluice gates to the front of saltwater wedge in one tidal day, and the moving range of saltwater wedge was about from 1.53 km to 2.48 km from the sluice gates, implicating that movement amplitude of the front of saltwater wedge was around 0.95 km under this condition.

Continuous measurement

For continuous survey in one tidal day, the average river discharge during the survey period was 37 m^3/s, and the tide level difference between lower low water and higher high water was 38 cm.

(1) Vertical distribution of salinity

The measurement results at one of the positions which is 0.39 km from the sluice gates are shown in Fig. 3-10. In the continuous measurement the stratified water bodies were observed once more, with an average halocline of 0.25 m, suggesting again that seawater intruded in the form of saltwater wedge in this estuary. Moreover, the vertical distribution of salinity also changed with the tide. The elevation of density interface increased all the time from lower low water to higher high water, and then decreased from higher high water to next lower low water. This variation trend of density interface with the change of tide level is shown in Fig. 3-10 (b). The whole variation processes of the density interface are shown in Fig. 3-10 during one tidal day. For the other measurement positions, the variation tendencies of density interface were similar under these conditions and can be read from Fig. 3-11.

(2) Longitudinal distribution of salinity

As well as the vertical variation of salinity, the longitudinal changes of salinity were also observed, and results are shown in Fig. 3-11. During first flood tide with tide range of 28 cm, the front of saltwater wedge moved from 1.62 km to 2.16 km from the sluice gates as shown in Fig. 3-11 (b) and (c). It didn't move downward during the first ebb tide with tide range of 5 cm, but moved upward continuously, extended to about 2.48 km around higher low water as shown in Fig. 3-11 (d), illustrating that seawater didn't

change its flow direction during the shorter ebb tide in this river. After this, the second flood tide with tide range of 15 cm started, and the range of saltwater wedge reached to about 3.07 km around higher high water as in Fig. 3-11 (e). When the tide converted into the second ebb tide with tide range of 37 cm, the intruded seawater didn't immediately change flow direction, but kept the constant distance of 3.07 km for about 2 hours. And then it started to move seaward until the next flood tide, shown in Fig. 3-11 (f) and (g). With the alternative changing between flood tide and ebb tide, the whole length of saltwater wedge also had similar variation trend during one tidal day.

The continuous observation of salinity in one tidal day once again confirmed that the classification of seawater intrusion in Shinkawa River estuary is well stratified type. The same as the results above, the change amplitude of density interface at one position approximately declined from sluice gates to the front of saltwater wedge in one tidal day, and the moving range of saltwater wedge's front was about from 1.62 km to 3.07 km from the sluice gates.

3.2.1.2 The variation of seawater intrusion on spring tide day and neap tide day

The variations of saltwater wedge on spring tide day and neap tide day were observed on July 15 and August 23, 2011. The specific information of tide is listed in the Table 3-7. In these two survey days, SC-3 was applied to measure the longitudinal distribution of salinity of river water around higher high water of spring tide and lower low water of neap tide.

On spring tide day, the average river discharge supplied from upstream during the observation period (10:00–13:00) was 18.9 m^3/s, and the average river discharge near the river mouth sluice gates during the observation period was 38.7 m^3/s. Under this condition, the longitudinal profile of the saltwater wedge is shown in Fig. 3-12 (a). The length of the saltwater wedge extended to about 4.7 km from the river mouth sluice gates around the higher high water. On neap tide day, the average river discharge from upstream during the observation period (15:00–16:00) was 10.3 m^3/s, and discharge near the sluice gates was 35.4 m^3/s. under this condition, the longitudinal profile of the saltwater wedge is shown in Fig. 3-12 (b). The extent of saltwater wedge was about 2.2 km from the sluice gates around the lower low water. Compared with the spring tide condition, the saltwater wedge was approximately 2.5 km shorter and 0.80 m thinner.

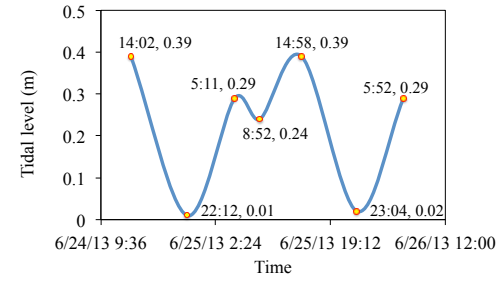

(a) Tide level

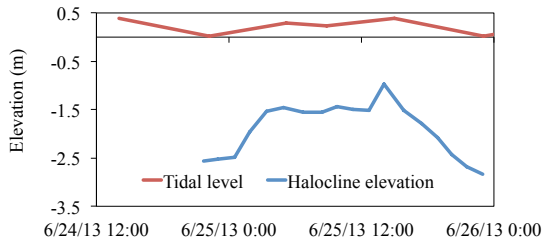

(b) Variation trend of density interface

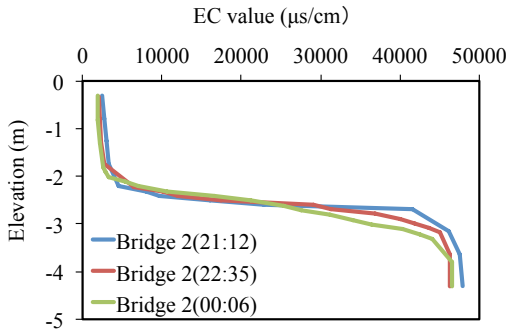

(c) First flood tide

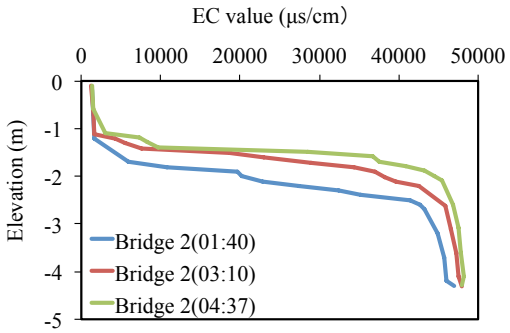

(d) First flood tide

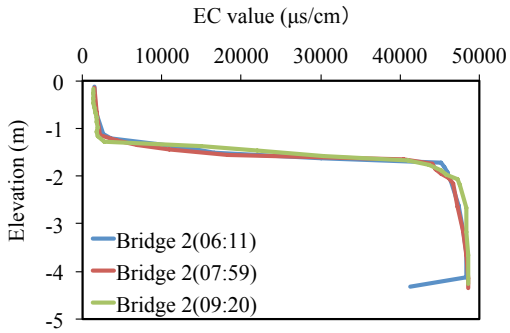

(e) First ebb tide

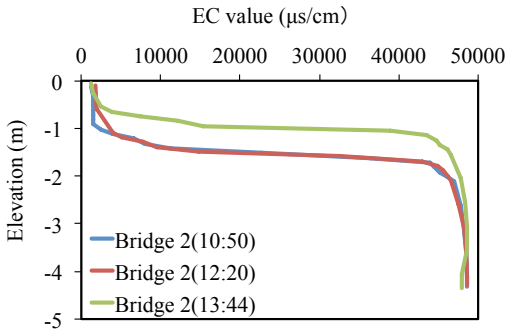

(f) Second flood tide

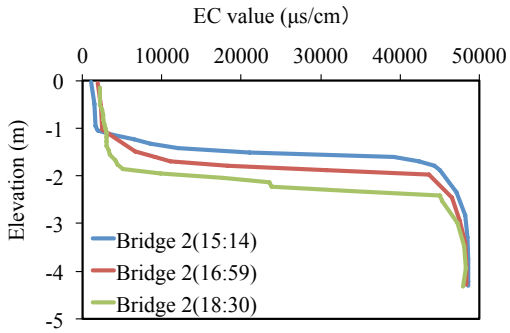

(g) Second ebb tide

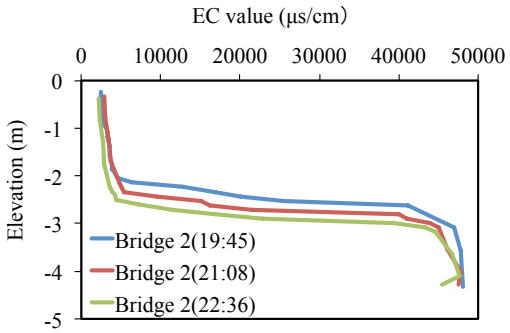

(h) Second ebb tide

Fig. 3-10 The vertical distribution of salinity at the position of 0.39 km from the sluice gates

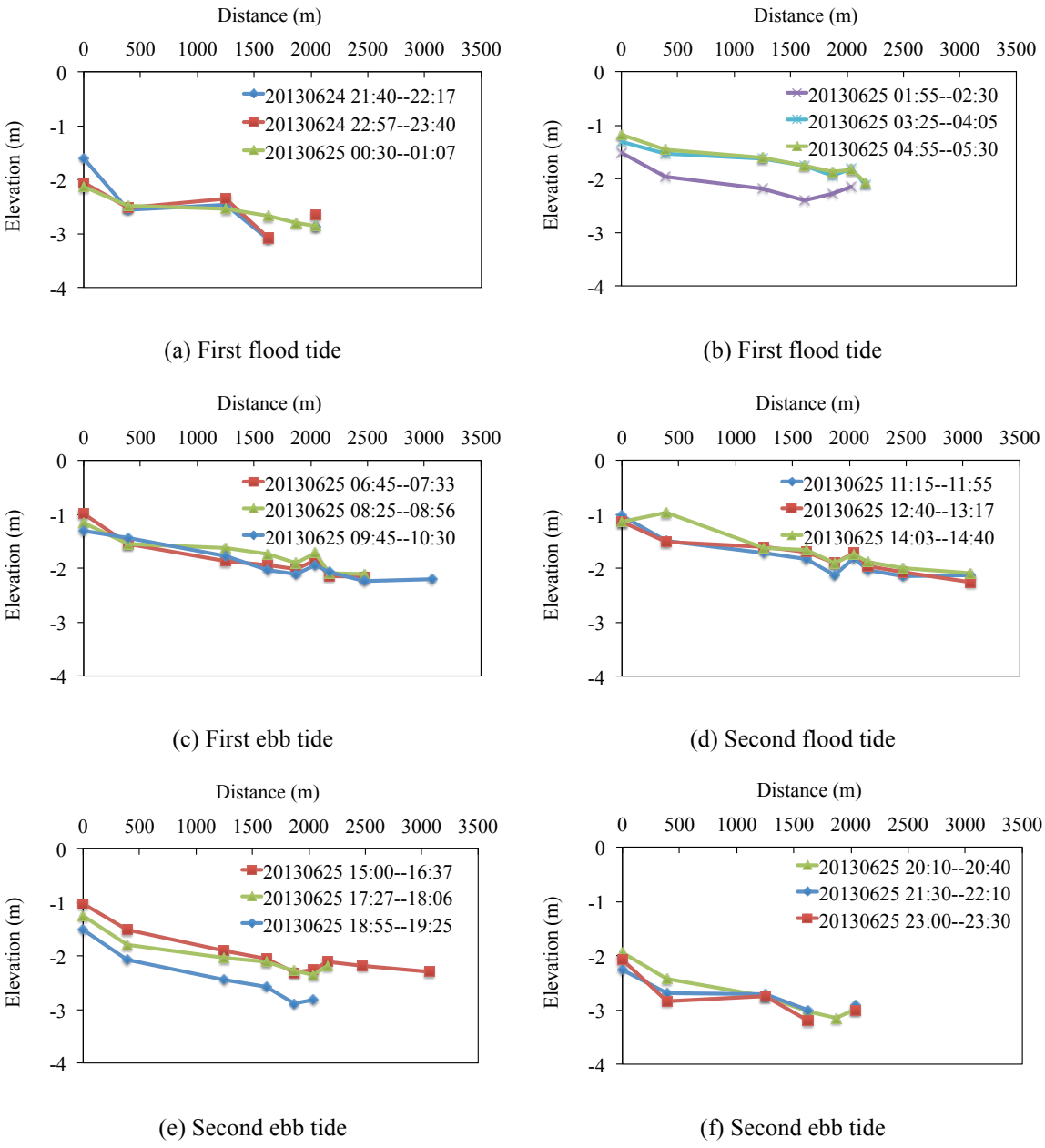

Fig. 3-11 The longitudinal variation of seawater intrusion on the survey day of continuous measurement

Table 3-7 Tide information on spring tide day and neap tide day

Date	Lower high water	Higher low water	Higher high water	Lower low water
Jul 15, 2011	04:22	07:20	13:32	21:46
Tide level (cm)	33	31	42	10
Aug 23, 2011	07:29			16:26
Tide level (cm)	41			24

3.2.2 The variation of seawater intrusion under different discharge

In this research area, the river discharge changes with the irrigation season and non-irrigation season, resulting in the season variation of saltwater wedge intrusion in Shinkawa River. This variation investigation was conducted on July 2, 2011 (spring tide day), irrigation season, and September 29, 2011 (spring tide day), non-irrigation season. More specific information of tide is listed in the Table 3-8. In these two surveys, EC meters were adopted to recognize the density interface and extent of saltwater wedge.

On Jul 2, 2011, the survey day of irrigation season, the average discharge of Shinkawa River was 30 m^3/s. The range of saltwater wedge is shown in Fig. 3-13 (a). The extent of saltwater wedge was about 5.04 km around higher high water. For non-irrigation season, the saltwater wedge was also observed under the condition of spring tide. The upstream average discharge of Shinkawa River was 5.6 m^3/s on September 29, 2011. Under this condition, the range of saltwater wedge is shown in Fig. 3-13 (b) around the higher high water. The extent of saltwater wedge was about 12.0 km, almost occurring in entire Shinkawa River during non-irrigation season.

During irrigation season, the movement range of saltwater wedge was approximately between 1.5 km and 6.0 km according to all observations. The range of saltwater wedge in non-irrigation season is longer than that in irrigation season, appearing the entire river, due to the less freshwater discharge.

3.2.3 Particular variation of the seawater intrusion

The sluice gates, an the important flood control facility in the Shinkawa River mouth, are often operated to not only drain more river water but also block the seawater, which disrupts regular rules of the saltwater wedge during irrigation season. In this case, two surveys were implemented. One is that the seawater's landward movement was observed when the saltwater drainage was finished and sluice gates were fully opened. The other is that the saltwater movement was observed seaward when the sluice gates were fully closed and the drainage pumps ran to drain saltwater. The tide conditions on two survey days are listed in Table 3-9.

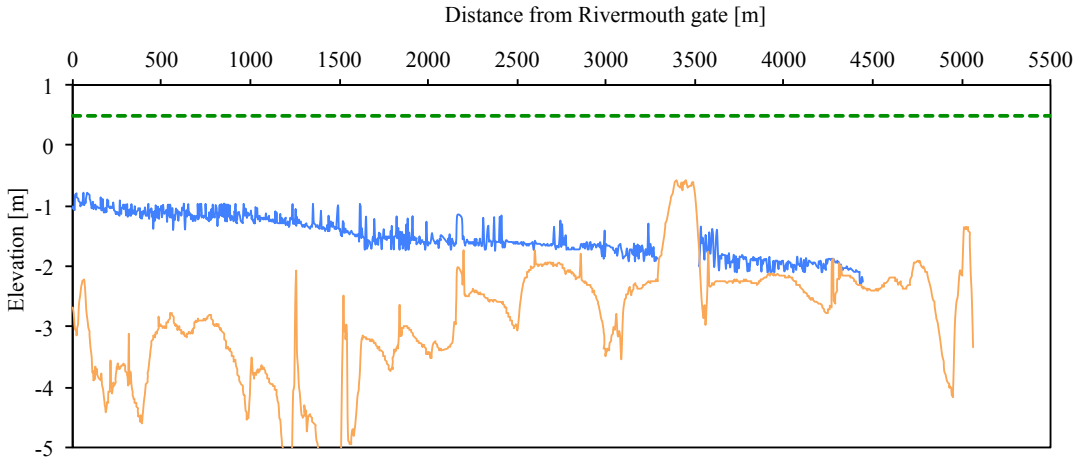

(a) On spring tide day

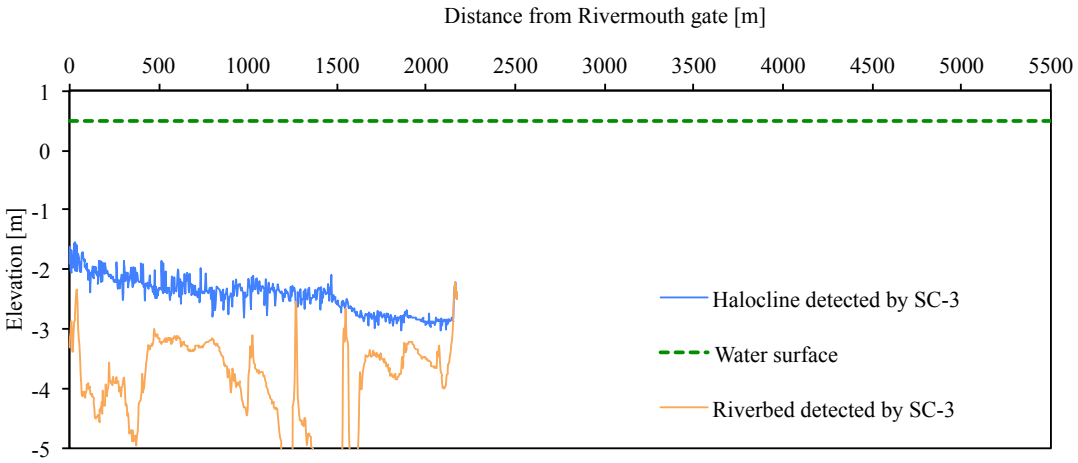

(b) On neap tide day

Fig. 3-12 The saltwater wedge under different tides

Table 3-8 Tide information on the survey days with different river discharge

Date	Lower high water	Higher low water	Higher high water	Lower low water
Jul 2, 2011	05:00	07:51	14:01	22:13
Tide level (cm)	30	28	39	6
Sep 29, 2011	02:45	09:48	16:28	22:10
Tide level (cm)	36	11	38	24

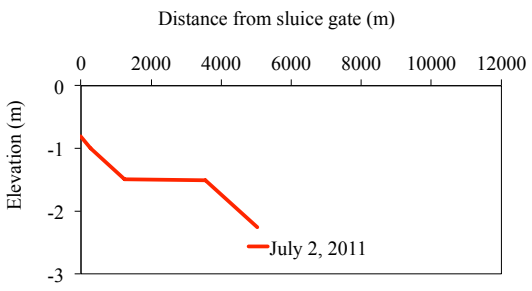

(a) Relatively large discharge (Irrigation season)

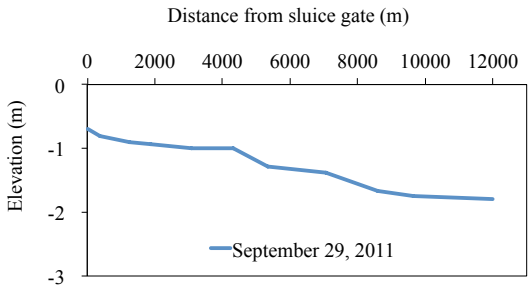

(b) Relatively small discharge (Non-irrigation season)

Fig. 3-13 The variation of saltwater wedge under different river discharge

Intrusion process of saltwater wedge

The intrusion process was conducted from 0:00 to 23:27 on September 1, 2012, and its results are shown in Fig. 3-14. The average river discharge draining into the sea was 29.5 m^3/s during the observation period on Sep 1, 2012. Fig. 3-14 (a) shows the intrusion processes within about 4.5 hours after the sluice gates had been opened, while the distance of saltwater wedge reached 1.25 km from the sluice gates. The saltwater wedge continued to intrude toward upstream, even during ebb tide, and its distance reached 2.04 km from the sluice gates as shown in Fig. 3-14 (b). Within the next flood tide (8:49 to 14:48), the distance of saltwater wedge reached most upstream, 3.56 km from the sluice gates as shown in Fig. 3-14 (c), and the elevation of whole density interface gradually increased from the beginning of measurement to the higher high water. The distance of saltwater wedge didn't immediately decline after it reached the most upstream, keeping constant, but the elevation of density surface gradually decreased during the second ebb tide (14:28 to 21:58) as shown in Fig. 3-14 (d).

Table 3-9 Tide information on the operation days of sluice gates

Date	Lower high water	Higher low water	Higher high water	Lower low water
Sep 1, 2012	03:26	08:49	14:48	21:58
Tide level (cm)	34	24	41	19
Sep 6, 2012	05:06	12:34	19:10	22:50
Tide level (cm)	38	22	34	31

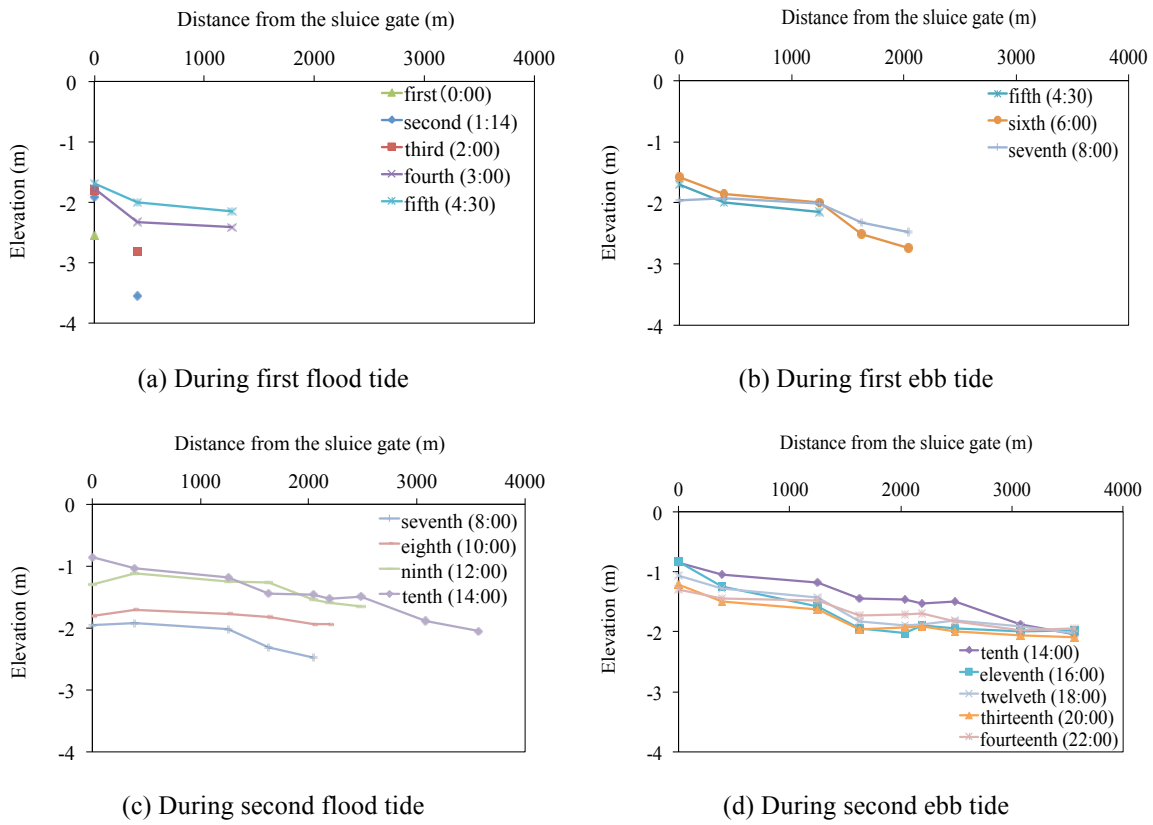

Fig. 3-14 The process of seawater intrusion after the sluice gates was opened

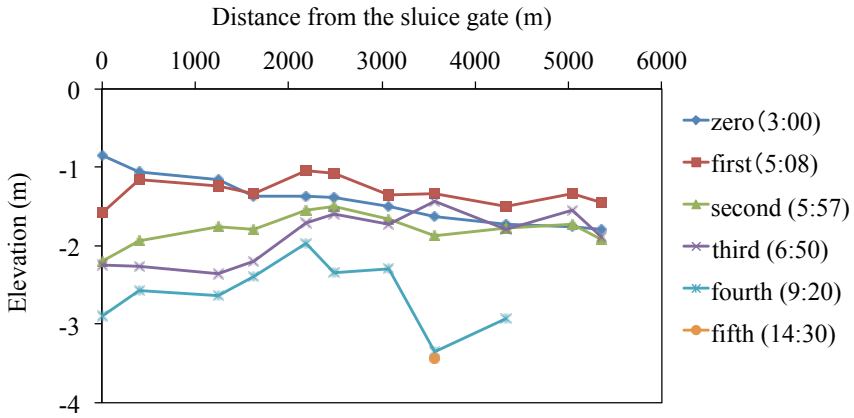

Fig. 3-15 The variation of saltwater wedge after the sluice gates was closed

Drainage process

The drainage process was carried out from 3:00 to 15:01 on September 6, 2012, and its net results are shown in Fig. 3-15. After the sluice gates were fully closed, the density interface between saltwater and freshwater near the sluice gates became lower and lower, then disappeared with the operation of Shinkawa River Mouth drainage pumping station. The variation trends of the density interface at other positions had similar rule. It passed about 9 hours that the whole saltwater wedge, with a range of 5.36 km, disappeared in waterway since the sluice gates had been fully closed and the drainage pumps started to run.

3.2.4 Velocities and flow directions of freshwater and saltwater

The velocities and flow directions of freshwater and saltwater were measured using electromagnetic current meters from September 29 to October 1, 2011. The specific setups of current meters for sampling data are listed in Table 3-10.

Table 3-10 The instructions of velocity measurement

Date	Observation sites	Height off the riverbed	River depth (m)	The mounting time
Sep 29,30 and Oct 1, 2011	1.62 km from sluice gates	0.8 m (for saltwater) 2.6 m (for freshwater)	3.6 (2.0 m for saltwater layer)	8:00 Sep 29, 2011

Fig. 3-16 shows the velocities and directions of freshwater and saltwater observed from September 29 to October 1, 2011 (two tidal cycles). The velocity of freshwater shown in Fig. 3-16 (a) fluctuated between 0.5 cm/s and 43.7 cm/s with the tide level variation, with an average of 14.9 cm/s. And the velocity tended to become smaller during the flood tide period, and larger during the ebb tide period. The flow directions were mostly seaward. Variation of the velocity of underlying saltwater shown in Fig. 3-16 (b) was between 0.1 cm/s and 28.2 cm/s, with an average of 5.7 cm/s. The flow direction of the saltwater layer was more sensitive to the tidal movement than that of freshwater. During the observation period, 43.6 % of the flow was seaward and 51.8 % was landward.

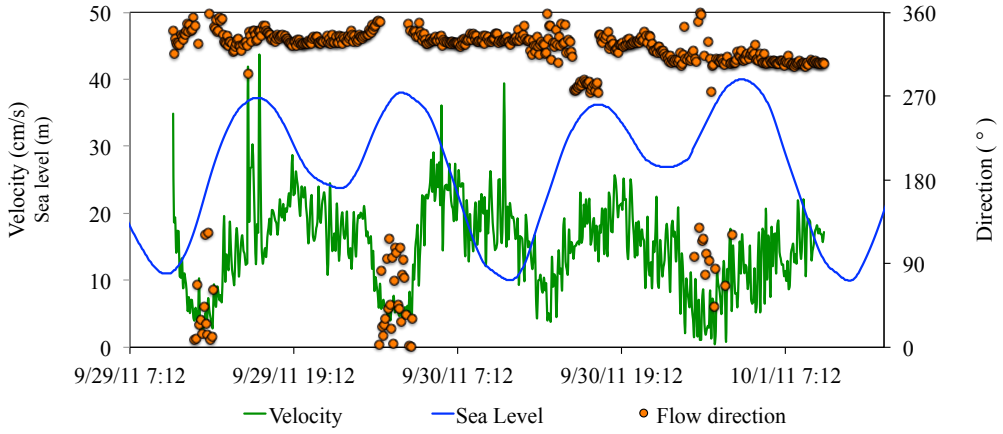

(a) Freshwater

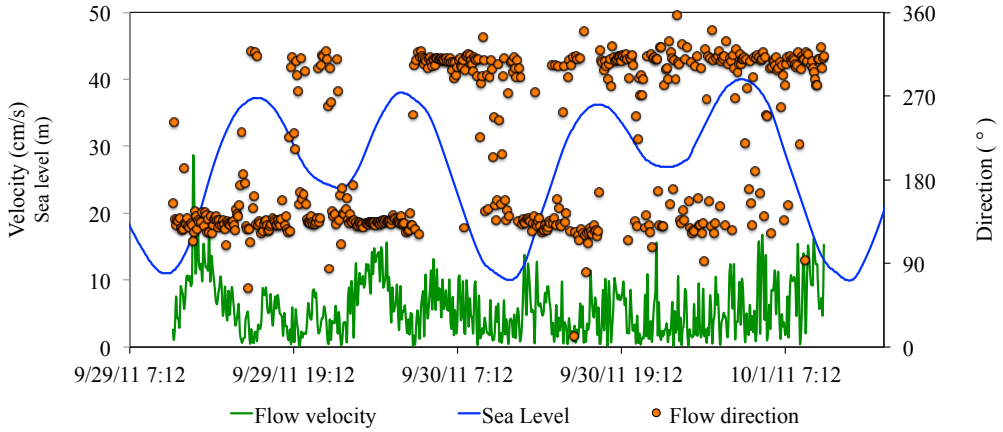

(b) Saltwater

Fig. 3-16 The velocities and directions of freshwater and saltwater from Sep 29 and Oct 1, 2011

3.3 Discussions

The characteristics of the seawater intrusion in Shinkawa River showed similar with the tide variation, and responded to the different discharge. During irrigation season, the river discharge is relatively constant, and the seawater moves into and out of the river with flood tide and ebb tide during one tidal day. Although there are twice uneven floods and ebbs during one tidal day near Shinkawa River estuary, the tide range between lower high water and higher low water is so small (see chapter 2) that it cannot cause the change of intrusion direction of seawater in this estuary. Thus the longitudinal and vertical variation of seawater intrusion increased from lower low water to higher

high water (flood tide) and decreased from higher high water to next lower low water (next ebb tide). And the continuous observations of seawater intrusion in one tidal day confirmed the feature of seawater intrusion in Shinkawa River once more. For the half month variation, the front of seawater intrusion will experience from the most upstream to the most downstream on spring tide and neap tide. What's more, the seasonal variation of seawater intrusion is mainly caused by the river discharge. Within a special period, for instance irrigation season or non-irrigation season, a relatively constant discharge results a smaller variation of intrusion range than that between different seasons. That is to say, during irrigation season, a relatively stable but large discharge causes a relatively stable but small seawater intrusion, which is much smaller than that of non-irrigation season when the discharge is much smaller. However, without a discharge influence, the extent of seawater intrusion yields to the force of tide, and gradually increases during the irrigation season in one year, because the tide level at higher high water near Shinkawa River estuary gradually increases from April to September.

Table 3-11 The positions of intake pumping stations from the sluice gates

Order	Intake pumping station	Distance from sluice gates (km)
1	Shinsensuirokyo	2.20
2	Shindorimakio	2.24
3	Nakasai	3.21
4	Chikusenbou	3.59
5	Shinsenkaryu	4.38
6	Masugatahokyu	7.64
7	Nishikawahokyusonei	10.06

Based on the extent of seawater intrusion investigated above, and the information of intake pumping stations (see Table 3-11), there are at least five intake pumping stations (the first five in Table 3-11) having the possibility of being influenced by the saltwater wedge during different conditions of discharge and stage of tide, threatening the paddy fields they irrigate. The first two intake pumping stations are more seriously threatened

than the others for they are almost always surrounded by the saltwater wedge in July and August of every irrigation season. Other pumping stations are only within the range of saltwater wedge in the period of demand peak of irrigation water and relatively high tide level, such as flood tides and spring tides in July and August of every irrigation season, but not on neap tide and ebb tides.

3.4 Summary

Based on the salinity observations of the Shinkawa River estuary for three years, the seawater intrusion was determined as the well stratification type, and the intrusion rules were summarized as follow:

(1) The saltwater wedge moves in and out of Shinkawa River estuary with the tide. The movement of saltwater wedge has one tidal day periodicity. From lower low water to higher high water, the saltwater wedge propagates landward. From higher high water to next lower low water, it moves seaward. The movement of saltwater wedge has also half lunar month periodicity. The front of saltwater wedge can reach the most upstream on spring tide day, then recede to the most downstream on neap tide day, and then return to similar position on next spring tide day.

(2) The saltwater wedge moves in and out of Shinkawa River estuary with the river discharge. During every irrigation season, the saltwater wedge intrudes with the longest extent in July or August owing to the highest tide level and relatively less freshwater discharge. During non-irrigation season, the saltwater wedge appears in the entire Shinkawa River due to smaller river discharge.

(3) The elevation of density interface also varies with the tide. The elevation of density interface increases during the flood tide (from lower low water to higher high water), and decreases during the ebb tide (from higher high water to lower low water) on every tidal day.

(4) Both velocities of freshwater and saltwater are influenced by the tide. The velocity of freshwater reaches the peak around lower low water during every tide, and lowers to the minimum around higher high water. The freshwater flows seaward all the time. The saltwater moves landward during flood tide, and flows downstream during ebb tide.

(5) During the irrigation season, the movement extent of saltwater wedge is about from 1.5 km to 6.0 km. Within this range, there are five intake pumping stations along Shinkawa River, which are easily threatened by the saltwater wedge during the irrigation season.

4. Evaluation the impact of seawater intrusion on irrigation water in Shinkawa River

Numerical simulation, with the characteristics of prediction and trails, can let the designers make an evaluation and decision on multi-schemes in the most economical and quickest way. The numerical simulation can not only reduce the workload of the in-situ experiment, but also achieve the target that the optimum design scheme can be determined under multi-constraints. In this chapter, the saltwater wedge in Shinkawa River will be reproduced by a one-dimensional, two layer unsteady flow model, and this model is further applied to evaluate the effect of seawater intrusion on irrigation water during irrigation season.

4.1 Modeling

4.1.1 Brief description of the model

In this study, the adopted numerical model is a one-dimensional, two-layer, unsteady flow model, originally developed by Suga (1977; 1979; 1981). The model consists of the following six equations:

$$\frac{\partial h_1}{\partial t}+\frac{1}{B}\frac{\partial Q_1}{\partial x}=E \tag{4-1}$$

$$\frac{\partial h_2}{\partial t}+\frac{1}{B}\frac{\partial Q_2}{\partial x}=-E \tag{4-2}$$

$$\frac{\partial}{\partial t}\left(\rho_1 h_1\right)+\frac{1}{B}\frac{\partial}{\partial x}\left(\rho_1 Q_1\right)=\rho_2 E \tag{4-3}$$

$$\frac{\partial \rho_2}{\partial t}+u_2\frac{\partial \rho_2}{\partial x}=D_x\frac{\partial^2 \rho_2}{\partial x^2} \tag{4-4}$$

$$\frac{1}{g}\frac{\partial u_1}{\partial t}+\frac{\partial h_1}{\partial x}+\frac{\partial h_2}{\partial x}+\frac{u_1}{g}\frac{\partial u_1}{\partial x}+i_{f1}-i_0=0 \tag{4-5}$$

$$\frac{1}{g}\frac{\partial u_2}{\partial t}+\frac{\partial}{\partial x}\left(1-\varepsilon\right)h_1+\frac{\partial h_2}{\partial x}+\frac{u_2}{g}\frac{\partial u_2}{\partial x}+i_{f2}-i_0=0 \tag{4-6}$$

, where subscripts 1 and 2 denote the freshwater and saltwater layers respectively, u is

the flow velocity, Q is the discharge, ρ is the cross-sectionally averaged density of each layer, B is the river width, E is the saltwater entrainment coefficient, i_f is the friction slope, i_0 is the riverbed slope, ε is the relative density difference, and D_x is the vertical diffusion coefficient. All the variables in these equations are shown in Fig. 4-1.

Equations (4-1) and (4-2) represent the volume conservation of the freshwater and the saltwater layer; equation (4-3) is a mass conservation of freshwater; equation (4-4) is a diffusion equation; and equations (4-5) and (4-6) are the motion equations of freshwater and saltwater, respectively.

All parameters are given as following:

(1) Relative density difference ε

$$\varepsilon = \frac{\rho_2 - \rho_1}{\rho_2} \tag{4-7}$$

(2) Saltwater entrainment coefficient E

$$E = 2 \times 10^{-3} F_1^3 |u_1 - u_2| \tag{4-8}$$

$$F = \frac{u}{\sqrt{\varepsilon g h}} \tag{4-9}$$

, while F is the internal Froude number

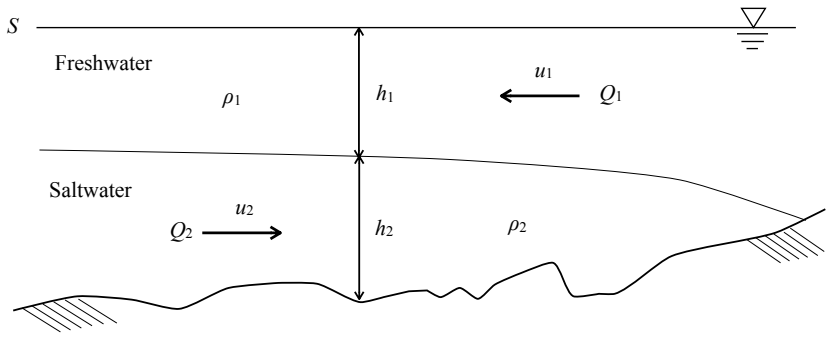

Fig. 4-1 Symbols in control equations

(3) Interfacial friction coefficient

$$i_{f1} = \frac{\tau_1}{\rho_1 g h_1} = \frac{f_i}{2gh_1}(u_1 - u_2)|u_1 - u_2| \tag{4-10}$$

$$i_{f2} = \frac{\tau_2 - \tau_1}{\rho_2 g h_2} = \frac{f_b}{gh_2} u_2 |u_2| - \frac{f_i}{2gh_2}(1-\varepsilon)(u_1 - u_2)|u_1 - u_2| \tag{4-11}$$

$$f_i = 0.35\Psi^{-0.5} + \frac{2E}{|u_1 - u_2|} \tag{4-12}$$

$$\Psi = R_e \cdot F_1^2 \tag{4-13}$$

$$R_e = \frac{|u_1| h_1}{\nu} \tag{4-14}$$

, while f_i is the interfacial friction coefficient, f_b (=0.01) is riverbed friction coefficient, and Re is the Reynolds number.

(4) Vertical diffusion coefficient

$$D_x = 5.93 u_{*2} h_2 \tag{4-15}$$

$$|u_{*2}| = \sqrt{\frac{\tau_2 - \tau_1}{\rho_2}} = \left\{ f_b u_2 |u_2| - \frac{f_i}{2}(1-\varepsilon)(u_1 - u_2)|u_1 - u_2| \right\}^{\frac{1}{2}} \tag{4-16}$$

where u_{*2} is the shear velocity.

Equation (4-8) and (4-10) are obtained based on the large-scale flume experiments and observation results of Mogamigawa River, Yamagata prefecture, Japan conducted by Suga and Takahashi (1975; 1976). Equation (4-15) is to calculate the vertical diffusion coefficient originally defined by Elder (1959)

For the sake of numerical calculation, terms with small order are ignored and the motion equation (4-5) and (4-6) are transformed as follows:

$$\frac{\partial h_1}{\partial x} = \frac{1}{\phi}\left[-i_{f1} + i_{f2} - \epsilon F_2^2 i_0 + \epsilon\left(1 - F_1^2 - \frac{u_1}{u_2} F_2^2\right)\frac{E}{u_1} + \frac{u_1^2 - u_2^2}{gB}\frac{\partial B}{\partial x} \right.$$
$$\left. - \frac{h_1}{u_1 \rho_2}\frac{\partial \rho_1}{\partial t} - \frac{\rho_1 h_1}{\rho_2^2}\frac{\partial \rho_2}{\partial x} + \frac{2u_1}{gh_1}\frac{\partial h_1}{\partial t} - \frac{2u_2}{gh_2}\frac{\partial h_2}{\partial t} - \frac{1}{gh_1 B}\frac{\partial Q_1}{\partial t} + \frac{1}{gh_2 B}\frac{\partial Q_2}{\partial t} \right] \tag{4-17}$$

$$\frac{\partial h_2}{\partial x} = \frac{1}{\phi}\left[i_{f1} - i_{f2} + \epsilon(1-F_1^2)i_0 - \epsilon\left(1 - F_1^2 - \frac{u_1}{u_2}F_2^2\right)\frac{E}{u_1} - \frac{u_1^2 - u_2^2}{gB}\frac{\partial B}{\partial x} \right.$$

$$\left. + \frac{h_1}{u_1\rho_2}\frac{\partial \rho_1}{\partial t} + \frac{\rho_1 h_1}{\rho_2^2}\frac{\partial \rho_2}{\partial x} - \frac{2u_1}{gh_1}\frac{\partial h_1}{\partial t} + \frac{2u_2}{gh_2}\frac{\partial h_2}{\partial t} + \frac{1}{gh_1 B}\frac{\partial Q_1}{\partial t} - \frac{1}{gh_2 B}\frac{\partial Q_2}{\partial t} \right] \tag{4-18}$$

$$\phi = \epsilon(1 - F_1^2 - F_2^2) \tag{4-19}$$

Within the extent that water surface is assumed to be horizontal, equation (4-18) is unnecessary since the depth of the saltwater layer (h_2) is automatically determined by the provided tide stage (S) and the depth of the freshwater layer (h_1).

4.1.2 Numerical solution

Numerical grid and symbols are defined as shown in Fig. 4-2. Implicit finite difference scheme was applied to discretize the equations (4-1), (4-2), (4-3), (4-4) and (4-17). For example, the first term of the equation (4-1) can be discretized as follows:

$$\frac{\partial h_1}{\partial t} = \frac{1}{2\Delta t}\left(h_{1\,m}^{n+1} - h_{1\,m}^{n} + h_{1\,m-1}^{n+1} - h_{1\,m-1}^{n}\right) \tag{4-20}$$

, where superscript *n* and subscript *m* denote time step and grid-point number counted from downstream. After discretizing all of terms in the equation (4-1), (4-2), (4-3), (4-4) and (4-17), general forms of discretized equations are listed as below:

$$\frac{\Delta x_{m-1}}{2\Delta t}\left(h_{1\,m}^{\,n+1} - h_{1\,m-1}^{\,n+1}\right) + \frac{2}{B_m + B_{m-1}}\left(Q_{1\,m-1}^{\,n+1} - Q_{1\,m}^{\,n+1}\right) = \Delta x_{m-1}E_m^n + \frac{\Delta x_{m-1}}{2\Delta t}\left(h_{1\,m}^{\,n} - h_{1\,m-1}^{\,n}\right) \tag{4-21}$$

$$\frac{\Delta x_{m-1}}{2\Delta t}\left(h_{2\,m}^{\,n+1} - h_{2\,m-1}^{\,n+1}\right) + \frac{2}{B_m + B_{m-1}}\left(Q_{2\,m-1}^{\,n+1} - Q_{2\,m}^{\,n+1}\right) = -\Delta x_{m-1}E_m^n + \frac{\Delta x_{m-1}}{2\Delta t}\left(h_{2\,m}^{\,n} - h_{2\,m-1}^{\,n}\right) \tag{4-22}$$

$$\left(\frac{\Delta x_{m-1}}{2\Delta t} - \frac{u_{1\,m}^{\,n} + u_{1\,m-1}^{\,n}}{2}\right)\rho_{1\,m}^{\,n+1} + \left(\frac{\Delta x_{m-1}}{2\Delta t} + \frac{u_{1\,m}^{\,n} + u_{1\,m-1}^{\,n}}{2}\right)\rho_{1\,m-1}^{\,n+1}$$

$$= \left(\frac{\Delta x_{m-1}}{2\Delta t} - \frac{2E_m^n \Delta x_{m-1}}{h_{1\,m}^{\,n} + h_{1\,m-1}^{\,n}}\right)\rho_{1\,m}^{\,n} + \frac{2E_m^n \Delta x_{m-1}}{h_{1\,m}^{\,n} + h_{1\,m-1}^{\,n}}\rho_{2\,m}^{\,n} + \frac{\Delta x_{m-1}}{2\Delta t}\rho_{1\,m-1}^{\,n} \tag{4-23}$$

$$\left(\frac{\Delta x_{m-1}}{2\Delta t} - \frac{u_{2\,m}^{\,n} + u_{2\,m-1}^{\,n}}{2}\right)\rho_{2\,m}^{\,n+1} + \left(\frac{\Delta x_{m-1}}{2\Delta t} + \frac{u_{2\,m}^{\,n} + u_{2\,m-1}^{\,n}}{2}\right)\rho_{2\,m-1}^{\,n+1}$$

$$= \left(\frac{\Delta x_{m-1}}{2\Delta t} + \frac{D_x}{\Delta x_{m-1}} \right) \rho_{2\,m}^{\ n} + \left(\frac{\Delta x_{m-1}}{2\Delta t} - \frac{2D_x}{\Delta x_{m-1}} \right) \rho_{2\,m-1}^{\ n} + \frac{D_x}{\Delta x_{m-1}} \rho_{2\,m-2}^{\ n} \tag{4-24}$$

$$- \left[\frac{\varepsilon_{m-1}^{n} \left\{ 1 - \left(F_{1\,m-1}^{\ n} \right)^2 - \left(F_{2\,m-1}^{\ n} \right)^2 \right\}}{\Delta x_{m-1}} + \frac{u_{1\,m}^{\ n} + u_{1\,m-1}^{\ n}}{2g h_{1\,m-1}^{\ n} \Delta t} \right] h_{1\,m}^{\ n+1} + \left[\frac{\varepsilon_{m-1}^{n} \left\{ 1 - \left(F_{1\,m-1}^{\ n} \right)^2 - \left(F_{2\,m-1}^{\ n} \right)^2 \right\}}{\Delta x_{m-1}} - \frac{u_{1\,m}^{\ n} + u_{1\,m-1}^{\ n}}{2g h_{1\,m-1}^{\ n} \Delta t} \right] h_{1\,m-1}^{\ n+1}$$

$$+ \frac{u_{2\,m}^{\ n} + u_{2\,m-1}^{\ n}}{2g h_{2\,m-1}^{\ n} \Delta t} \left(h_{2\,m}^{\ n+1} + h_{2\,m-1}^{\ n+1} \right) + \frac{1}{2g h_{1\,m-1}^{\ n} \left(B_m + B_{m-1} \right) \Delta t} \left(Q_{1\,m}^{\ n+1} + Q_{1\,m-1}^{\ n+1} \right) - \frac{1}{2g h_{2\,m-1}^{\ n} \left(B_m + B_{m-1} \right) \Delta t} \left(Q_{2\,m}^{\ n+1} + Q_{2\,m-1}^{\ n+1} \right)$$

$$+ \frac{h_{1\,m-1}^{\ n} + h_{1\,m}^{\ n}}{2 \left(u_{1\,m-1}^{\ n} + u_{1\,m}^{\ n} \right) \rho_{2\,m-1}^{\ n} \Delta t} \left(\rho_{1\,m}^{\ n+1} + \rho_{1\,m-1}^{\ n+1} \right) + \frac{\rho_{1\,m-1}^{\ n} \left(h_{1\,m-1}^{\ n} + h_{1\,m}^{\ n} \right)}{2 \left(\rho_{2\,m-1}^{\ n} \right)^2 \Delta x_{m-1}} \left(\rho_{2\,m-1}^{\ n+1} - \rho_{2\,m}^{\ n+1} \right)$$

$$+ i_{f1\,m-1}^{\ n} - i_{f2\,m-1}^{\ n} + \varepsilon_{m-1}^{n} \left(F_{2\,m-1}^{\ n} \right)^2 \frac{i_{0\,m-1} + i_{0\,m}}{2} - \varepsilon_{m-1}^{n} \left\{ 1 - \left(F_{1\,m-1}^{\ n} \right)^2 - \frac{u_{1\,m-1}^{\ n}}{u_{2\,m-1}^{\ n}} \left(F_{2\,m-1}^{\ n} \right)^2 \right\} \frac{E_{m-1}^{n}}{u_{1\,m-1}^{\ n}}$$

$$- \frac{2 \left\{ \left(u_{1\,m-1}^{\ n} \right)^2 - \left(u_{2\,m-1}^{\ n} \right)^2 \right\}}{g \left(B_m + B_{m-1} \right) \Delta x_{m-1}} \left(B_{m-1} - B_m \right) - \frac{h_{1\,m-1}^{\ n} + h_{1\,m}^{\ n}}{2 \left(u_{1\,m-1}^{\ n} + u_{1\,m}^{\ n} \right) \rho_{2\,m-1}^{\ n} \Delta t} \left(\rho_{1\,m}^{\ n} + \rho_{1\,m-1}^{\ n} \right)$$

$$+ \frac{u_{1\,m}^{\ n} + u_{1\,m-1}^{\ n}}{2g h_{1\,m-1}^{\ n} \Delta t} \left(h_{1\,m-1}^{\ n} + h_{1\,m}^{\ n} \right) - \frac{u_{2\,m}^{\ n} + u_{2\,m-1}^{\ n}}{2g h_{2\,m-1}^{\ n} \Delta t} \left(h_{2\,m-1}^{\ n} + h_{2\,m}^{\ n} \right)$$

$$- \frac{1}{g h_{1\,m-1}^{\ n} \left(B_m + B_{m-1} \right) \Delta t} \left(Q_{1\,m-1}^{\ n} + Q_{1\,m}^{\ n} \right) + \frac{1}{g h_{2\,m-1}^{\ n} \left(B_m + B_{m-1} \right) \Delta t} \left(Q_{2\,m-1}^{\ n} + Q_{2\,m}^{\ n} \right) = 0 \tag{4-25}$$

After all variables coefficients in the equation (4-21), (4-22), (4-23), (4-24) and (4-25) were reorganized, general forms of discretized equations are finally transformed as follows:

$$a_{1\,m} h_{1\,m}^{n+1} + a_{2\,m} Q_{1\,m}^{n+1} + a_{3\,m} Q_{2\,m}^{n+1} + a_{4\,m} \rho_{1\,m}^{n+1} + a_{5\,m} \rho_{2\,m}^{n+1} = a_{6\,m} \tag{4-26}$$

$$a_{7\,m} Q_{1\,m-1}^{n+1} + a_{8\,m} Q_{1\,m}^{n+1} + a_{9\,m} h_{1\,m}^{n+1} + a_{10\,m} \rho_{1\,m}^{n+1} + a_{11\,m} \rho_{2\,m}^{n+1} = a_{12\,m} \tag{4-27}$$

$$a_{13\,m} Q_{2\,m-1}^{n+1} + a_{14\,m} Q_{2\,m}^{n+1} + a_{15\,m} h_{1\,m}^{n+1} + a_{16\,m} \rho_{1\,m}^{n+1} + a_{17\,m} \rho_{2\,m}^{n+1} = a_{18\,m} \tag{4-28}$$

$$a_{19\,m} \rho_{1\,m-1}^{n+1} + a_{20\,m} \rho_{1\,m}^{n+1} = a_{21\,m} \tag{4-29}$$

$$a_{22\,m} \rho_{2\,m-1}^{n+1} + a_{23\,m} \rho_{2\,m}^{n+1} = a_{24\,m} \tag{4-30}$$

where $a_1 - a_{24}$ are determinate values when all the variables within one time step before (n) are given.

To solve these equations, the following six boundary conditions are given: the depth of freshwater (h_1), the tide stage (S), and the density of saltwater layer (ρ_2) as downstream boundary conditions; the discharge of freshwater (Q_1) and saltwater (Q_2) and density of freshwater (ρ_1) as upstream boundary conditions.

The first step is calculation of $a_1 - a_{24}$, which are determined using the values of variables at the initial conditions n = 1, and those calculated one time step before for n ≥ 2. Then ρ_1 and ρ_2 are calculated, by solving equation (20) from the furthest upstream grid-point, downstream, and equation (21) from the furthest downstream grid-point, upstream. Given longitudinal values of ρ_1 and ρ_2 and boundary conditions, h_1 at the furthest upstream boundary ($h_{1\,m}^{n+1}$) is calculated by equation (17), then Q_1 and Q_2 of one grid-point downstream ($Q_{1\,m-1}^{n+1}$, $Q_{2\,m-1}^{n+1}$) by equation (18) and (19), respectively. The values of h_2 are determined as a difference between the total water depth and freshwater depth h_1. By repeating this procedure, all the longitudinal values are calculated, and then repeated for the next time step.

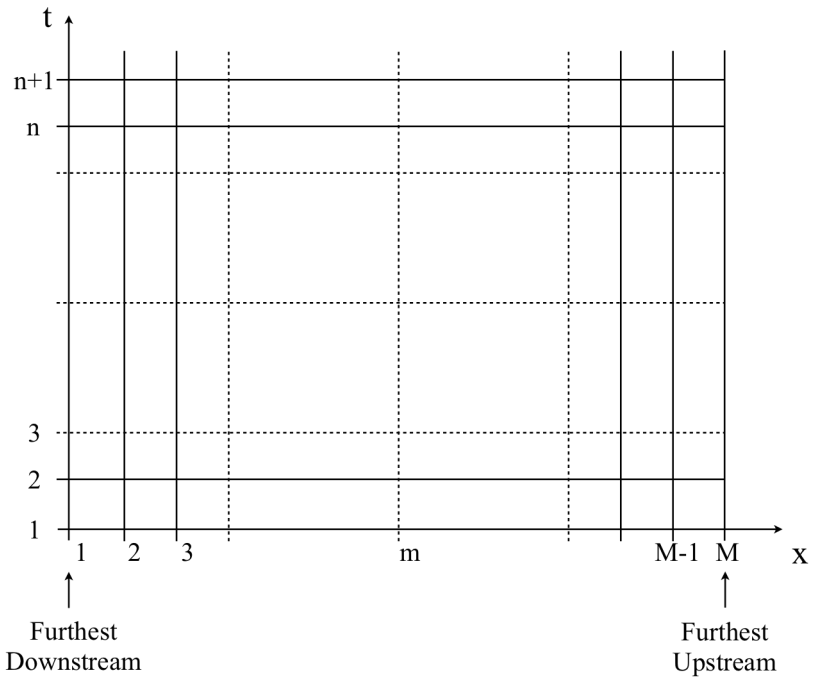

Fig. 4-2 Grid-points covering the computational domain and symbols

4.1.3 Model application

To apply the model to the study river, the computational domain was set from the river mouth sluice gates to 15 km upstream, a location where no seawater intrusion occurs. The computational domain was divided into 150 sections of 100 m each. The model bathymetry and river width are based on the drawings of longitudinal sections and cross-sectional profiles obtained from the Water Management Office. The riverbed profile obtained by SC-3 was not applied because of the difficulty encountered in the numerical calculation when an abrupt change in the riverbed occurs. The time interval was 300 s.

The values of ρ_2 was assumed to be constant at 1.025 kg/m^3 based on field observations. The value of h_1 was determined by the function of river discharge. The value of S was given by the time series data with a 10-min interval provided by the Water Management Office. The value of h_2 was determined by the difference between S and h_1. The value of ρ_1 at furthest upstream was assumed to be constant at 1.00 kg/m^3 according to the values obtained indirectly by measuring the EC value of the freshwater supplied from upstream. The time-series data of Q_1 supplied from the upstream area was obtained from the Water Management Office. The Q_2 at the furthest upstream point was set as 0 m^3/s because the saltwater wedge did not reach that point.

In addition to the freshwater supplied from the furthest upstream point, the freshwater volume varies by the operation of nine intake pumping stations and ten drainage pumping stations within the computational domain. The intake and discharge volumes of these pumping stations were incorporated in the model as positive and negative lateral flows, respectively. The time series data of pump operation were provided by the Water Management Office.

4.2 Verification of model

4.2.1 The distribution of the saltwater wedge

Fig. 4-3 shows the simulated saltwater wedge intrusions on July 15 and August 23 compared with that observed in the field. Halocline elevations were reproduced well in both cases. However, the longitudinal extent of the simulated saltwater wedge on July 15 was about 1 km longer, and on August 23 was about 1.3 km longer than the observed

extent. The difference was mainly due to the adoption of a smoother riverbed profile based on the drawing of the longitudinal section in the model, whereas the actual bathymetry of the river is fairly rough. Since the purpose of this study is to evaluate the influence of the saltwater wedge on agricultural water intake, the relative vertical position of the density interface needs to be simulated accurately, while the longitudinal extent is less important.

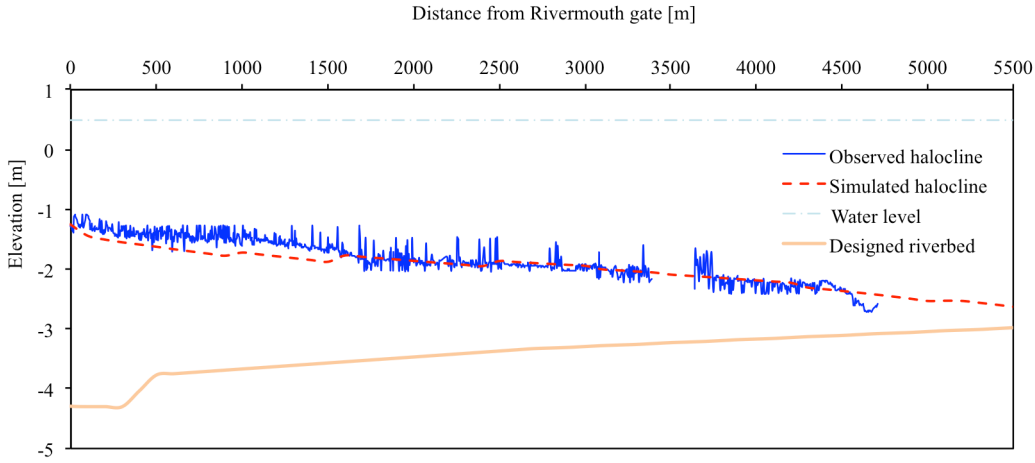

(a) Spring tide (July 15, 2011)

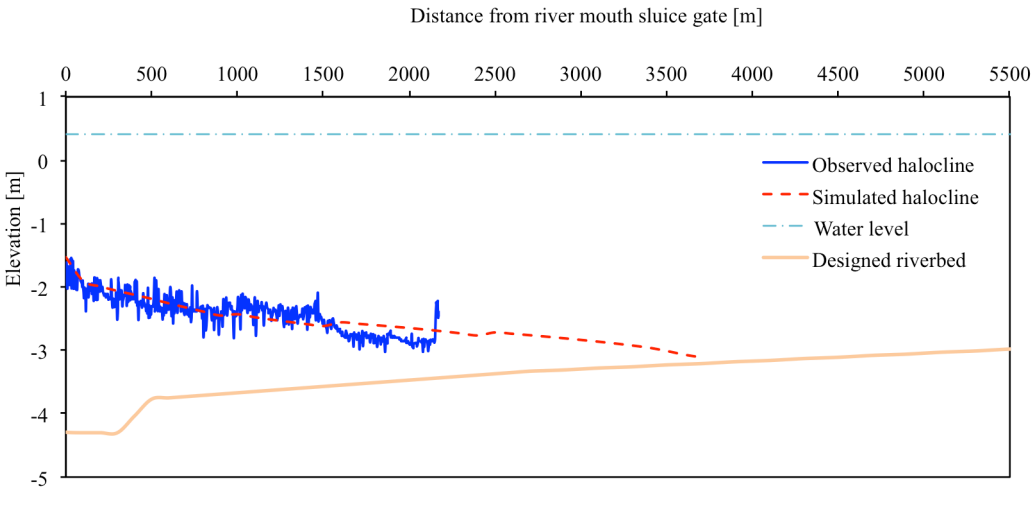

(b) Neap tide (August 23, 2011)

Fig. 4-3 Longitudinal halocline profile by observation and numerical simulation

4.2.2 Velocities of saltwater and freshwater

The calculated velocities of freshwa ter and saltwater during the survey period are shown in Fig. 4-4. Positive values indicate seaward flow, and negative values indicate landward flow. The calculated range of fluctuation is smaller than the observed range for both freshwater and saltwater layers. This may be caused by the influence of wind, which is not accounted for in the model. The calculated flow direction and average velocities are fairly consistent with the observed values. The calculated and observed average velocities of freshwater were 0.144 and 0.141 m/s seaward, and those of saltwater were 0.058 and 0.064 m/s landward, with a less than 10 % error difference. These results demonstrate that the one-dimensional, two-layer, unsteady flow model can satisfactorily simulate the seawater intrusion in the Shinkawa River under a range of tidal level and river discharge conditions.

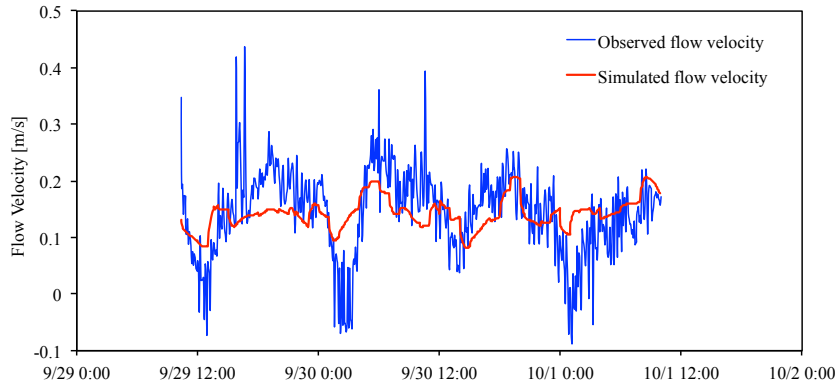

(a) Freshwater

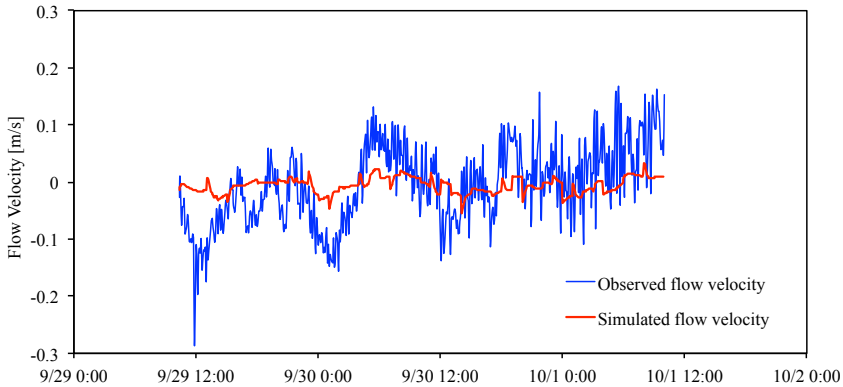

(b) Saltwater

Fig. 4-4 Velocities of freshwater and saltwater by observation and numerical simulation

4.3 Evaluation of the impact of seawater intrusion on irrigation water

Saltwater enters the irrigation channel through the inlet of the intake pumping station when saltwater level is close to the intake's altitude. Therefore, the relative vertical positions of the inlet of intake pumping station inlets and the halocline are the critical factor that determines the degree of saltwater mixing. Because the river mouth sluice gates close when the EC value of the river water near the monitoring station at the Nakasai intake pumping station reaches 1500 μs/cm, the behavior of the saltwater wedge and the extent of saltwater mixing without operation of the gate throughout an irrigation period are unknown. This model was used to simulate saltwater wedge behavior without the gate operation during the irrigation period in 2011.

The relationship between the vertical position of the halocline and the EC value observed at the Nakasai intake pumping station 3.21 km from the sluice gates is shown in Fig. 4-5. EC values greater than 1500 μs/cm were observed immediately before the countermeasure was practiced, and the height difference between the inlet and halocline is the simulated result. This result implies that when the vertical position of the halocline rises to 1.2 m below the inlet of the water intake pumping station, the EC value rises sharply over the unsuitable standard for irrigation water, 1500 μs/cm. Since the EC value of the seawater is about 45000 μs/cm, even minor mixing of saltwater due to the suction by pumps would cause makes the irrigation water unsuitable for irrigation use. According to the simulation result, this condition would occur for about 23 % of the irrigation period if the countermeasures were not practiced in 2011.

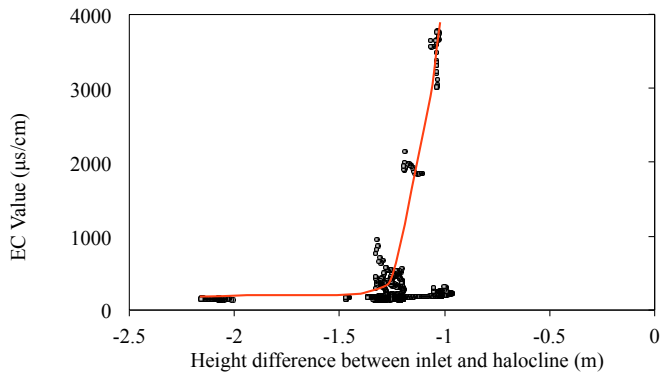

Fig. 4-5 Relationship between EC Values observed at monitoring station (Nakasai intake pumping station) and relative halocline position to the inlet simulated by the model

4.4 Summary

Saltwater wedge intrusion was investigated by field observations and numerical simulations in the estuary of the Shinkawa River. As indicated by longitudinal and vertical profile visualization, the saltwater wedge in Shinkawa River moves into the estuary at each tidal event with strong stratification, causing salinization of irrigation water. Since the vertical position of the halocline is the determining factor of the extent of the mixture of saltwater into irrigation water, the present countermeasure, closing the river mouth sluice gates in combination with discharging the river water out of the sluice gates by pumps, is effective to lower the position of the halocline and to avoid the intrusion of high-salinity water into irrigation water. However, operation of the drainage pumps is costly, and this countermeasure brings about a shortage of irrigation water because the intake pumping stations cease operation. In drought years in particular, the frequency and magnitude of saltwater intrusion increases because of a lower freshwater supply from upstream; this is problematic because of the higher water demand to supplement high rates of evapotranspiration during these times. Therefore, more effective and efficient countermeasures to lower the vertical position of the halocline must be introduced. We are currently developing proposals for several alternative countermeasures, such as increases in the volume of freshwater supply in the river by manipulating the operation timing of the drainage pumps equipped further upstream than the longitudinal profile of the saltwater wedge, or controlling the aperture of sluice gates to eliminate only the saltwater layer out of the river with only a head difference between inside and outside the gate. These proposals will be tested in-situ experiment, and, if successful, will help alleviate the costs associated with operation of the river mouth pump, and allow for continuous intake of irrigation water.

5. Control experiments of saltwater wedge in Shinkawa River

Based on the problems and characteristics of seawater intrusion in Sinkawa River discussed above, three methods, which are the freshwater flow increase, the operation of sluice gates and the selective intake structure, were attempted to impede or present the landward intrusion of saltwater wedge.

5.1 Discharge increase

5.1.1 Methods and materials

The idea of discharge increase is that change the upstream freshwater flow rate when other factors are kept the constant. In Shinkawa River, the discharge increase of freshwater upstream was achieved by operating the intake and drainage pumping stations along this river.

July 3 and 4, 2012 (spring tide days) and Aug 6 and 7, 2013 (spring tide days) were determined to implement the increasing of freshwater discharge, because the upstream discharge principally determines the extent of saltwater wedge under similar tidal condition. On July 3, 2012, all pump stations were kept on the normal usage, but they were operated to increase the discharge from 9:50 to 13:50 on July 4, 2012 (3 hours before to 1 hour after the higher high water). The specific operations of the pump stations on July 4 were that the intake pumping stations stopped providing water or pumped less water, while drainage pumping stations kept running or drained more water under the premise of satisfying the demand of irrigation water on that day. For the second freshwater increase experiment on Aug 6, 2013, the drainage pumping stations were limited to discharge as less as possible, and intake pumping stations were set up to take more water than that in normal situation. The operation method of pumping stations on Aug 7, 2013 was the same as that on July 4, 2012. The second experiment's conducing time was from 2 hours before to 2 hours after the higher high water of flood tide, keeping the same duration as that during first experiment. The distribution of saltwater wedge was surveyed two hours after all pumping stations' operations. The specific information of tide on survey days is listed in Table 5-1.

Table 5-1 Tide information on the days of discharge increase

Date	Lower high water	Higher low water	Higher high water	Lower low water
Jul 3, 2012	03:42	06:49	12:53	21:09
Tide level (cm)	30	28	41	5
Jul 4, 2012	04:22	07:45	13:49	21:59
Tide level (cm)	31	28	41	5
Aug 6, 2013	03:47	07:18	13:28	21:16
Tide level (cm)	32	30	40	16
Aug 7, 2013	04:04	08:02	14:09	21:49
Tide level (cm)	32	29	40	16

During the period of observation, the SC-3 and EC meters (see Chapter 3) were adopted to recognize the density interface between saltwater and freshwater and extent of saltwater wedge. The velocities and the flow directions of the freshwater and saltwater were measured using current meters (see Chapter 3), which were programmed to obtain 30 samples every 10 min, and one sample is recorded with the interval of 1 sec. The record periods were from 10:00 on July 3, 2012 to 18:00 July 4, 2012, and from 7:00 on Aug 6, 2013 to 16:00 on Aug 7, 2013. The other setup instructions are listed in Table 5-2.

Table 5-2 The instructions of velocity measurement on the days of discharge increase

Date	Observation sites	Height off the riverbed	River depth (m)	The mounting time
Jul 3, 4, 2012	1.62 km from sluice gates	0.9 m (for saltwater) 3.1 m (for freshwater)	4.2 (2.5 m for saltwater layer)	9:00 July 3, 2012
Aug 6, 7, 2013	0.26 km from sluice gates	1.1 m (for saltwater) 3.1 m (for freshwater)	4.7 (2.4 m for saltwater layer)	15:20 Aug 5, 2013

5.1.2 Experimental results

5.1.2.1 First experiment

(1) Tide and discharge

The average discharges at the most upstream site of this river were 19.3 m^3/s on July 3, 2012 and 21.4 m^3/s on July 4, 2012, and at the most downstream site were 17.3 m^3/s and 27.0 m^3/s on July 3 and 4, 2012, respectively. The total average discharge was increased by about 9.7 m^3/s during the survey periods as shown in Fig. 5-1. Tide levels on survey days were shown in Fig. 5-2.

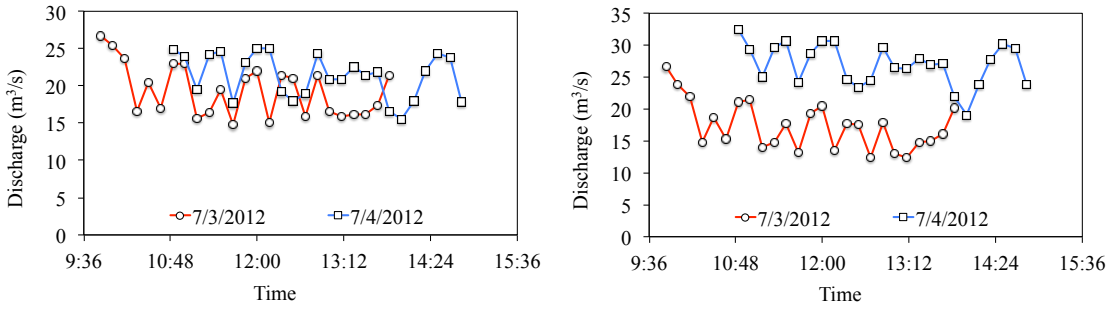

(a) Upstream (b) Downstream

Fig. 5-1 Discharge during the survey period on July 3 and 4, 2012

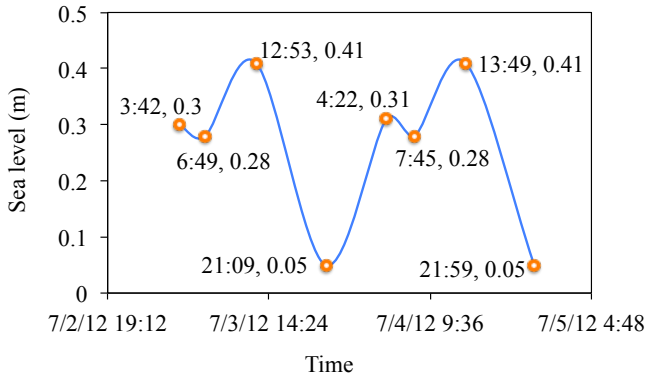

Fig. 5-2 Tide level on July 3 and 4, 2012

(2) Longitudinal profile

The survey results were concentrated on the distance of saltwater wedge and the interface between saltwater and freshwater, for the extent and height of saltwater wedge

are chief factors that estimate the effect of the controlling method.

The longitudinal distribution of the density interface between saltwater and freshwater is shown in Fig. 5-3, illustrating that the height of the density interface was decreased after the upstream discharge was increased. The average elevations of the density interface were about -1.74 m on July 3, 2012, and about -1.93 m on July 4, 2012, and it was reduced by 0.19 m under the added freshwater flow of 9.7 m^3/s during the survey period. The part of density interface whose variation of elevation was relative obvious between two survey days started at 0.58 km upstream from the sluice gates, having a whole length of approximately 2.16 km, indicating that the action range of increased flow was about 1.60 km under this tidal situation.

(3) Velocity

The velocities of saltwater and freshwater near 1.62 km upstream from the sluice gates are showed in Fig. 5-4. It can be seen from Fig. 5-4 (a) that the freshwater always flowed downstream (northwest between 270° and 360°) with a velocity varied with the tide level. The velocity rose to the highest value after higher high water, and lowered to the lowest value before the next higher high water. The average velocity was 0.23 m/s during the survey period. In Fig. 5-4 (b), the direction of saltwater changed due to flood tide and ebb tide. The maximum velocity was close to 0.35 m/s about near the lower low water, with the direction of seaward, and the minimum velocity was close to 0 m/s near higher high water, with the direction of landward.

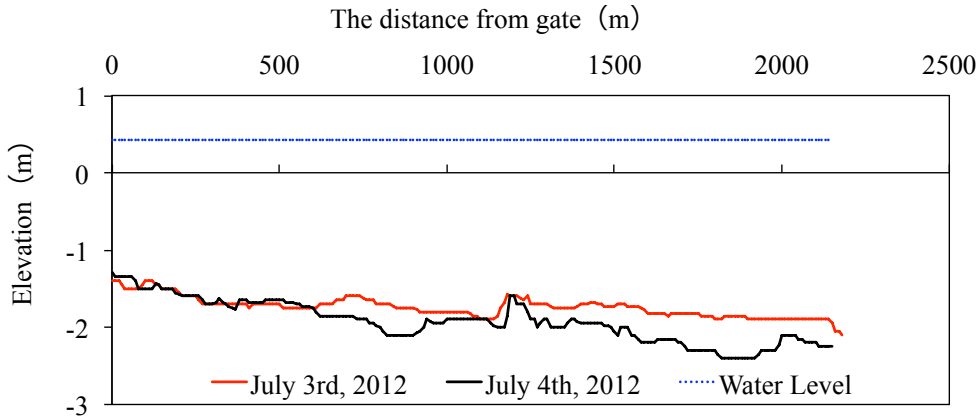

Fig. 5-3 Density interfaces on July 3 and 4, 2012

5.1.2.2 Second experiment

(1) Tide and discharge

The average discharges at the most upstream site of this river were 27.8 m^3/s on Aug 6, 2013 and 26.2 m^3/s On Aug 7, 2013, and at the most downstream site were 22.5 m^3/s and 37.6 m^3/s on Aug 6 and 7, 2013, respectively. The total average discharge was increased by about 15.1 m^3/s during the survey periods as shown in Fig. 5-5. Tide levels on survey days are shown in Fig. 5-6.

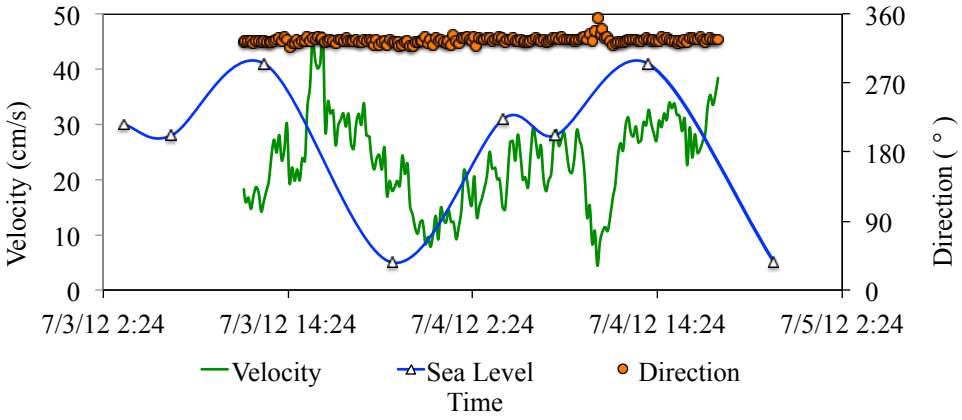

(a) Freshwater

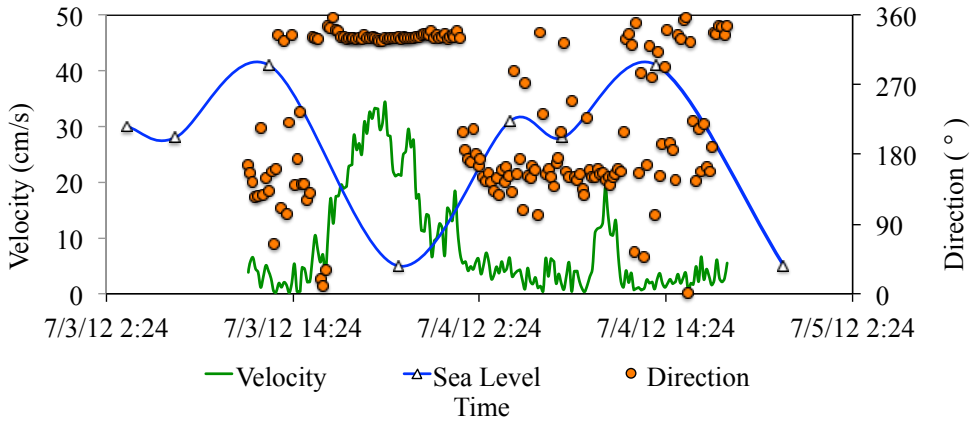

(b) Saltwater

Fig. 5-4 The velocities and directions of freshwater and saltwater on July 3 and 4, 2012

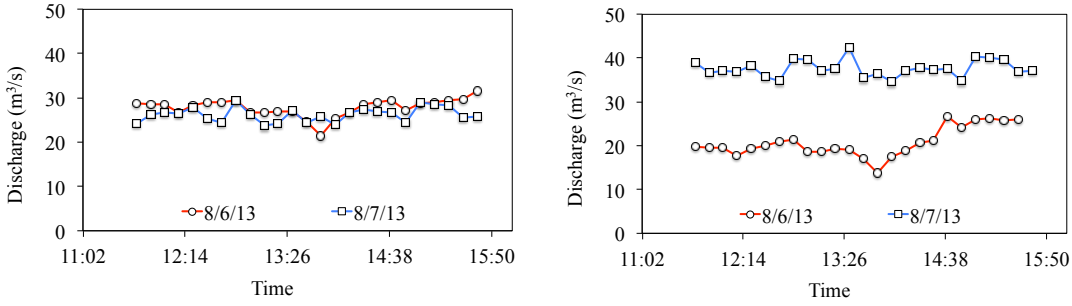

(a) Upstream (b) Downstream

Fig. 5-5 Discharge during the survey period on Aug 6 and 7, 2013

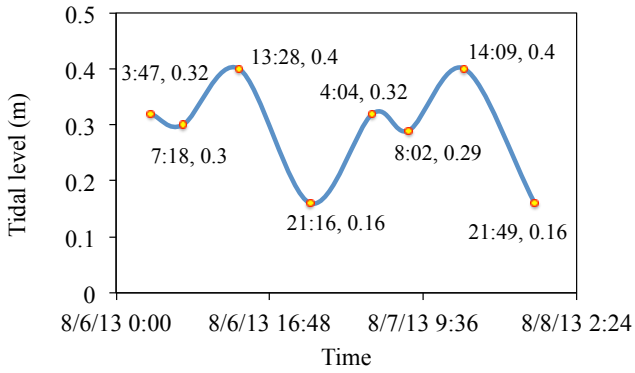

Fig. 5-6 Tide level on Aug 6 and 7, 2013

(2) Longitudinal profile

The longitudinal distribution of the density interface between saltwater and freshwater is shown in Fig. 5-7. It can be found that the extent of saltwater wedge was obviously shortened, and the height of the density interface slightly decreased as well after the upstream discharge was increased. The decreased distance of saltwater wedge was about 0.49 km, from 3.56 km to 3.07 km, and the height of density interface was declined by about 0.2 m during the survey period.

(3) Velocity

The velocities of saltwater and freshwater near 0.26 km upstream from the sluice gates are showed in Fig. 5-8. Fig. 5-8 (a) reveals that the freshwater always flowed downstream (northwest between 270° and 360°) with a velocity varied with the tide level. The velocity reached the highest value after higher high water, and decreased to the lowest value before the next higher high water. The average velocity was 0.32 m/s

during the survey period. In Fig. 5-8 (b), the direction of saltwater changed due to flood tide and ebb tide, and the average velocity was 0.06 m/s. During one tidal cycle, 52 % of flow was seaward and 48 % was landward.

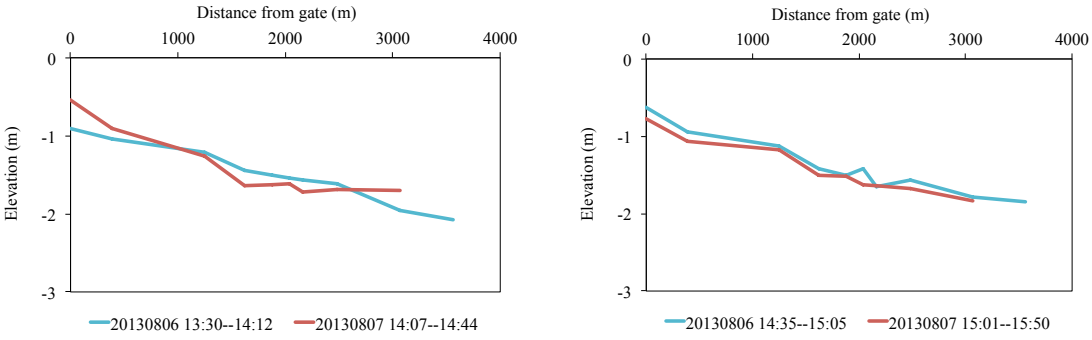

(a) First survey (b) Second survey

Fig. 5-7 Density interface on Aug 6 and 7, 2013

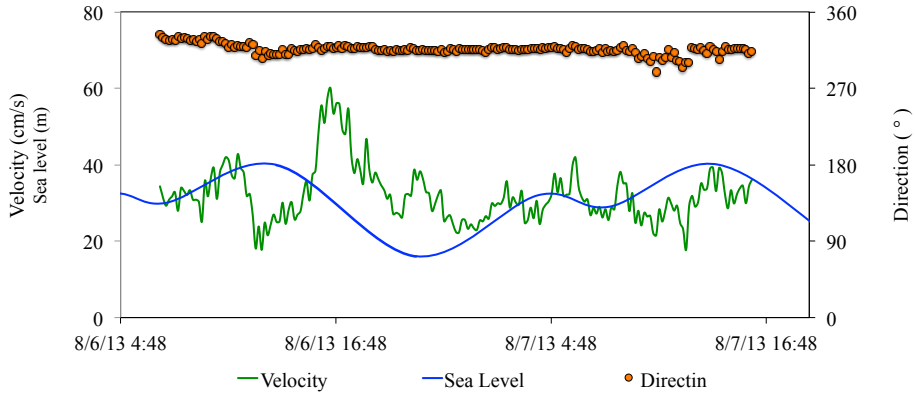

(a) Freshwater

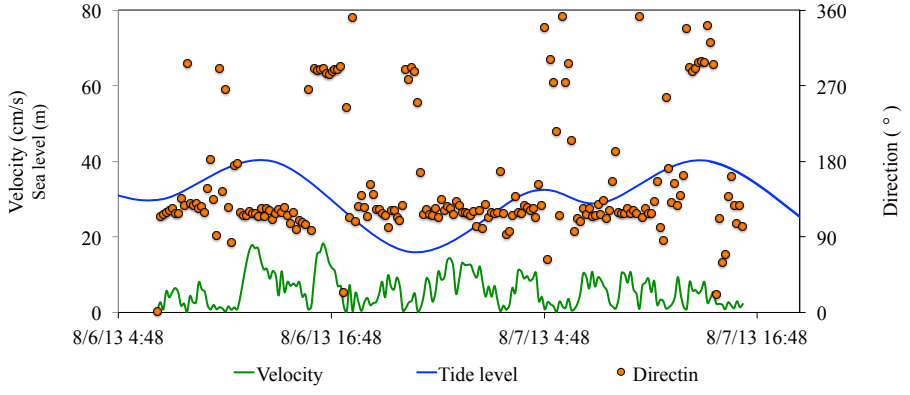

(b) Saltwater

Fig. 5-8 The velocities and directions of freshwater and saltwater on Aug 6 and 7, 2013

5.1.3 Discussions

According to the results above, the decreased height and extend of the saltwater wedge were very limited, because the implementation periods of this control method were carried out during the irrigation season, thus the amount of water that could be added from upstream pump stations was not only restricted by the need of agricultural water, but also by the discharge capacity of the narrowest cross section of the river. Since the agricultural water consumed by upstream paddy fields was large amount, the water volume that can be added is limited, resulting in little effect on preventing seawater intrusion. If the discharge exceeded the maximum that this river allows, the overflow might have damage on buildings and agricultural production along this river. In addition, the position of increased discharge also has influence on the effect of control saltwater wedge. Some pumping stations are within the movement range of saltwater wedge along this river. If discharge was increased by operating these pumps, less effect would be got on the result. This seems to be one of the reasons that this control method was not completely successful. Therefore, this method should be implemented as upstream as possible beyond the movement range of saltwater wedge, under reasonable water management and fully considering the reliable discharge capacity of the waterway.

5.1.4 Conclusions

The method of discharge increase can reduced the height of the density interface between saltwater and freshwater and extent of saltwater wedge in Shinkawa River. However, the effect of this mean is limited by the upstream discharge that can be ultilized. This method did not control the extent of the saltwater wedge beyond the most downstream of the intake of irrigation water.

5.2 Selective intake

5.2.1 Methods and materials

The basic idea of selective intake is constructing one kind of structure which can only let freshwater freely enter the gate of pumping station, and block saltwater outside of the gate. This attempt was conducted at the Nakasai intake pumping station (3.21 km from the sluice gates) to verify whether this method could work.

The selective intake structure was first built by fixing the top of a blue waterproof cloth on the steel pipes and fixing its bottom on the riverbed along the pipes. It should be noted that the size of waterproof cloth is needed to adequately meet the length and depth of trash rack (longer than the sum of edge A, B and C shown in Fig. 5-9), and the capacity of pump should be ensured by keeping enough height difference between the top of blue waterproof cloth and water surface. In this case, the size of waterproof cloth was identified as 20 m × 4.5 m, and the height difference was calculated as 0.5 m on the survey day, which can satisfy the amount of pumping water even under the lowest water level. To assure the saltwater being blocked outside of selective intake structure, the pipe clips were used to fix the top of the waterproof cloth, and the earth bags were arranged at the riverbed along the pipes as shown in Fig. 5-10.

Fig. 5-9 The inlet at Nagasai intake pumping staion

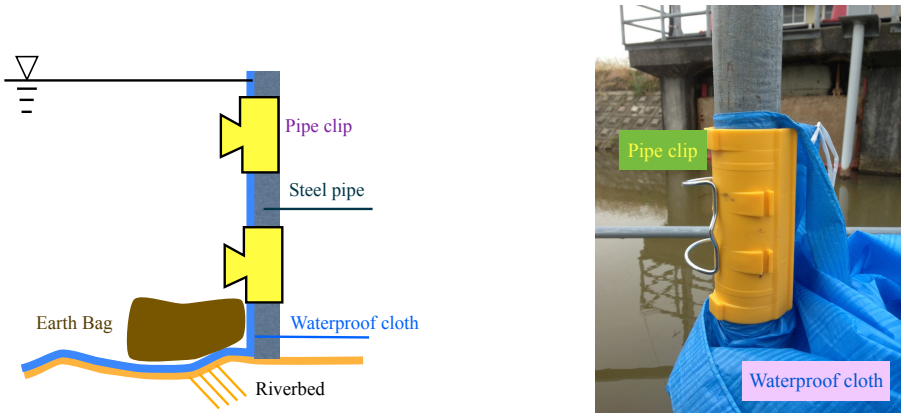

(a) Scheme (b) Materials

Fig. 5-10 The scheme of selective intake structure

The premise of this observation being implemented is that the front of saltwater wedge appears more upstream than Nakasai intake pumping station. This has been confirmed before the survey day of August 19, 2013, and the implement duration was determined 4 hours around higher high water (at 12:02), from 10:00 to 14:00 on August 19, 2013. EC meters were used in this in-situ experiment to continuously monitor the salinity of water inside and outside of the waterproof cloth during the period when the pump run, and the scope of saltwater wedge was also observed on the downstream and upstream bridges near this pumping station.

5.2.2 Experimental results

During the experimental period, the extent of saltwater wedge increased from about 3.07 km to 3.56 km. The salinity variations of inside and outside of the waterproof cloth during the survey period are shown in Fig. 5-11. At the beginning of the measurement, both salinities inside and outside the waterproof cloth were lower than 600 μs/cm that is the standard of freshwater. With the tide level rising, the saltwater gradually appeared outside of the waterproof cloth, and become higher and higher. At this point, the salinity inside of waterproof cloth, in the layer with the elevation from 0.25 m to 0.40 m, also gradually increased, and exceeded 1000 μs/cm. This possibly because that the saltwater was mixed into the upper layer freshwater under the high-speed flow of upper layer water. At the end of this experiment, the average salinity of water inside the waterproof cloth reached about 1000 μs/cm, which illustrates that the freshwater was contaminated by the saltwater outside of the waterproof cloth. It can be found in Fig. 5-11 (f) that the salinities inside the waterproof cloth in upper layer, with the elevation between 0.25 m and 0.40 m, and bottom layer were greater than 1500 μs/cm, but it was less than 1000 μs/cm in the middle layer, implying the problem of leakage between the riverbed and the waterproof cloth. In these three special cases, the salinity of water inside at the bottom of the riverbed decreased with the salinity outside of the waterproof cloth, suggesting that it was also influenced by the tide.

5.2.3 Discussions

Based on the results of selective intake experiment, this structure only achieved the aim of taking the upper layer water, but the freshwater and saltwater were not separated thoroughly by the selective intake structure. However, the average salinity of water

inside the waterproof cloth during the survey period was always less than 1200 μs/cm, less than the standard of irrigation water for paddy fields. Therefore, this method can basically satisfy the quality requirement of agricultural water. In addition, the results of this selective intake experiment also suggest that a new intake structure, with a larger area of wetted cross-section that can decrease the velocities of different water layer, should be constructed to avoid the underlying saltwater mixing into the upper layer.

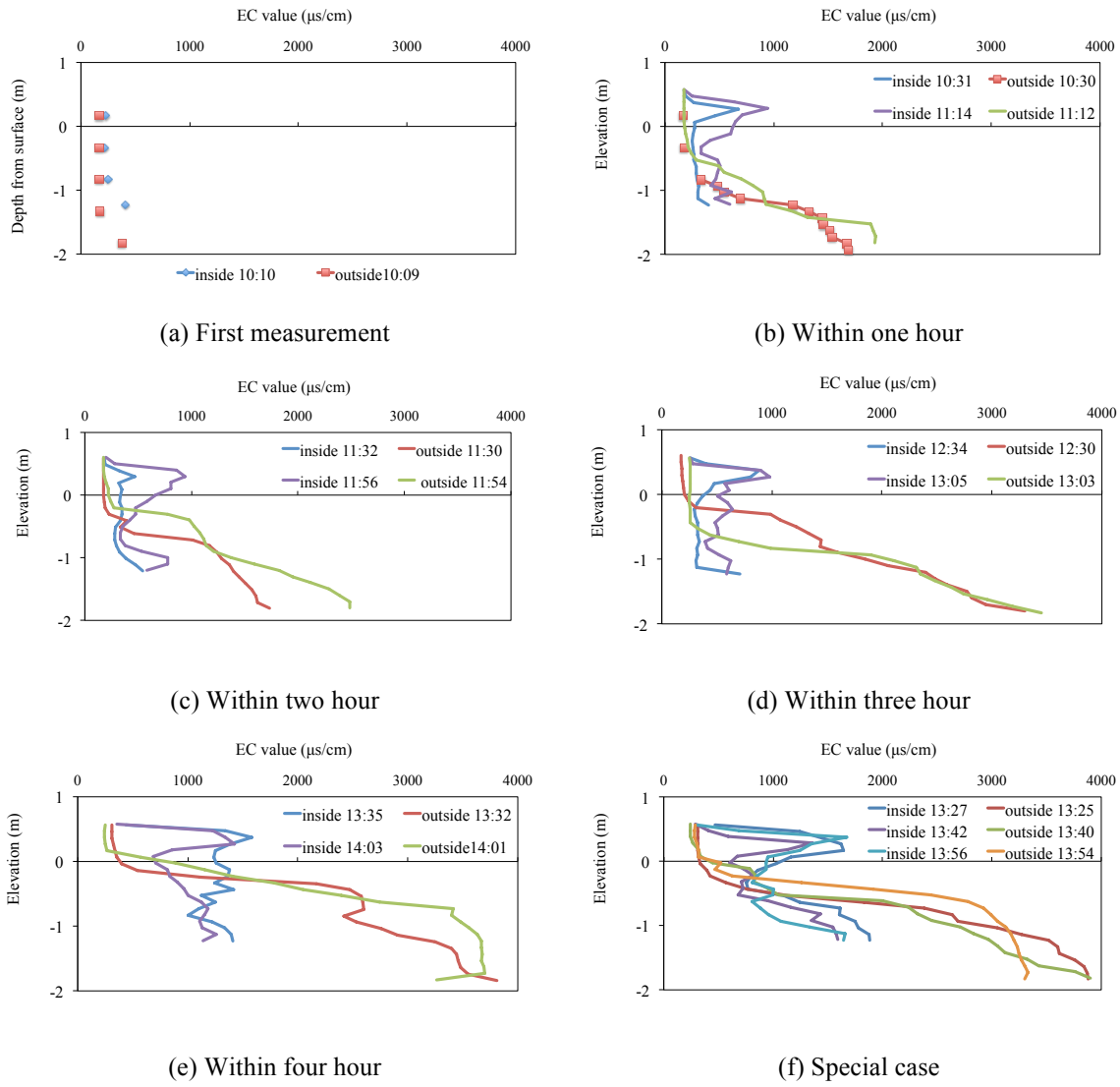

Fig. 5-11 The salinity variations of inside and outside of the waterproof cloth

5.2.4 Conclusions

The selective intake structure basically guaranteed the quality of irrigation water. However, the effect of this mean is limited due to the small area of wetted cross-section. This selective intake structure might be attempted to apply with a larger area of wetted cross-section.

5.3 The operation of sluice gates

5.3.1 Methods and materials

The idea of the operation of sluice gates was to push-out the saltwater outside the sluice gates, reducing the height and length of the saltwater wedge and constraining the seawater intrusion through a submerged orifice. The submerged orifice was successfully achieved by controlling the aperture of the sluice gates to keep a constant water level difference of 0.25 m between inside and outside of the gates. This water level difference was determined by the average discharge every month during irrigation season this river mouth. The created process of submerged orifices is that the sluice gates were first fully closed to create the water level difference between inside and outside of the sluice gates, and then the sluice gates were opened to the aperture that was adjusted due to the water level difference.

Two spring tide days, August 16 and 17, 2012 with similar tide level and upstream discharge, were selected to evaluate the effectiveness of the operation of sluice gates. The survey period was determined around higher high water each day, while more specific tide information is shown in Fig. 5-12 (a). The operation of sluice gates started at 10:00 and ended at 15: 40, on August 16, 2012. During this period, the measurements of longitudinal profiles were implemented five times by SC-3 and EC meters, and one in the four was before the operation of sluice gates. On the second survey day, the observation period of saltwater wedge was from 13:00 to 15:00 (around higher high water) without sluice gates operation.

In addition, another experiment was designed to verify the extent of saltwater wedge, as one sluice gate is closed and the other is open. If this experiment could achieve that the saltwater wedge only moved within the limited range, beyond the sites of all intake pumping station, the navigation and the expensive cost consumed by drainage pumps

when the sluice gates are fully closed can be carried out completely. This mean was implemented around higher high water on Aug 21 and 22, 2013, when the tide conditions are shown in Fig. 5-12 (b).

During the periods of observations, the SC-3 was employed to obtain the longitudinal profiles of the saltwater wedge before and after the sluice gates were operated. Simultaneously, the vertical salinity distribution was also measured by using EC meters at 10 cm intervals from surface to bottom at bridges crossing Shinkawa River. Besides, current meters were adopted to record the velocities of saltwater and freshwater at 0.26 km and 1.62 km upstream from the sluice gates. All current meters were programmed to collect 30 samples within 30 sec each time, and the interval between two times was 10 min. Other setups of current meters are listed in Table 5-3.

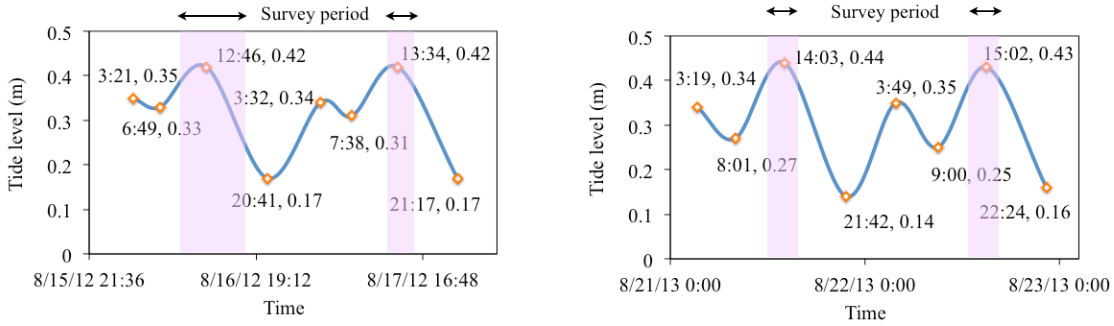

(a) On Aug 16 and 17, 2012

(b) On Aug 21 and 22, 2013

Fig. 5-12 The tide and survey period on the days of the operation of sluice gates

Table 5-3 The instructions of velocity measurement on the operation days of sluice gates

Date	Observation sites	Height off the riverbed	River depth (m)	The mounting time
Aug 16, 17, 2012	0.26 km from sluice gates	0.9 m (for saltwater) 3.1 m (for freshwater)	4.4 (2.6 m for saltwater layer)	16:00 Aug 15, 2012
	1.62 km from sluice gates	1.1 m (for saltwater)	4.5 (2.06 m for saltwater layer)	17:00 Aug 15, 2012
Aug 21 22, 2013	0.26 km from sluice gates	1.23 m (for saltwater) 3.5 m (for freshwater)	4.6 (2.45 m for saltwater layer)	8:46 Aug 21, 2013

5.3.2 Experimental results

5.3.2.1 Submerged orifice

The average upstream freshwater flow rates were 19.9 m^3/s and 18.7 m^3/s on Aug 16 and 17, 2012, and the average downstream discharges were both 20.9 m^3/s on both survey days. The aperture of the sluice gate and water level difference between outside and inside of the gates are shown in Fig. 5-13. The average water level difference was 0.22 m during the period when the saltwater was eliminated.

(1) Vertical variation of saltwater wedge

The vertical salinity distribution of the saltwater is shown in Fig. 5-14 measured by EC meters. It can be seen that during the whole survey period, the height of density interface decreased with time, and the reduced magnitude gradually abated from downstream to upstream. Near the sluice gates, maximum height variation of the density interface was 1.85 m between natural situation and after the operation of sluice gate. Near the front of the saltwater wedge, the minimum height variation of density interface was about 0.25 m between the conditions when the saltwater wedge was under natural situation and 3.5 hours after the sluice gate operation. Simultaneously, the electrical conductivity of saltwater at the bottom of every measured position also decreased from downstream to upstream, but the boundary between saltwater and freshwater was always been recognizable.

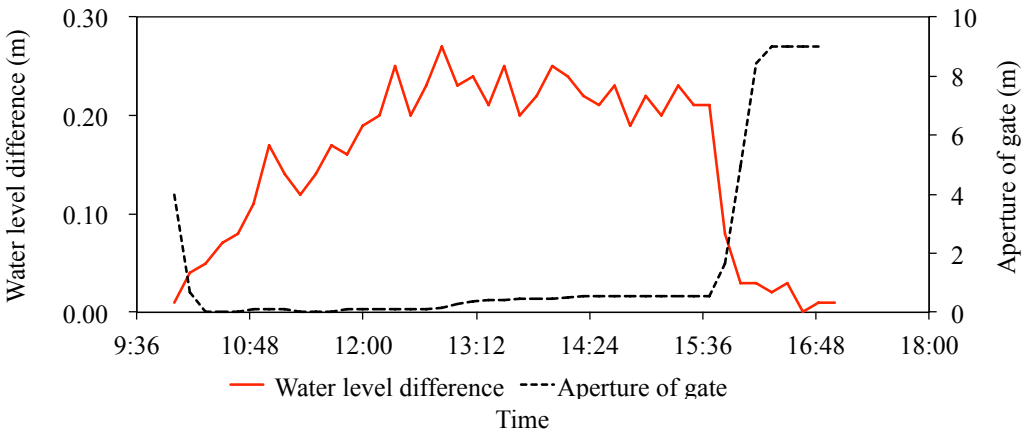

Fig. 5-13 The aperture of gates and water level difference between outside and inside of sluice gates

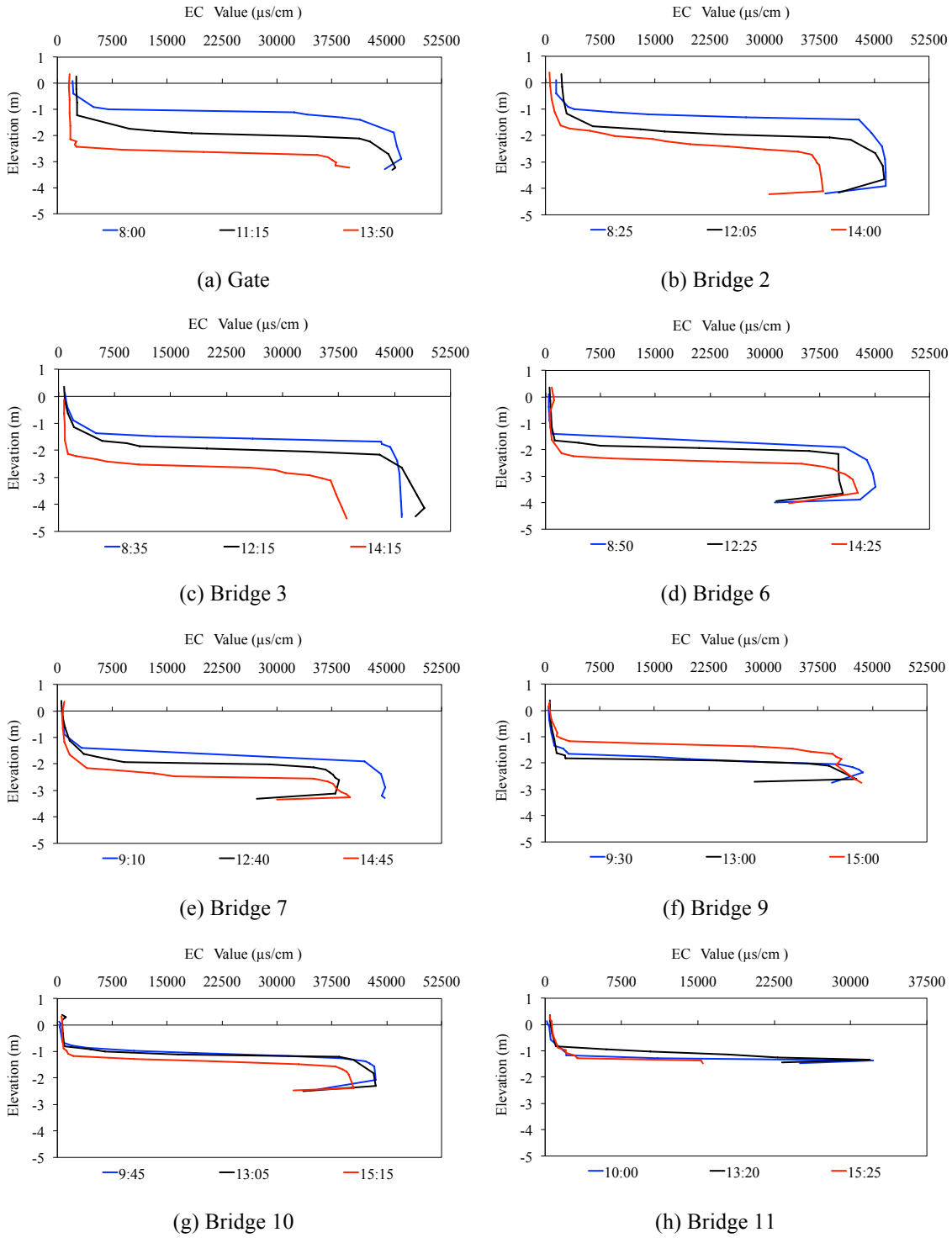

Fig. 5-14 The vertical distribution of salinity during the operation process of sluice gates

The vertical variation of density surface of the saltwater wedge measured by SC-3 is shown in Fig. 5-15. The average elevation of the density interface was about -1.32 m before the operation of sluice gates started on August 16, 2012, and reduced to about -1.79 m within 0.5 hour when the submerged orifice was created, with a variation of 0.47 m. With the drainage of saltwater, the height of the density interface continued to decline, while its average elevation changed from -2.04 m to -2.36 m from the second hour to the third hour when the saltwater started to be eliminated, demonstrating that the total height variation of density interface was 1.04 m under this submerged orifices and upstream discharge. The height of the density surface lowered more during the second observation (11:55 to 12:22) compared to the other surveys (0.25 m and 0.32 m) on August 16, 2012. As a whole, the density interface could be decreased when the operation of sluice gates was implemented.

Under the similar boundary situation (tide level and discharge), the comparison of density surfaces measured by SC-3 between the operation of sluice gates day (August 16, 2012) and natural situation day (August 17, 2012) is shown in Fig. 5-16. The average elevation of density surface at the last survey on August 16, 2012 was -2.36 m, but was -1.49 m on August 17, 2012 with the same tide level, suggesting that this method successfully drained the saltwater out of the sluice gates.

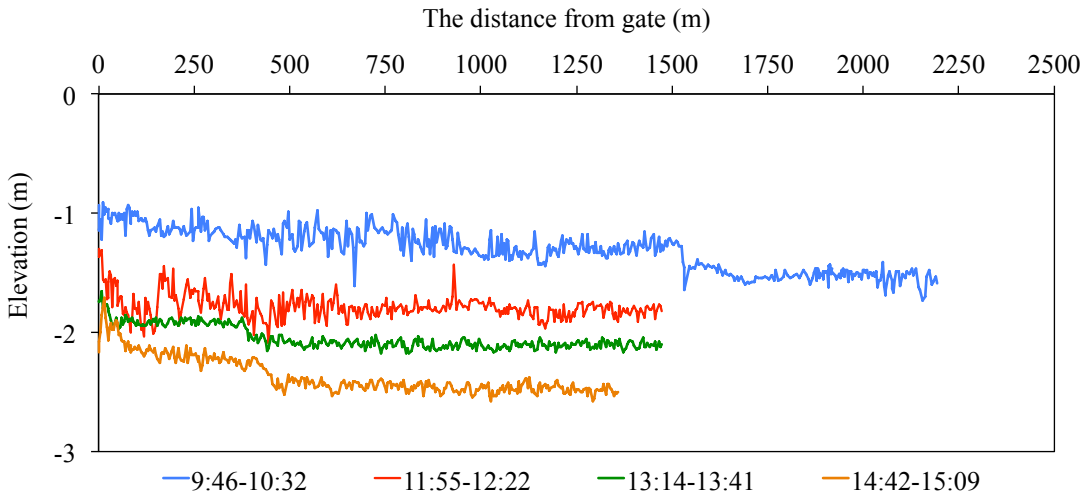

Fig. 5-15 The variation of density interfaces before and after the operation of sluice gates

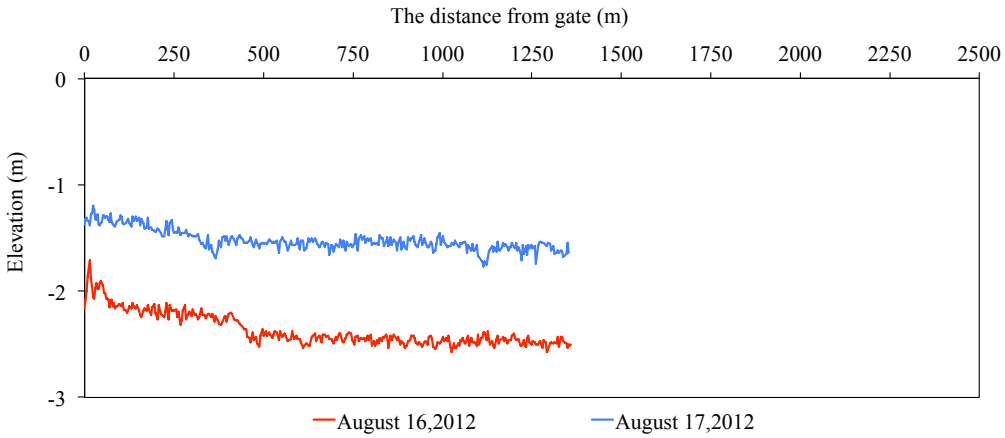

Fig. 5-16 The variation of density interfaces between two survey days

(2) Longitudinal variation of saltwater wedge

The longitudinal variation of the saltwater wedge measured by EC meters is shown in Fig. 5-17. The extent of saltwater wedge was about 4.33 km from the sluice gates before the sluice gates were closed. Within 1.5 hours after the submerged orifices was created, the distance of saltwater wedge decreased to about 3.56 km. With the drainage of saltwater, the distance was shortened to about 2.48 km. During the whole period of the sluice gates operation, the shortened distance of saltwater wedge was 1.85 km. Comparing with the results of non-operation of sluice gates, on Aug 17, 2012, the longitudinal distances of saltwater wedge were similar to each other, shown in Fig. 5-17 (b). This shorter saltwater wedge, on the day of non-operation of sluice gates, was potentially caused by the operation of sluice gates the day before. Also, the average height of the density surface was 0.68 m, at the same positions that was lowered by the previous operation of sluice gates.

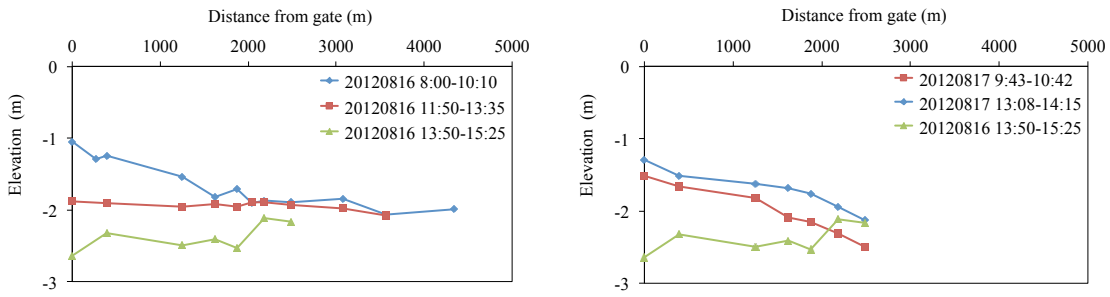

(a) Operation of sluice gates

(b) Non-peration of sluice gates

Fig. 5-17 The longitudinal variation of saltwater wedge

(3) Velocities of saltwater and freshwater

In Fig. 5-18, for the freshwater near the Nagisa Bridge (0.26 km upstream from the sluice gates), the variation tendency of velocity was more relative with the operation of the sluice gates than that of saltwater during the experiment period. After the operation of sluice gates was finished, the velocity of freshwater changed with the tidal situation. When the sluice gates were fully first closed, the velocity of freshwater almost decreased to 0 cm/s. Contrarily, when the sluice gates were fully opened, the velocity of freshwater raised to the peak value (60.63 cm/s). When the gates were subsequently closed again, it also decreased quickly. When the sluice gates were opened again, it declined again. Because the difference of average water levels inside and outside of the sluice gates was about 0 m, the drainage of freshwater was blocked. Besides, the direction of freshwater flow was scarcely changed (northwest between 270° and 360°), flowing seaward all the time.

For the saltwater layer, the velocity near Nagisa Bridge sharply changed twice with the operation of sluice gates and tide, as well as its transformed directions. When the sluice gates were first opened to predetermined aperture at about 12:00 on August 16, 2012, the saltwater started to flow seaward, while its velocity changed from 0.58 cm/s to 12.32 cm/s. Once the sluice gates were fully opened at about 16:00, its velocity reached the first peak value (22.34 cm/s), and then decreased quickly as the sluice gates was closed again. At that time, the drainage pumps were running, so the flow direction didn't turn round and the velocity was controlled by the discharge drained by pumps. After 6.5 hours when the saltwater was drained out by pumps, the sluice gates were opened again. Then the saltwater flowed landward, and its velocity increased to second peak value (27.00 cm/s) around higher high water, suggesting that saltwater intruded upstream again during the period of flood tide.

In Fig. 5-19, the velocity of saltwater near Sakiyama Bridge (1.62 km upstream from gates) also changed with the operation of sluice gates and tide, but it can be seen that the hysteretic nature was less obvious than the velocity near Nagisa Bridge, probably due to the distance from the sluice gates to this bridge. When the sluice gates were first closed on August 16, 2012, the saltwater still flowed upstream from 10:00 to 11:40, similarly flowed downstream from 0:00 to 3:20 on August 17, 2012, after the sluice

gates were fully opened. When the sluice gates were first opened fully around at 16:00 on August 16, 2012, the velocity of saltwater increased to a peak value (34.3 cm/s), and then gradually decreased because of the following closure of the sluice gates. Under the condition of the sluice gates were closed, the velocity of saltwater was controlled by the discharge drained by pumps, and they were similar of the velocities near two bridges because of the drainage through pumps. Moreover, the average velocity of saltwater intrusion near Sakiyama Bridge was lower than that near Nagisa bridge, implying that the intrusion velocity decreased with upstream distance.

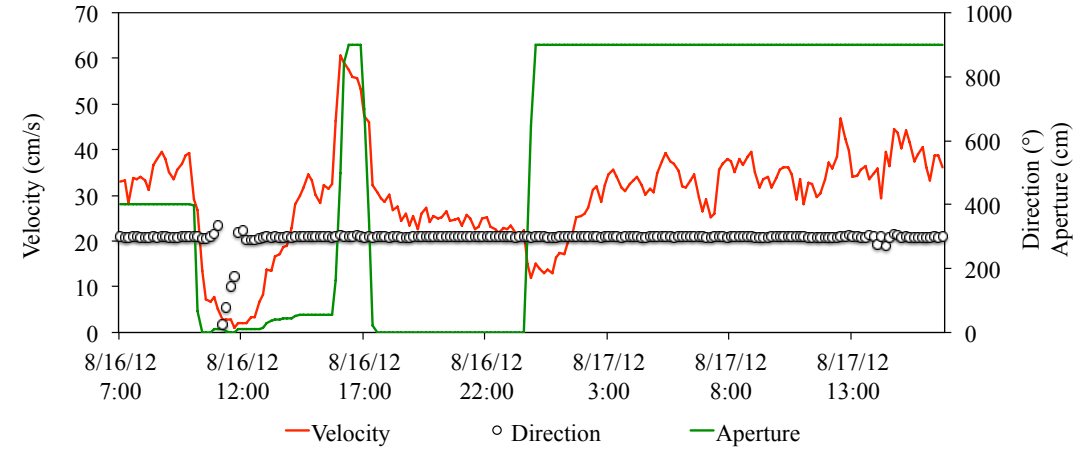

(a) Freshwater

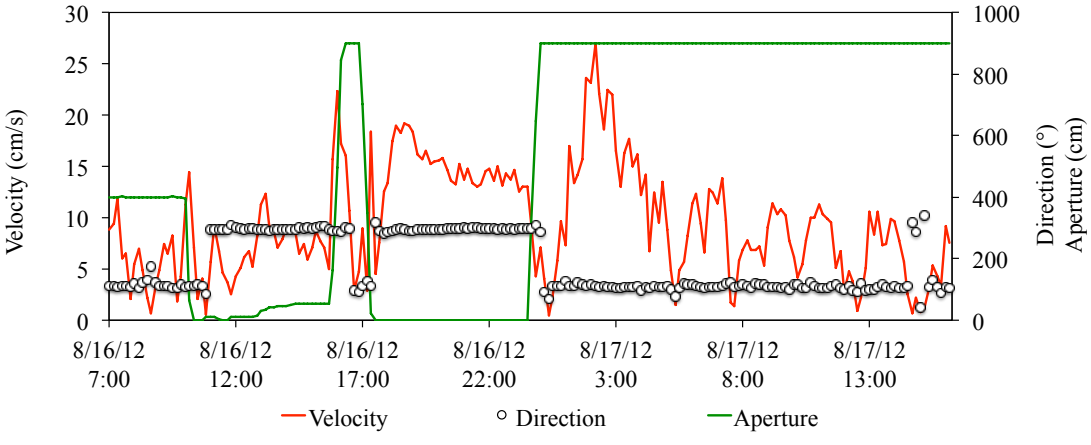

(b) Saltwater

Fig. 5-18 The velocities of freshwater and saltwater at 0.26 km from the gate on August 16 and 17, 2012

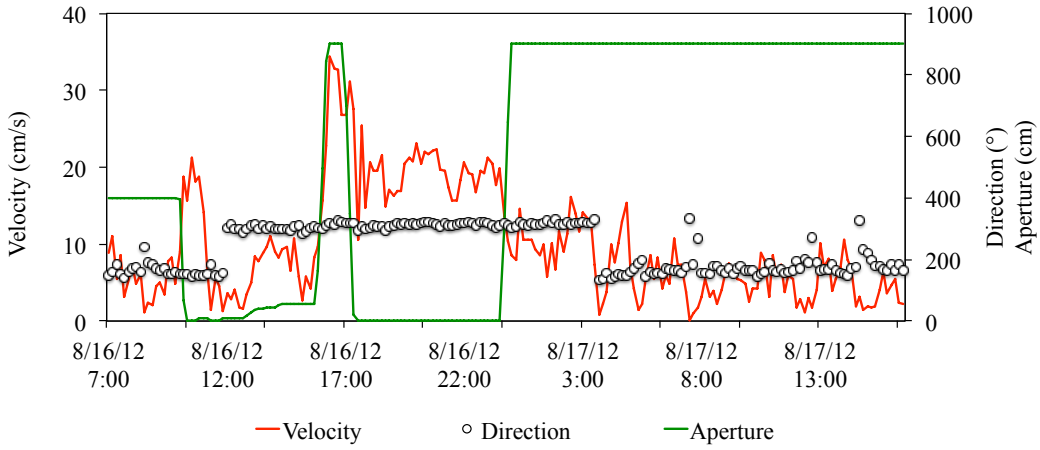

Fig. 5-19 The velocities of saltwater at 1.62 km from the sluice gates on August 16 and 17, 2012

5.3.2.2 Operation of one sluice gate

The average upstream freshwater flow rates were 16.9 m^3/s and 18.5 m^3/s on Aug 21 and 22, 2013, and the average downstream discharges were 34.8 m^3/s and 33.3 m^3/s during survey period.

(1) Vertical variation of saltwater wedge

The vertical salinity distribution of the saltwater measured by EC meters on Aug 16 and 17, 2013 at 0.26 km from the sluice gates, is shown in Fig. 5-20. Near the Nagisa Bridge, the height differences of density interface were 0.55 m, 0.87 m, 0.95 m and 0.88 m respectively, between the operation and non-operation of sluice gates. During the whole survey period, the average height difference of density interface was decreased by 0.81 m. For other measurement sites, the vertical heights of density interfaces were also decreased as shown in Fig. 5-22.

The vertical variation of density surface of the saltwater wedge measured by SC-3 is shown in Fig. 5-21. The average elevation of the density interface was about -1.23 m before the operation of one sluice gate started on August 21, 2013, and was reduced to about -1.77 m when the operation was finished within 4 hours, with a height variation of density surface was of 0.54 m. Comparison with the results on Aug 22, 2013, the height of the density interface was always lower than that of on non-operation of sluice gate. The average height difference of the density surface lowered was 0.43 m. As a whole, the density interface could be decreased when only the operation of one sluice

gate was implemented.

(2) Longitudinal variation of saltwater wedge

The longitudinal variations of the saltwater wedge measured by EC meters on two survey days are shown in Fig. 5-22. For the first two measurements of saltwater wedge, on Aug 21 and 22, 2012, the extent of saltwater wedge was decreased from about 5.04 km to 3.07 km from the sluice gates, with a distance difference of 1.97 km. With the flood tide, the shortened distance became shorter on the third measurement, from 5.04 km to 3.56 km. For the last measurement, the distance changed from 5.36 km to 3.56 km, with a distance difference of 1.80 km. During the whole observation, the average shortened distance of saltwater wedge was 1.81 km with this operation of one gate.

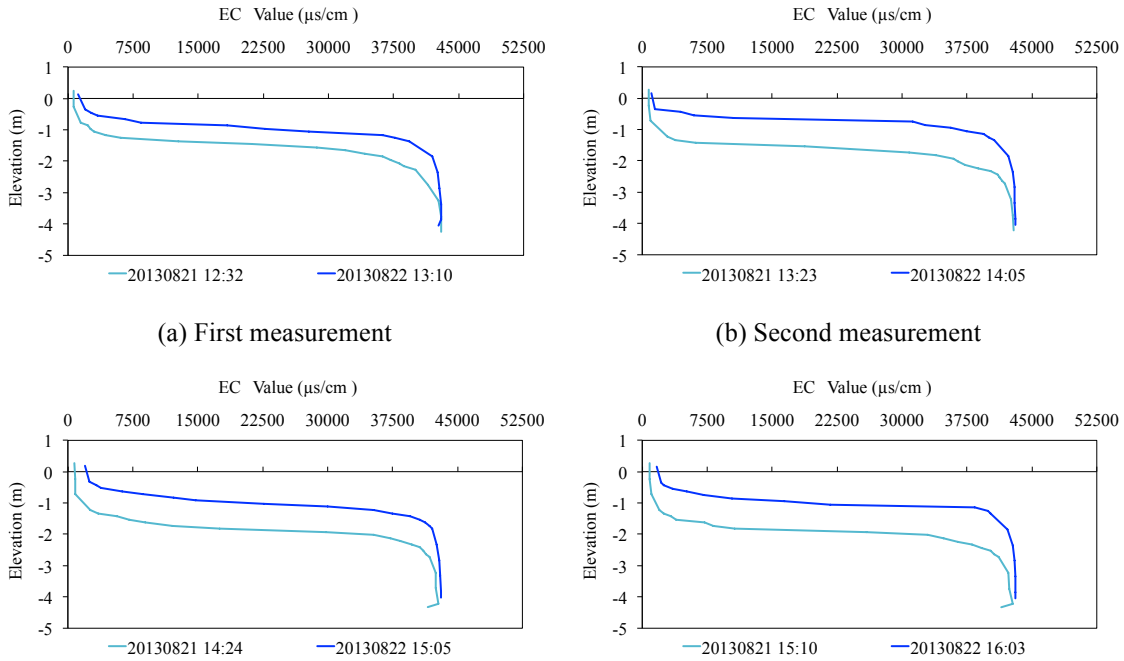

(a) First measurement (b) Second measurement

(c) Third measurement (d) Fourth measurement

Fig. 5-20 The vertical distribution of salinity at 0.26 km from the sluice gates on Aug 21 and 22, 2013

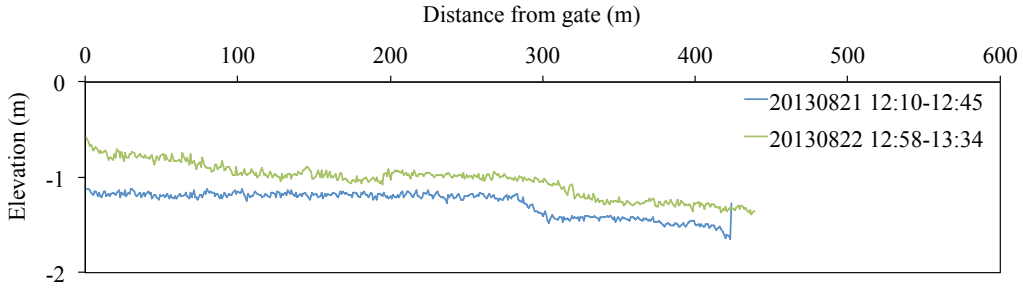

(a) First way

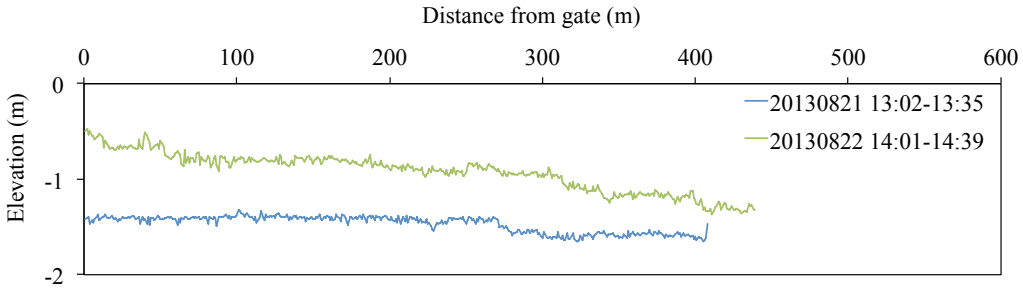

(b) Second way

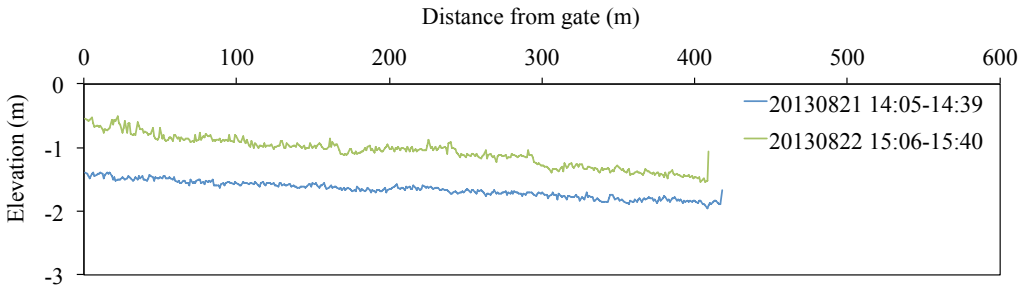

(c) Third way

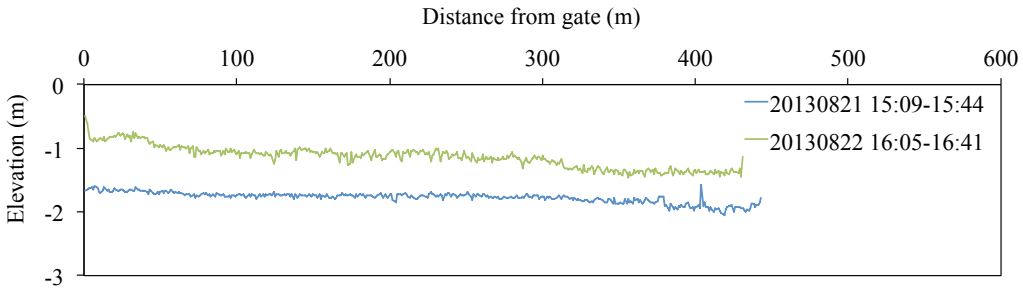

(d) Fourth way

Fig. 5-21 The vertical variation of density interface on August 21 and 22, 2013

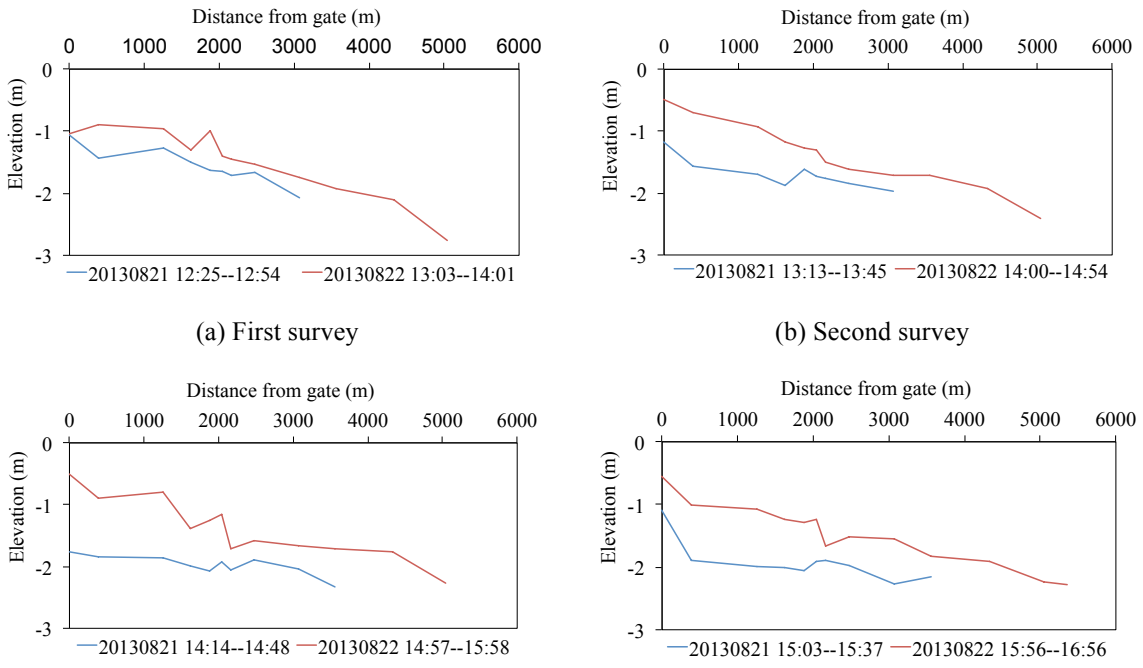

Fig. 5-22 The longitudinal variation of saltwater wedge

(3) Velocities of saltwater and freshwater

The velocities of saltwater and freshwater near 0.26 km upstream from the sluice gates are showed in Fig. 5-23. It can be seen from Fig. 5-23 (a) that the freshwater always flowed downstream (northwest between 270° and 360°) with a velocity varied with the tide level. The velocity reached the highest value after higher high water, and lowered to the lowest value before next higher high water, with an average velocity of 0.33 m/s during the survey period. In Fig. 5-23 (b), the direction of saltwater changed due to flood tide and ebb tide, and the average velocity of saltwater was 0.06 m/s. During one tidal cycle, 24 % of flow was seaward and 76 % was landward.

5.3.3 Discussions

According to the results of twice operations of sluice gates, the shortened distances of saltwater wedges were similar to each other, which are 1.85 km and 1.81 km. The heights of density interfaces were also decreased by 0.87 m and 0.43 m, respectively. It is obviously that the effect achieved by submerged orifice is better than that of the operation of one sluice gate. So the operation of sluice gates for creating submerged

orifice is more effective for controlling saltwater wedge in Shinkawa River.

In addition, these two experiments are to control the saltwater wedge beyond all intake pumping stations where the most downstream one is located at 2.20 km from the sluice gates (see Table 3-12). That means the final range of saltwater wedge should be less than 2.20 km. But the extents of saltwater wedges after first operation of two sluice gates were about 2.48 km, still making two intake pumping stations within saltwater wedge. The reason seems to be that the drainage time of saltwater was shorter than actual needs. However, the one sluice gate operation, resulted in a net distance of saltwater wedge of 3.56 km, made four intake pumping stations within saltwater wedge.

Based on the discussions above, the submerged orifices should be implemented within adequate period to guarantee the quality of irrigation water and navigation.

5.3.4 Conclusions

Both operations of sluice gates controlled the saltwater wedge intrusion to some extent, guaranteeing the normal drainage discharge of Shinkawa River and saving the energy taken by drainage pumps near the mouth of the river when the sluice gates were fully closed. But the effect of submerged orifice is better than the other. So this method can be applied to control the saltwater wedge intrusion in sufficient operation period.

5.4 Discussions

The driving force of seawater intrusion is the density difference between saltwater and freshwater, associating with vertical mixing of the saltwater and freshwater resulting from the turbulence produced by tidal currents, and the phenomenon of saltwater wedge is the result of the minimum degree of vertical mixing, causing the maximum vertical density gradients (Henry 1967). At present, several control methods of saltwater intrusion that have been implemented, either laboratory experiments or engineering practices, are all based on the mechanism of disturbing the driving force and turbulence structure of the tidal current. For instance, the river bottom barrier (Army U.S. Army Corps of Engineers 1993) can prevent the advancing saltwater wedge, providing adequate blockage of the saltwater supply. The vertical air curtain is also a method to control saltwater intrusion. Besides, freshwater flush, water barriers and the construction of sumps in the path of advancing saltwater wedge, can also be applied to

prevent or control the seawater intrusion (Abraham 1973).

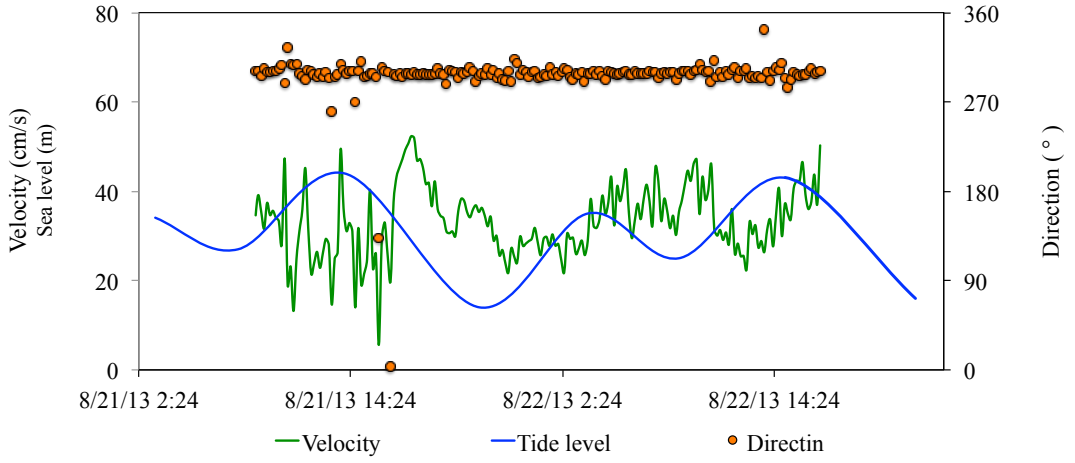

(a) Freshwater

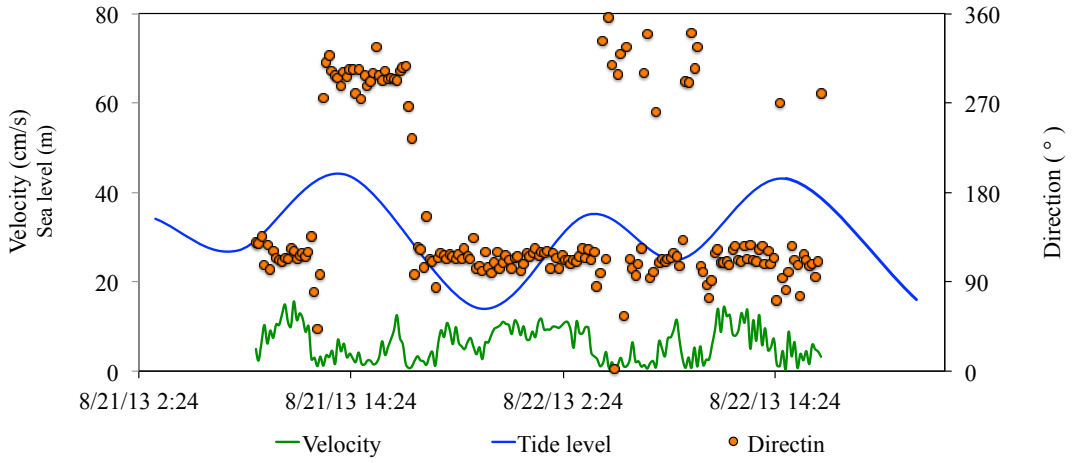

(b) Saltwater

Fig. 5-23 The velocities of freshwater and saltwater on August 21and 22, 2013

Based on the mechanism of controlling saltwater wedge intrusion and countermeasures, discharge increase and the operation of sluice gates were applied to limit the saltwater wedge intrusion in the Shinkawa River, but neither of them could completely achieve the designed objective owing to be limited by the supply and the demand of irrigation water for paddy fields and navigation of this river. In addition, one selective intake structure was also built only to pump overlying freshwater, yet still didn't fulfill desired goal thoroughly. However, the most effective method for controlling saltwater wedge in

Shinkawa River, the operation of sluice gates, has been found. The biggest obstacle for this method is that this in-situ experiment opportunity was strongly restricted by the currently implemented countermeasures of the sluice gates closing and pumping stations ceasing.

According to the analyses stated above, the numerical simulation method that can predict and evaluate the seawater intrusion (Fatemeh et al. 2008; Sangman et al. 2010; Gong 2011) is proposed to apply with the in-situ experiment, in order to prevent or control the seawater intrusion in the Shinkawa River. The concrete research idea is that a regimen controlling saltwater wedge can be designed by numerical calculation under the real conditions, and then the effectiveness of these designed regimens should be verified by in-situ experiment. In this research, the most effective method for controlling seawater intrusion in Shinkawa River has been estimated, but the most adequate aperture of the sluice gates is till unknown. So the aperture of sluice gates and its operation time can be first determined by the numerical model under real tide level and river discharge, and then the conducting scheme of the operation of sluice gates determined based on the results of numerical model will be carried out in the real river.

5.5 Summary

Based on the results of discharge increase, the operation of sluice gates and one mean of only pumping upper freshwater, some summary is list as following:

(1). Discharge increase reduced the height of density interface between saltwater and freshwater, and make the extent of saltwater wedge shorter in Shinkawa River as well. But this method did not thoroughly limit the saltwater wedge beyond the irrigation pumping stations. However, this method might be applied to control the saltwater wedge in this river under sound water management and sufficient upstream runoff.

(2). The selective intake structure basically guaranteed the quality of irrigation water during the survey period as well. But this method did not achieve the original goal, only taking overlying freshwater and blocking underlying saltwater. The selective intake structure can be reconstructed to improve the quality of pumped water from Shinkawa River by increasing the area of the wetted cross-section of the structure.

(3). The operation of sluice gates reduced the height of the density interface between

saltwater and freshwater, and the intrusion extent of saltwater wedge in Shinkawa River. And the operation of sluice gates, among these three methods, is most effective for controlling the saltwater wedge in Shinkawa River. The submerged orifice created by the sluice gates can be implemented with adequately aperture and period to fully control the saltwater wedge intrusion, guaranteeing the normal drainage discharge of Shinkawa River and saving the energy taken by drainage pumps near the mouth of the river when the sluice gates was fully closed.

6. Conclusions

Before determining some effective and inexpensive countermeasures for preventing seawater intrusion, the behavior of seawater intrusion in Shinkawa River has been visualized by field surveys and numerical simulation. Then the effects of three proposed countermeasures, discharge increase, the operation of sluice gates and selective intake, were verified by in-situ experiments. The corresponding conclusions can be summarized as following:

(1) The rules of seawater intrusion in Shinkawa River were summarized based on the field surveys. The seawater intrusion in this river is mainly subject to the river discharge and tide. During irrigation season (relative large discharge), the longitudinal extent of seawater intrusion changes twice in one day with flood tide and ebb tide, and reaches maximum and minimum on spring tide day and neap tide day, respectively. That is the rules of seawater intrusion in Shinkawa River have periodicity, one tidal day and half lunar month. With the variation of tide level from April to September, the longitudinal extent of seawater intrusion into the river gradually increased, with a range of 1.5 km to 6.0 km. Within the intruded part of river, the vertical distribution of salinity is featured by a sharply transition zone of about 25 cm, which is called as the density interface, with an EC value of 20,000 μs/cm between saltwater and freshwater. The density interface also changes with the tide, increasing during flood tide and decreasing during ebb tide. During non-irrigation season (relative small discharge), the seawater intrusion moves into and out of river with flood tide and ebb tide as well, with an obvious transition zone between saltwater and freshwater, only the extent is longer than that in irrigation season, existing in the entire river. Based on these rules, the seawater intrusion in Shinkawa River is classed into the well-stratified type (saltwater wedge)

For velocities and directions of saltwater and freshwater, freshwater almost flows seaward all the time, but the direction of saltwater is usually influenced by tide, moving seawater during flood tide and moving landward during ebb tide. Velocities of both freshwater and saltwater increase and decrease with flood tide and ebb tide. The average velocity of freshwater is greater than that of saltwater.

(2) The processes of seawater intrusion in Shinkawa River during the whole irrigation

season were successfully reproduced by the one-dimensional, two layer unsteady flow model. By this model, a long series data of seawater intrusion in Shinkawa River was obtained without the sluice gates operation. The simulated positions of density interfaces near the inlet of one intake pumping station were compared with the position of the inlet. It was found that when the salinity of pumped water reached to the standard of irrigation water of 1500 μs/cm, the height difference between density interface and the inlet was 1.2 m. That means when the height difference is less than 1.2 m, the salinity of pumped water might be more than 1500 μs/cm, and the paddy fields irrigated by this water suffer influence. And this high saline water situation occupied about 23 % of the time during total irrigation season under non-operation of sluice gates.

(3) Three selected countermeasures based on the conditions of the Shinkawa River, discharge increase, the operation of sluice gates and selective intake, were all verified by in-situ experiments. Among these three methods, the discharge increase and selective intake had less effect on controlling seawater intrusion than the operation of sluice gates, which successfully pushed the saltwater out of the river. Within 3 hours after the submerged orifice was created, the extent of saltwater wedge was decreased from 4.33 km to 2.48 km, with a distance difference of about 1.85 km, and the decreased height of density interface was about 1.04 m.

Based on this study, the operation of sluice gates can be applied to solve out the seawater intrusion in other estuaries where have similar conditions with Shinkawa River in the world.

Reference

[1] Tuin H van der (1991) Guidelines on the study of seawater intrusion into rivers. The united Nations Educational, Scientific and Cultural Organization 7, Place de Fonternoy, 75700 Pairs. ISBN 92-3-102765-4

[2] McLusky D S and Elliott M (2004) The Estuarine Ecosystem: Ecology, Threats and Management. New York: Oxford University Press. ISBN 0-19-852508-7

[3] Huang HM (2006) Study of one and two dimensional simulation of saltwater intrusion in estuary of Yangtze River. Dissertation, Hohai University

[4] Li Chunchu (1990) The overview and problems of the influence of high saline water intrusion on the estuaries in China. Marine Sciences 3: 54-59

[5] Xu Ning, Lv Songhui, Chen Jufang et al (2004) The influence of water temperature and salinity on the growth of Scrippsiella trochoidea. Marine Environment Sciences 23(3): 36-38

[6] Zhu Yamin (2006) Hydrologic characteristics and salt flux mechanism in Inner Lindingyang firth of the Pearl River. Dissertation, Sun Yat-Sen Universtiy

[7] Song ZY and Mao LH (2002) Study of seawater intrusion in estuary of Yangtze River. Water Resources Protection 3: 27-30

[8] Yang LL (2007) Study of saltwater intrusion in estuary by simulation modeling. Dissertation, Shanghai Jiaotong University

[9] Mao Zhicang, Shen Huanting and Yao Yunda (1993) Analysis on the resource of saltwater intrusion in the south bank of South branch of Yangtze River estuary. Marine Science Bulletin 12 (3): 17-25

[10] Shen Huanting, Mao Zhicang and Gu Guochuan (1980) The preliminary study of saltwater intrusion in the Yangtze River estuary – South-North Water Diversion Project. The Changjiang River (3): 20-26

[11] Van der Meer JJM (1993) Microscopic evidence of subglacial deformation. Quaternary Science Reviews (12): 553-587

[12] Mao ZC and Shen HT (1995) Study on Type of Saltwater Intrusion for Tidal Branching Estuaries – A Case Study on the Changjiang Estuary. Journal of East China Normal University (Natural Science) 2: 77-85

[13] Zeng Yifei (2007) Ocean Engineering Environment. Shanghai Jiao Tong University Press, Shanghai, pp 124-126

[14] Huang Xinhua, Zeng Shuiquan, Yi Shaozhen et al (1962) the problem of salt injury in the West River Delta. Journal of Geographical Science 28 (02): 137-147

[15] He Chao (2010) Wind effects on salt intrusion in Modaomen estuary in winter. Dissertation, Sun Yat-Sen University

[16] Xiao CQ and Shen HT (1998) The Analysis of Factors Affecting the Saltwater Intrusion in Changjiang Estuary. Journal of East China Normal University (Natural Science) 3: 74-80

[17] Liu JW (2010) The studies of movement of salty border in wet and dry season and the vertical distribution of salinity in modaomen waterway. Dissertation, Sun Yat-sen University

[18] Nguyen AD and Savenije HHG (2006) Salt intrusion in multi-channel estuaries: a case study in the Mekong Delta, Vietnam. Hydrology and Earth System Sciences 10: 743-754

[19] Wang Yigang, Feng Weibing, Jing ying et al (1997) Study on the impact of the Three Gorges Project on the saltwater intrusion and navigation in the Yangtze River estuary. The 8th colloquium of coast engineering in China – the proceedings of the port and coastal development both China and Taiwan. Ocean Press, Beijing, pp 21-28

[20] Wang Cangjie (2001) River Dynamic. China communication press, Beijing, pp 144-145

[21] Simmons HS and Brown FR (1969) Salinity effects in estuarine hydraulics and sedimentation. Proc.13th Congress of IAHR C-34: 311-325

[22] Suga G (1979) Fundamental study on hydraulics of salt wedge in tidal river,

technical note of the Public Work Research Institute. No. 1537: 255

[23] Hansen DV and Rauray M Jr (1966) New dimensions in estuary classification. Limnology and Oceanography (1): 319-326

[24] Wang Yucheng, Liu Zhe, Gao Huiwang, Ju Lian and Guo, Xinyu (2011) Response of salinity distribution around the Yellow River mouth to abrupt changes in river discharge. Continental Shelf Research 31: 685-694

[25] Zuo Qidong (1984) The theory and method of physical model test. Water Resources and Electric Power Press, Beijing

[26] China Institute of Water Resources and Hydropower Research and Nanjing Hydraulic research institute (1985). Hydraulic model test. Water Resources and Electric Power Press, Beijing

[27] Farmer Harlow G (1951) An experimental study of salt wedges. Woods Hole Oceanographic Institution 51-59

[28] Yasuo Kaneko (1965). Experiment study on salt wedge in a channel of non-uniform depth. Report of port and harbor technical research institute ministry of transportation, Japan 4 (5)

[29] Grigg Nicola (1995) A laboratory study of the dynamics and mixing in a salt wedge estuary. Dissertation, The University of Western Australia

[30] Banks J, Carson J, Nelson B and Nicol D (2001) Discrete-Event System Simulation. Prentice Hall, 3. ISBN 0-13-088702-1

[31] Starogatz and Steven (2007) "The End of Insight". In Brockman, John. What is your dangerous idea?. HarperCollins. ISBN 9780061214950

[32] Suga K (1977) Numerical calculation of one-dimensional and two layers unsteady flow. The 24th proceeding of coastal engineering, 544-548 (in Japanese)

[33] Suga K (1979) Numerical calculation of one-dimensional and two layers unsteady flow. The 26th proceeding of coastal engineering, 567-571 (in Japanese)

[34] Suga K (1981) Numerical calculation method of saline-wedge in tidal rivers. Civil

Engineering Journal 23-11: 31-36 (in Japanese)

[35] Zhu Liuzheng (1980) The problem of Yangtze River estuary. The institute of ocean engineering of the College of Hydraulic in Western China

[36] Yi Jiahao (1987) The model calculation study of saltwater in Yangtze River estuary. Nangjing Hydraulic Research Institute

[37] Arita Masamitsu and Gerhard H Jirka (1987) Two-layer model of saline wedge I: entrainment and interfacial friction. J. Hydraul. Eng. 113:1229-1246

[38] Arita Masamitsu and Gerhard H. Jirka (1987) Two-layer model of saline wedge I: II: Prediction of mean properties. J. Hydraul. Eng. 113:1249-1263

[39] Chen XinJian (2004) Modeling hydrodynamics and salt transport in the Alafia River estuary, Florida during May 1999–December 2001. Estuarine, Coastal and Shelf Science 61: 477–490

[40] Liu Wen-Cheng, Hsu Ming-Hsi, Wu Chi-Ray, Wang Chi-Fang and Kuo Albert Y (2004) Modeling Salt Water Intrusion in Tanshui River Estuarine System—Case-Study Contrasting Now and Then. Journal of Hydraulic Engineering 130: 849-859

[41] Meselhe EA, Noshi HM (2001) Hydrodynamic and Salinity Modeling of the Calcasieu-Sabine Basin. World Water Congress 1-10

[42] Jeong S, Yeon K, Hur Y and Oh K (2010) Salinity intrusion characteristics analysis using EFDC model in the downstream of Geum River. Journal of Environment Science (China) 22(6): 934-939

[43] Gong W and Shen J (2011) The response of salt intrusion to change in river discharge and tidal mixing during the dry season in the Modaomen Estuary, China. Cont Shelf Res 31: 769-788

[44] Liu Junwei and Tong Chaofeng (2004) A Review on Salt Water Intrusion in Yangtze Estuary. http://www.paper.edu.cn

[45] Schonfeld JC (1960) The mechanism of longitudinal diffusion in a tidal river.

International Association of Scientific Hydrology, General Assembly of Helsincki, Publication No.51

[46] Pritchard DW (1952) Salinity distribution and circulation in the Chesapeake Bay estuarine system; Sears found. Marine Research (11): 106-123

[47] Pritchard DW (1954) A study of the salt balance of a coastal plain estuary. Marine research (13): 133-144

[48] Bowden KF, Fairbairn LA and Hughes P (1959) The distribution of shearing stresses in a tidal current. Geophsical Journal of the Royal Astronomical Society (2): 288-305

[49] Bowden KF (1963) The mixing processes in a tidal estuary. International Journal of Air and Water Pollution (7): 344-356

[50] Bowden KF (1966) Circulation, salinity and river discharge in the Mersey estuary. Geophysical Journal of the Royal Astronomical Society (10): 383-400

[51] Hansen DV (1965) Currents and mixing in the Columbia River Estuary. Transactions of a Joint Conference of Ocean Science and Ocean Engineering 943-955

[52] Bowden KF (1967) Circulation and diffusion. Estuaries. Publication by Association for the Advancement of Science 15-36

[53] Pritchard DW (1967) Observation of circulation in coastal plain estuaries. Estuaries. Pub lication by Association for the Advancement of Science 37-44

[54] Hanawa Kimio and Takashige Sugimoto (1980) Effect of the variation of river discharge on flushing and recovery of salt wedge (2). Sci. Rep. Tohoku University, Ser. 5, (Tohoku Geophysical Journal) 27 (1): 1-17 1980

[55] Uncles RJ and Stephens JA (1996) Salt Intrusion in the Tweed Estuary. Estuarine, Coastal and Shelf Science 43: l-293

[56] Uncles R J and Stephens JA (1997) Dynamics of Turbidity in the Tweed Estuary. Estuarine, Coastal and Shelf Science 45: 745-758

[57] Austin Jay A (2004) Estimating effective longitudinal dispersion in the Chesapeake Bay. Estuarine, Coastal and Shelf Science 60: 359-368

[58] Lerczak James A and Geyer W Rochwell (2006) Mechanisms Driving the Time-Dependent Salt Flux in a Partially Stratified Estuary. Journal of physical oceanography 36: 2296-2311

[59] Ippen Arthur T and Harleman Donald R E (1961) One-dimensional Analysis of Salinity Intrusion in Estuaries. Technical Bulletin Sep 55 - Nov 59

[60] Leendertsc J J et al (1973) A Three-Dimensional Model for Estuaries and Coastal Seas: Volum I, Principles of Computation. Rand Santa Monica CA 90406

[61] Leendertsc JJ et al (1975) A Three-Dimensional Model for Estuaries and Coastal Seas: Volum II, Aspects of Computation. Rand Santa Monica CA 90406

[62] Backhaus JO (1983) A Semi-Implicit Scheme for the Shallow Water Equations for Application to Shelf sea Modeling. Continental Shelf Research Vol. 4

[63] Simpson JH el at (1990) Tidal straining, Density current, and stirring in the control of estuarine stratification. Estuaries 13(2): 125-132

[64] Gillibrand PA and Balls PW (1998) Modeling Salt Intrusion and Nitrate Concentrations in the Ythan Estuary. Estuarine, Coastal and Shelf Science 47: 695-706

[65] Hagy James D, Sanford Lawrence P and Boynton Walter R (2000) Estimation of Net Physical Transport and Hydraulic Residence Times for a Coastal Plain Estuary Using Box Models. Estuaries 23 (3): 320-340

[66] Aceas JCJ, II'Hassan A, Savenije HHG et a1 (2000) Using GIS tools and Rapid Assessment Techniques for Determining salt intrusion: STREAM, a river basin management instrument. Physics and Chemistry of the Earth (Part B): Hydrology Oceans and Atmosphere 25(3): 265-273

[67] Hetland Robert D and Geyer W Rockwell (2004) An Idealized Study of the Structure of Long, Partially Mixed Estuaries. Journal of Physical Oceanography 34: 2677-2691

[68] Sylaios G, Tsihrintzis V and Haralambidou K (2006) Modeling stratification-mixing processes at the mouth of a dam-controlled river. European Water 13/14: 21-28

[69] Zahed Fatemeh, Etemad-Shahidi Amir and Jabbari Ebrahim (2008) Modeling of salinity intrusion under different hydrological conditions in the Arvand River Estuary. Canada Journal of Civil Engineering 35: 1476-1480

[70] Xue Pengfei, Chen Changsheng, Ding Pingxing, Beardsley, Robert C, Lin Huichan, Ge Jianzhong and Kong Yazhen (2009) Saltwater intrusion into the Changjiang River: A model-guided mechanism study. Journal of Geophysical Research 114, C02006. Doi: 10.1029/2008JC004831

[71] Twigt Daniel J, De Goede Erik D, Zijl Firmijn, Schwanenberg Dirk and Chiu Alex YW (2009) Coupled 1D–3D hydrodynamic modeling, with application to the Pearl River Delta. Ocean Dynamics 59:1077-1093

[72] Ralston David K, Geyer Rockwell W, Lerczak James A (2010) Structure, variability, and salt flux in a strongly forced salt wedge estuary. Journal of Geophysical Research: Oceans 115. Issue C6. DOI: 10.1029/2009JC005806

[73] Zhang W, Feng HC, Zheng JH, Hoitink AJF, Van Der Vegt M, Zhu Y and Cai HJ (2013) Numerical simulation and analysis of saltwater intrusion lengths in the Pearl River delta, China. Journal of Coastal Research 29 (2): 372-382. DOI: http://dx.doi.org/10.2112/JCOASTRES-D-12-00068.1

[74] Department of the Army U.S. Army Corps of Engineers (1993) Control methods for salinity intrusion in well-stratified estuaries and waterways. Engineer Technical Letter 1110-2-347

[75] Abraham DRIRG, Van Der Burgh IRP and DE Vos IRP (1973) Pneumatic barriers to reduce salt intrusion through locks. RIJKSWWATERSTAAT Communications 17

[76] Zhu zhiwei (1996) Exchange flow through a channel with an underwater sill. Dissertation, University of British Columbia, Canada

[77] Fagerburg Timothy L and Alexander Michael P (1994) Underwater sill construction for mitigating salt wedge migration on the lower Mississippi River. Miscellaneous Paper HL-94-1

[78] Jirka GH and Arita M (1987) Density Currents or Density Wedges: Boundary Layer Influence and Control Methods. Journal of Fluid Mechanics 177: 187-206

[79] Jirka GH and Sutherland ND (1988) Experimental Study of Salinity Intrusion Control Methods in Estuaries and Waterways, Contract Technical Report (in preparation), U.S. Army Engineer Waterways Experiment Station, Vicksburg, MS.

[80] Masanori Nakai and Masamitsu Arita (2002) An experimental study on prevention of saline wedge intrusion by an air curtain in rivers. Journal of Hydraulic Research 40 (3): 333-339

[81] Haralambidou K, Tsihrintzis VA and Sylaios GK (2003) Control of saline wedge intrusion in the estuary of Strymonas River using an air curtain. 8th international conference on environmental science and technology lemnos island, Greece 302-309

[82] Luyun Jr Roger, Momii Kazuro, Nakagawa Kei and Takahashi Masahiro (2009) Effects of Artificial Recharge and Physical Barrier on Seawater Intrusion. Annual Journal of Hydraulic Engineering, JSCE 53: 895-909

[83] Ranganna G (1975) Estimation of fresh water flow into a tidal estuary from salinity records. Proc. IAHR congress, Saopaulso

[84] Garvine RW, McCarthy RK and Wong KC (1992) The Axial Salinity Distribution in the Delaware Estuary and its Weak Responds to River Discharge. Estuarine Coastal Shelf Science 35: 157-165

[85] Hu Song, Zhu Jianrong and Fu Dejian (2003) Estuarine circulation and salinity intrusion II - the effects of runoff and sea level rise. Journal of Ocean University of Qingdao 33 (3): 337-342

[86] Tang Chengjia and Mao Zhichang (2004) The effect of the South-North Water Diversion Project and intake water in Jiangsu and Anhui on salinity intrusion in

Yangtze River estuary 21(2): 37-41

[87] The homepage of Japan Meteorological Agency. http://www.jma.go.jp/jma/indexe.html

[88] Tateshi M, Honda Y, Tokuoka T, Fukita A, Anma K, Nishimura K (2006) Saline water intrusion into the Aganogawa River. Laguna 13: 43-62 (in Japanese)

[89] Tateshi M, Nguyen VL, TA TKO, Tokuoka T, Fukita A, Nishimura K, Matsuda S (2007) Salt water intrusion in the Mekong River estuary, Vietnam: Observation at low flow season in May 2005. Sci Rep Niigata Univ, Ser E 22: 57-78

[90] Tokuoka T, Fukita A, Tateishi M, Nishimura K, Anma K, Matsuda S, Kawasumi T, Seki T (2005) Saline wedge observation by echo-sounding equipment (SC-3) and towing type water quality monitor (TPM CLOROTEC). Laguna 12: 81-87 (in Japanese)

[91] Henry B Simmons, 1967. Potential benefits of pneumatic barriers in estuary. Journal of the hydraulics division, Proceedings of the American Society of Civil Engineers, Vol. 93, No. HY3: 1-16

[92] Sangman Jeong, Kyusung Yeon, Youngteck Hur and Kukryul Oh, 2010. Salinity intrusion characteristics analysis using EFDC model in the downstream of Geum River. Journal of Environmental Science 22 (6): 934-939

[93] Gong Wenping, Shen Jian, 2011. The response of salt intrusion to changes in river discharge and tidal mixing during the dry season in the Modaomen Estuary, China. Continental Shelf Research 31: 769-788

[94] Fatemeh Zahed, Amir Etemad-Shahidi and Ebrahim Jabbari, 2008. Modeling of salinity intrusion under different hydrological conditions in the Arvand River Estuary. Canadian Journal of Civil Engineering 35: 1476-1480